# PES-ENZYME IMMOBILISED MEMBRANES FOR THE SIMULTANEOUS BIODEGRADATION AND FILTRATION OF NATURAL ORGANIC MATTER (NOM)

---


**by**

**PRETTY PHUMLILE MAMBA**


**Dissertation in fulfilment of the requirement for the degree**

**MAGISTER TECHNOLOGIAE**

**in**

**CHEMICAL ENGINEERING**

**in the**

**COLLEGE OF SCIENCE, ENGINEERING AND TECHNOLOGY**

**of the**

**UNIVERSITY OF SOUTH AFRICA**


**Supervisor : PROF THABO T.I NKAMBULE**

**Co-supervisors : PROF TITUS A.M MSAGATI**

**PROF BHEKIE B MAMBA**

**Dr. MACHAWE M MOTSA**


February 2020

## DECLARATION

Name: Pretty Phumlile Mamba

Student number: 65103718

Degree: Magister Technologiae: Chemical Engineering

**PES-ENZYME IMMOBILISED MEMBRANES FOR THE SIMULTANEOUS BIODEGRADATION AND FILTRATION OF NATURAL ORGANIC MATTER (NOM)**

I herewith declare that the above dissertation is my own work and that all the quoted and used sources have been shown and recognised by means of complete references.

SIGNATURE _____ DATE _____

## DEDICATION

This dissertation is dedicated to my late parents Mr. Simon Mahwayela and Mrs. Lillian Dwana Mamba for trying their level best when raising us even though it was not easy. Their hard work resulted to who I am today. MAY YOUR SOULS REST IN ERTENAL PEACE.

And

To my son Percy Junior Fourie, you are the reason I work hard.

## PUBLICATIONS AND PRESENTATIONS

**Peer-reviewed Publications:**

- P.P Mamba, P. Tshindane, T.A.M Msagati, B.B Mamba, T.T.I Nkambule, M.M. Motsa. *Ideal membrane structure for high permeate flux and DOM removal from water: Insight into the influence of preparation parameters*. 10 January 2020, Industrial & Engineering Chemistry Research (**Submitted**).

**Presentations:**

P.P Mamba, M.M Motsa, T.A.M Msagati, B.B Mamba, H.J Ogola, T.T.I Nkambule. *Screening of fungal isolates for humic acid removal and decolourization*. Oral presentation. NOM Indaba. Thamsanqa Kambule Auditorium. University of South Africa, South Africa, 20 November 2019.

## ACKNOWLEDGEMENTS

**This research would have not been a success without the support, contributions and encouragements from the following people and organisations:**

- Firstly, my appreciation goes to my supervisors; **Prof. Thabo T.I Nkambule** for granting me an opportunity to pursue my studies under his supervision. He saw potential and believed that I could do the project. He was always pushing me to do only the best and meet deadlines. I used to pray for him to find it in his heart to take it easy on me, little did I know that he was grooming a future academic. I will forever be grateful for not giving up on me; **Dr. Machawe M Motsa**, I always tell people that he was a God sent from heaven. My sincere gratitude goes to him for always believing in me throughout the journey though it was not easy, but his assistance in doing laboratory work and correcting my scientific writing kept me going. I will forever be grateful; **Prof. Titus A.M Msagati** for his guidance on the microbiological part of the project and making sure that I get access to the microbiology laboratory; **Prof. Bhekie B Mamba** for always encouraging us with wise words and being our inspiration in the academic field.

- I wish to acknowledge Dr. Henry Joseph Ogola for taking his precious time to assist with microbiology work, I would have not done it without him.

- My appreciation goes to the Nanotechnology and Water Sustainability (NanoWS) research technical team Dr. Hlengilizwe Nyoni and Mr Kagiso Mokalane for their assistance with technical instruments and analyses. My sincere gratitudes to the NanoWS admin team Mrs Gcinaphi Shabalala and Mr Bheki-mfundo Makgabo.

- I would also like to pour out my sincere gratitude to the NOM and ESG group for sharing thoughts and ideas. Special thanks to Dr. Olayemi Fakayode, Dr. Gcina Mamba and Mr Welldone Moyo for always availing themselves

whenever I needed assistance especially with presentations. Many thanks to Sylvia, Hailemariam, Thabile, Adewale, Adeeyo and Ester for their contributions.

- My acknowledgement goes to the college of Agriculture and Environmental Science, department of microbiology, especially Mr Hosana Mkoyi and Nthabiseng for letting me use their laboratory facilities and consumables.

- To the University of South Africa and NanoWS research unit for funding the research project.

- Many thanks to Dr. Tshepo Malefetse for editing this dissertation and to the examiners for reviewing the dissertation.

- Lastly, I would like to give thanks to my family and friends for their love and support emotionally and financially throughout the journey.

- Above all, I give thanks to the Almighty God for giving me strength and ability to persevere in undertaking this research study. It was not easy but his unfailing love, great purpose for my life and his word kept me going.

## ABSTRACT

Natural organic matter (NOM) removal is one of the challenges encountered by water treatment utilities in water treatment. NOM is found naturally in all surface waters and consists of compounds with complex structures emanating from decomposing plants and animal remains. NOM presence in water sources is a concern due to its ability to generate carcinogenic disinfection by-products (DBPs) with chlorine-based disinfectants, its ability to enable bacterial re-growth in distribution pipelines and introduction of organoleptic problems such as bad taste, odour and colour in drinking water. In attempt to remove NOM from water, conventional water treatment processes such as coagulation-flocculation have been employed. However, this can be achieved by optimising the coagulant dose and pH which not only increase the treatment costs but also time consuming. Therefore, fungal degradation of NOM into smaller fragments which can be easily removed by advance treatment methods such as membrane filtration could be a viable alternative to remove NOM from water. This work was aimed at developing and applying white rot fungi (WRF) enzyme-modified membranes for NOM degradation and removal in water.

The phase inversion method was used to prepare Polyethersulfone (PES) membranes using water as a non-solvent additive, N-methly-2-pyrrolidone (NMP) as a solvent and polyethylene glycol (PEG) as the pore-forming agent. This was carried out by varying the dope solution composition and concentration of the coagulation bath. Scanning electron microscopy (SEM) was used to study the changes in membrane structural arrangement and rejection studies were carried out using humic acid (HA) and bovine serum albumin (BSA) as NOM model compounds. Furthermore, eighteen (18) WRF isolates were collected from decaying wood and screened for their ability to produce lignolytic enzymes. Isolates (D, L and R) which tested positive for laccase were further screened for HA degradation from liquid media. Moreover, production of the desired enzymes in high quantities were carried out using solid-state fermentation (SSF) method and purified using 80 % ammonium sulfate. Thereafter, crude enzyme laccase was extracted and immobilised on the most promising PES membrane as a support material and 4-hydroxybenzoic acid

was used as a substrate for laccase stability. The changes in morphology of the modified membranes was also used as a confirmation for the successful immobilisation of the enzyme.

SEM micrographs revealed that the non-solvent additive impacts the morphology of the membrane pores and ultimately the permeation of water. High water flux was achieved from the membrane (M.5) with 0 wt.% water and 36 wt.% PEG. High flux performing membranes were selected for coagulation bath experiments. The highest water flux achieved for M.5 with 15 wt.% NMP was 568.66 $L.m^{-2}.h^{-1}$. The most permeable membranes recorded solute rejections as high as 88 % for BSA and 69 % for HA. Only three isolates (D, L, and R) identified as *Perenniporia* sp, *Trichoderma koningiopsis* and *Polyporaceae* sp, respectively, tested positive for laccase production. Colour change after fungal treatment was observed in all three isolates indicating the degradation of HA by the fungi. Ultraviolet visible (UV-vis) at 254 nm and dissolved organic carbon (DOC) measurement analysis revealed the highest percentage removal of (DOC) 52 % and ($UV_{254}$) 27.3 % for isolate R. After enzyme purification, results indicated laccase activity of 0.297 U/mL for isolate R and 0.152 U/mL for isolate D. In immobilisation studies, the interaction amongst the enzymes, the sulfonate groups and the substrate were confirmed by an intense colour change on the membrane surface. SEM images revealed the presence of spherically shaped structures on the surfaces of enzyme-modified membranes which in turn confirmed the successful immobilisation of the enzyme laccase. Moreover, a reduction in the permeability of the modified membranes served as confirmation for the immobilisation of the enzyme.

Rejection studies suggest that the enzyme-modified membranes can be used for HA removal and other similar pollutants from water with a 95 % HA removal using membrane modified with enzyme laccase from isolate R. Therefore, enzyme-modified membranes can be recommended for NOM removal from real water samples. However, the application of the enzyme-modified membranes in a large-scale water treatment is limited by challenges emanating with enzyme extraction, and high operational costs associated with higher pressure conditions.

## TABLE OF CONTENTS

## LIST OF FIGURES

## LIST OF TABLES

## LIST OF ABBREVIATIONS

| | |
|---|---|
| ABTS | 3-ethylbenzothiadine-6-sufunic acid |
| AOP(s) | Advanced oxidation processes |
| ATCC | American type culture collection |
| BDOC | Biodegradable organic carbon |
| BLAST | Basic local alignment search tool |
| Bp | Base pair |
| BSA | Bovine serum albumin |
| Da | Dalton |
| DBP(s) | Disinfection by-product(s) |
| DNA | Deoxyribonucleic acid |
| DOC | Dissolved organic carbon |
| DOM | Dissolved organic matter |
| EfOM | Effluent organic matter |
| ε | Extinction coefficient |
| FA | Fulvic acid |
| GAC | Granular activated carbon |
| HA | Humic acid |
| HAA | Haloacetic acid |
| HBT | 1-hydroxybenzotrialzole |
| HCCA | α-Cyano-4-hydroxycinnamic acid |
| HRT | Hydraulic retention time |
| HS | Humic substances |
| IEX | Ion exchange |
| ITS | Internal transcribed spacer |

| | |
|---|---|
| kDa | kilo Dalton |
| LiP | Lignin peroxidase |
| MALDI-TOF | Matric assisted laser desorption ionisation-time of flight |
| MBR | Membrane bioreactor |
| MIB | Methly-isoborneol |
| MnP | Manganese-dependent peroxidase |
| NCBI | National Center for Biotechnology Information |
| NMP | N-methly-2-pyrrolidone |
| NOM | Natural Organic Matter |
| PAC | Powdered activated carbon |
| PCR | Polymerase chain reaction |
| PEG | Polyethylene glycol |
| PES | Polyethersulfone |
| POM | Particulate Organic Matter |
| SANS 241 | South African National Standards 241 |
| SDA | Sabouraud dextrose agar |
| SDB | Sabouraud dextrose broth |
| SEM | Scanning electron microscopy |
| SSF | Solid state fermentation |
| THM | Trihalomethane |
| TOC | Total organic carbon |
| UF | Ultrafiltration |
| UV | Ultraviolet |
| VA | Veratryl alcohol |
| WRF | White rot fungi |

# CHAPTER 1
# INTRODUCTION

## 1.1 Background

Increasing concerns over the augmentation of current safe drinking water supplies has driven the water industry to perform further research on alternative and efficient methods for water treatment. The current water treatment systems were not initially intended for the complete removal of organic substances present in raw water. The presence of natural organic matter (NOM) in water is therefore undesirable. Being a naturally occurring complex mixture of dissolved organic and particulate compounds, NOM emanates from the remains of vegetation and animal matter and it is to this end found in either soil or water sources (Chaukura *et al*., 2018). Despite their important role in plant growth and soil richness, NOM is problematic to remove, especially when present in drinking water sources (Haarhoff *et al*., 2013; Kosobucki & Buszewski, 2014).

## 1.2 Problem statement

The presence of NOM in water changes its colour, taste and smell, thus interfering with the quality of the final water (Ncibi & Matilainen., 2018; Pan *et al*., 2016). In addition, the re-growth of bacteria and formation of biofilm coupled with cumulative and high amounts of heavy metals in the supply pipelines, is caused by NOM thus leading to increased treatment costs (Haarhoff *et al.*, 2013; Matilainen *et al.*, 2010). Furthermore, during the disinfection stage, NOM reacts with chlorine to produce disinfection by-products (DBPs) such as haloacetic acids (HAA) and trihalomethanes (THM), which are potential carcinogens that impacts human health (Marais *et al*., 2019; Golea *et al.*, 2017; jiang *et al* ., 2016). The presence of NOM in water has also been linked to fouling in membrane filtration processes (Tshabalala *et al*., 2016). Given the above-mentioned challenges, lowering NOM content or its complete removal from water is of critical importance.

The removal of NOM depends on their geographic origin, character and occurrence in water (Moyo *et al*., 2019; Tshindane *et al*., 2019; Nkambule *et al*., 2012). The most used methods for NOM removal include the use of chemicals, which effectively increases the overall water treatment costs. Examples of the chemical-based methods include coagulation, adsorption and oxidation (Sillanpää *et al*., 2018). In a typical water treatment, the most reliable treatment method for NOM removal is coagulation-flocculation, which removes most of the hydrophobic fraction of NOM. The next steps are clarification followed by filtration, which remove low molecular weight substances such as the hydrophilic part of NOM (Marais *et al*., 2018; Matilainen *et al*., 2010). Although considered the best conventional water treatment process for NOM removal, enhanced coagulation has major limitations such as increased coagulant dose requirements, pH adjustment and production of large sludge quantities (Solarska *et al*., 2009).

Other methods for NOM removal from water involve degradation that use photocatalysts such as titanium dioxide (Ndlangamandla *et al*., 2018; Ng *et al*., 2014; Autin *et al*., 2013) and oxidation processes such as ozonation (Bose & Reckhow, 2007; Matilainen & Sillanpää, 2010). Adsorption processes have recently been used for NOM removal. However, these processes include the use of costly adsorbents such as activated carbon, ion exchange resin and nano adsorbents (Levchuk *et al*., 2018; Bhatnagar & Sillanpää, 2017). Although membrane technology has been reckoned as alternate treatment method for the removal of NOM (Motsa *et al*., 2018; Qin *et al*., 2006), its fouling limitations still persist. Therefore, there still exists a need for the development of eco-friendly and less cost water treatment methods that use naturally derived bio-systems such as microorganisms that degrade NOM in water. The use of naturally occurring microorganisms for the biodegradation of NOM into smaller metabolites that can possibly be removed with filtration processes such as membranes offers a viable solution for NOM removal from water.

## 1.3 Justification

Biological treatment methods such as the use of basidiomycetes white rot fungi (WRF) species could potentially be used for NOM removal from water. These organisms produce lignolytic enzymes such as laccase, lignin peroxidase and manganese-dependent peroxidases through their secondary metabolism (Huy *et al*., 2017). These enzymes can transform biodegradable NOM into less harmful products and thus reduce the formation of sludge and eventual treatment costs of drinking water (Zahmatkesh *et al*., 2016). It has been demonstrated that WRF enzymes can degrade a wide array of organic compounds including NOM (Zahmatkesh *et al*., 2017; Collado *et al*., 2018). Maintaining a conducive environment such as pH and temperature as well as nutrients such as carbon and nitrogen is known to enhance the ability of WRF to produce enzymes in high quantities to enables the degradation of organic compounds (Ergun *et al*., 2017; Batal *et al*., 2015).

These lignolytic enzymes can be attached to membranes as a substrate to avoid washout and enhance stability. Recently, membrane surfaces have been modified with enzymes from WRF for the degradation of a wide array of organic pollutants in water and wastewater in membrane bioreactor (MBR) systems (Asif *et al*., 2017; Vasina *et al*., 2017; Nguyen *et al.*, 2013). Such systems were successfully demonstrated in the effective and efficient removal of trace organic compounds (TrOCs) such as pharmaceuticals, personal care products, industrial chemicals and pesticides from wastewater (Asif *et al*., 2018; Asif *et al*., 2017; Nguyen *et al*., 2016; Nguyen *et al.*, 2013). In this research work, a similar principle that employs WRF enzyme system was adopted and investigated for the ability to degrade NOM using synthetic solutions such as humic acid. Specifically, this study was aimed at the modification of an ultrafiltration polymeric membrane infusing WRF enzymes such as laccase on its surface for application in the degradation and NOM removal in water. The method is preferred over basic membrane filtration due to its dual functionality of biodegradation and filtration, in addition there is the enhancement of anti-fouling properties.

## 1.4 Aim and objectives of the study

The aim of this study was to develop and modify polyethersulfone (PES) membranes with WRF enzyme extracts for the degradation and filtration of NOM in water.

To successfully accomplish the aim of this study, the following key objectives were formulated:

- Fabrication of high performing PES ultrafiltration membranes for NOM removal.
- Isolation, identification and characterization of white rot fungi (WRF) isolates.
- Extraction, purification and assaying of fungal enzymes from pure culture of WRF species.
- Immobilisation of the extracted enzymes by modifying the membrane surfaces.
- Application and evaluation of the developed enzyme-based PES membranes in the biodegradation and removal of NOM from water.

## 1.5 Dissertation outline

A summary of each chapter discussed in this dissertation is as follows:

- **Chapter 2** reviews the current literature on NOM by specifically focussing on its origin, fractions, impact on water treatment and currently available methods for the removal of NOM from water. Furthermore, literature on the WRF species and their corresponding extracellular enzymes, including their application, especially the application on the degradation of NOM in water, is reviewed. The chapter concludes with a review on the all-important application of MBR in water treatment.

- **In chapter 3**, the research methodology on membrane fabrication protocols, characterization techniques used to generate data is discussed. As part of the research methodology, methods undertaken for the isolation and identification of WRF using MALDI-TOF Biotyper software and molecular

method are presented. Moreover, method for enzyme production, extraction and purification is also discussed in this chapter.

- **Chapter 4** covers the results on an investigation of the effect of water as a non-solvent additive in preparation of high flux polyethersulfone (PES) ultrafiltration membranes.

- **Chapter 5** presents results emanating from the screening of white rot fungi isolates to produce lignolytic enzymes and humic acid degradation as a model compound for NOM. **Chapter 5** also covers a discussion on the optimisation of enzyme production and extraction of crude enzymes.

- **Chapter 6** provides evidence for the immobilisation of white rot fungi enzymes on the surface of PES membranes and the membrane matrix. Furthermore, the application of enzyme-modified PES membranes in the degradation and removal of NOM is demonstrated and evaluated.

- **Chapter 7** presents major conclusions from this research work and recommendations for future work.

## 1.6 References


Asif, M.B., Hai, F.I., Kang, J., Van De Merwe, J.P., Leusch, F.D., Price, W.E. and Nghiem, L.D., 2018. Biocatalytic degradation of pharmaceuticals, personal care products, industrial chemicals, steroid hormones and pesticides in a membrane distillation enzymatic bioreactor. *Bioresource Technology*, *247*, pp.528-536.

Asif, M.B., Nguyen, L.N., Hai, F.I., Price, W.E. and Nghiem, L.D., 2017. Integration of an enzymatic bioreactor with membrane distillation for enhanced biodegradation of trace organic contaminants. *International Biodeterioration & Biodegradation*, *124*, pp.73-81.

Autin, O., Hart, J., Jarvis, P., MacAdam, J., Parsons, S.A. and Jefferson, B., 2013. The impact of background organic matter and alkalinity on the degradation of the pesticide metaldehyde by two advanced oxidation processes: UV/$H_2O_2$ and UV/$TiO_2$. *Water Research*, *47*(6), pp.2041-2049.

Bhatnagar, A. and Sillanpää, M., 2017. Removal of natural organic matter (NOM) and its constituents from water by adsorption–A review. *Chemosphere*, *166*, pp.497-510.

Bose, P. and Reckhow, D.A., 2007. The effect of ozonation on natural organic matter removal by alum coagulation. *Water Research*, *41*(7), pp.1516-1524.

Chaukura, N., Ndlangamandla, N.G., Moyo, W., Msagati, T.A., Mamba, B.B. and Nkambule, T.T., 2018. Natural organic matter in aquatic systems–a South African perspective. *Water SA*, *44*(4), pp.624-635.

Collado, S., Oulego, P., Suárez-Iglesias, O. and Díaz, M., 2018. Biodegradation of dissolved humic substances by fungi. *Applied Microbiology and Biotechnology*, *102*(8), pp.3497-3511.

El-Batal, A.I., ElKenawy, N.M., Yassin, A.S. and Amin, M.A., 2015. Laccase production by Pleurotus ostreatus and its application in synthesis of gold nanoparticles. *Biotechnology Reports*, *5*, pp.31-39.

Ergun, S.O. and Urek, R.O., 2017. Production of ligninolytic enzymes by solid state fermentation using *Pleurotus ostreatus*. *Annals of Agrarian Science*, *15*(2), pp.273-277.

Golea, D.M., Upton, A., Jarvis, P., Moore, G., Sutherland, S., Parsons, S.A. and Judd, S.J., 2017. THM and HAA formation from NOM in raw and treated surface waters. *Water Research*, *112*, pp. 226-235.

Haarhoff, J., Mamba, B., Krause, R.W.M., Van Staden, S., Nkambule, T., Dlamini, S. and Lobanga, K.P., 2013. Natural organic matter in drinking water sources: Its characterisation and treatability, *Water Research Commission* Report No. 1883/1/12.

Huy, N.D., Tien, N.T.T., Huyen, L.T., Quang, H.T., Tung, T.Q., Luong, N.N. and Park, S.M., 2017. Screening and production of manganese peroxidase from Fusarium sp. on residue materials. *Mycobiology*, *45*(1), pp.52-56.

Jiang, Y., Goodwill, J.E., Tobiason, J.E. and Reckhow, D.A., 2016. Impacts of ferrate oxidation on natural organic matter and disinfection by-product precursors. *Water Research*, *96*, pp.114-125.

Kosobucki, P. and Buszewski, B., 2014. Natural organic matter in ecosystems-A review. *Nova Biotechnologica et Chimica*, *13*(2), pp.109-129.

Levchuk, I., Màrquez, J.J.R. and Sillanpää, M., 2018. Removal of natural organic matter (NOM) from water by ion exchange–A review. *Chemosphere*, *192*, pp.90-104.

Marais, S.S., Ncube, E.J., Msagati, T.A.M., Mamba, B.B. and Nkambule, T.T.I., 2019. Assessment of trihalomethane (THM) precursors using specific ultraviolet absorbance (SUVA) and molecular size distribution (MSD). *Journal of Water Process Engineering*, *27*, pp.143-151.

Marais, S.S., Ncube, E.J., Msagati, T.A.M., Mamba, B.B. and Nkambule, T.T., 2018. Comparison of natural organic matter removal by ultrafiltration, granular activated carbon filtration and full-scale conventional water treatment. *Journal of Environmental Chemical Engineering*, *6*(5), pp.6282-6289.

Matilainen, A. and Sillanpää, M., 2010. Removal of natural organic matter from drinking water by advanced oxidation processes. *Chemosphere*, *80*(4), pp.351-365.

Matilainen, A., Vepsäläinen, M. and Sillanpää, M., 2010. Natural organic matter removal by coagulation during drinking water treatment: a review. *Advances in Colloid and Interface Science*, *159*(2), pp.189-197.

Motsa, M.M., Mamba, B.B. and Verliefde, A.R., 2018. Forward osmosis membrane performance during simulated wastewater reclamation: Fouling mechanisms and fouling layer properties. *Journal of Water Process Engineering*, *23*, pp.109-118.

Moyo, W., Chaukura, N., Msagati, T.A., Mamba, B.B., Heijman, S.G. and Nkambule, T.T., 2019. The properties and removal efficacies of natural organic matter fractions by South African drinking water treatment plants. *Journal of Environmental Chemical Engineering*, *7*(3), p.103101.

Ncibi, M.C. & Matilainen, A.,2018. Removal of natural organic matter in drinking water treatment by coagulation : *Chemosphere. A comprehensive review*. 190:54–71.

Ndlangamandla, N.G., Kuvarega, A.T., Msagati, T.A., Mamba, B.B. and Nkambule, T.T., 2018. A novel photodegradation approach for the efficient removal of natural organic matter (NOM) from water. *Physics and Chemistry of the Earth, Parts A/B/C*, *106*, pp.97-106.

Ng, M., Kho, E.T., Liu, S., Lim, M. and Amal, R., 2014. Highly adsorptive and regenerative magnetic TiO2 for natural organic matter (NOM) removal in water. *Chemical Engineering Journal*, *246*, pp.196-203.

Nguyen, L.N., van de Merwe, J.P., Hai, F.I., Leusch, F.D., Kang, J., Price, W.E., Roddick, F., Magram, S.F. and Nghiem, L.D., 2016. Laccase–syringaldehyde-mediated degradation of trace organic contaminants in an enzymatic membrane reactor: Removal efficiency and effluent toxicity. *Bioresource technology*, *200*, pp.477-484.

Nguyen, T.T., Ngo, H.H. and Guo, W., 2013. Pilot scale study on a new membrane bioreactor hybrid system in municipal wastewater treatment. *Bioresource Technology*, *141*, pp.8-12.

Nkambule, T.I., Krause, R.W.M., Haarhoff, J., & Mamba, B.B.,2012. Natural organic matter

( NOM ) in South African waters : NOM characterisation using combined assessment techniques. *Water SA Vol*. 38(5):697–706.

Pan, Y., Li, H., Zhang, X. and Li, A., 2016. Characterization of natural organic matter in drinking water: sample preparation and analytical approaches. *Trends in Environmental Analytical Chemistry*, *12*, pp.23-30.

Qin, J.J., Cao, Y.M. and Oo, M.H., 2006. Preparation of poly (ether sulfone) hollow fiber UF membrane for removal of NOM. *Journal of Applied Polymer Science*, *99*(1), pp.430-435.

Sillanpää, M., Ncibi, M.C., Matilainen, A. and Vepsäläinen, M., 2018. Removal of natural organic matter in drinking water treatment by coagulation: A comprehensive review. *Chemosphere*, *190*, pp.54-71.

Solarska, S., May, T., Roddick, F.A. and Lawrie, A.C., 2009. Isolation and screening of natural organic matter-degrading fungi. *Chemosphere*, *75*(6), pp.751-758.

Tshabalala, T.G., Nxumalo, E.N., Mamba, B.B. and Mhlanga, S.D., 2016. Synthesis of robust flexible polyethersulfone ultrafiltration membranes supported on non-woven fabrics for separation of NOM from water. *Water SA*, *42*(4), pp.621-632.

Tshindane, P., Mamba, P.P., Moss, L., Swana, U.U., Moyo, W., Motsa, M.M., Chaukura, N., Mamba, B.B. and Nkambule, T.T., 2019. The occurrence of natural organic matter in South African water treatment plants. *Journal of Water Process Engineering*, *31*, p.100809.

Vasina, D.V., Moiseenko, K.V., Fedorova, T.V. and Tyazhelova, T.V., 2017. Lignin degrading peroxidases in white-rot fungus Trametes hirsuta 072. Absolute expression quantification of full multigene family. *PloS one*, *12*(3), p.e0173813.

Zahmatkesh, M., Spanjers, H. and van Lier, J.B., 2017. Fungal treatment of humic-rich industrial wastewater: application of white rot fungi in remediation of food-processing wastewater. *Environmental Technology*, *38*(21), pp.2752-2762.

Zahmatkesh, M., Spanjers, H., Toran, M.J., Blánquez, P. and Van Lier, J.B., 2016. Bioremoval of humic acid from water by white rot fungi: exploring the removal mechanisms. *AMB Express*, *6*(1), p.118.

# CHAPTER 2

# LITERATURE REVIEW

## 2.1 Introduction

In this chapter, applicable literature relating to the origin, fractions, impact on water treatment of natural organic matter (NOM) as well as available methods for its removal from water is reviewed. The white rot fungi (WRF) species and their corresponding lignolytic enzymes, including their role in the biodegradation of pollutants in water is also chronicled. The all-important application of membrane bioreactors in water and wastewater treatment is also discoursed in this chapter.

## 2.2 Natural Organic Matter (NOM)

All-natural waters contain NOM, a wide range of different organic compounds consisting mainly of organic carbon and hydrogen (Adusei-Gyamfi *et al*., 2019). NOM is found mostly in water bodies and soil, and it results from the degradation of vegetation and animal material (Adusei-Gyamfi *et al*., 2019). A representative complex structure of NOM is exhibited in **Figure 2.1**.

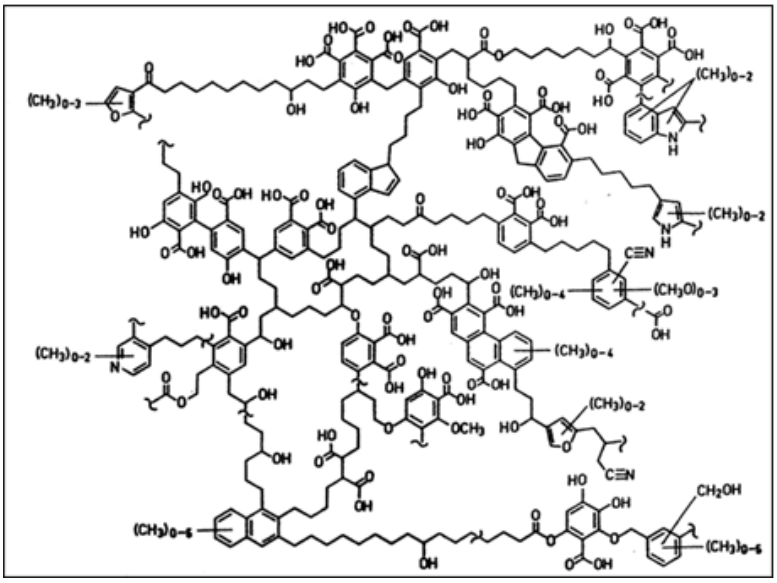

**Figure 2.1**: A representative chemical structure of NOM (adapted from Bhatnegar & Sillanpaa, 2017).

NOM is introduced into the ecosystem either naturally or anthropogenically (Derrien *et al*., 2019). It can be categorized based on its origin. NOM that occurs outside the water body is described as Allochthonous and is generally caused by leaching of vegetation and soil from the surface and transported into water sources through winds or surface washout (Artifon *et al*., 2019). Autochthonous NOM originates within the water body due to algal blooms, which imparts the aesthetical characteristics of the water and biological activities that occur in water sources (Koszelnik *et al*., 2018). Effluent NOM (EfOM) is another group of NOM derived from anthropogenic activities that can be introduced into water sources through wastewater discharge and degradation of organic litter (Derrien *et al*., 2019).

### 2.2.1 Composition of NOM

NOM is quantified through organic carbon measurements as total organic carbon (TOC) (Nkambule *et al*., 2012). It consists of particulate organic matter (POM), a fraction of organic matter that retains on the filter after filtration through 0.45 µm (Winogradow *et al*., 2019), and dissolved organic carbon (DOC), the portion that

goes through the filter and is mostly used as a quantification parameter for NOM (Zhao *et al*., 2019). DOC can be divided into hydrophobic such as humic substances (HS), and hydrophilic fractions such as non-humic substances (Hu *et al*., 2016). HS are composts of high molecular weight compounds such as humic acids, fulvic acid and humin and are the most abundant DOC fraction that causes yellow-brownish colour of most surface water (Pan *et al*., 2016). The hydrophilic component of DOC consists of low molecular weight compounds comprising of aliphatic carbon and nitrogenous compounds (Matilainen *et al*., 2011). A fraction of DOC that consist of the combination of hydrophobic and hydrophilic is described as transphilic (Bhatnagar, 2017; Matsebula & Haarhoff, 2009).

### 2.2.2 Organic matter components and their role in the environment

#### 2.2.2.1 Humic substances (HS)

Humic substances (e.g. humic acids, fulvic acids and humin) are some of the most persistent organic matter fraction in the soil. This type of NOM constitutes the major fraction of NOM in drinking water sources. Moreover, they can be classified according to their solubility, physical appearance and molecular size (Adusei-Gyamfi *et al*., 2019; Levchuk *et al*., 2018).

Humic acids (HA), which originates from the microbial degradation of plants, are the most abundant HS in ground and surface water. As shown in **Figure 2.2**, HA are made up of both aliphatic and aromatic alcohols and carboxylic acids (Basumallick & Santra, 2017). HA are dark brown in colour and soluble at pH > 2 (Mamba *et al*., 2009). This HS fraction is relatively large and their molecular weight ranges between 2 000 to 50 000 Da, which makes them easy to be extracted either from soil or water (Boguta *et al*., 2019). Despite the presence of HA in drinking water being undesirable, they are essential in agriculture by improving the chemical and physical qualities of the soil as well as protecting the soil from contamination with heavy metals. Furthermore, the presence of HA in soil improves the uptake of nutrients and the amount of humus (Liu *et al*., 2019; Zhou *et al*., 2019).

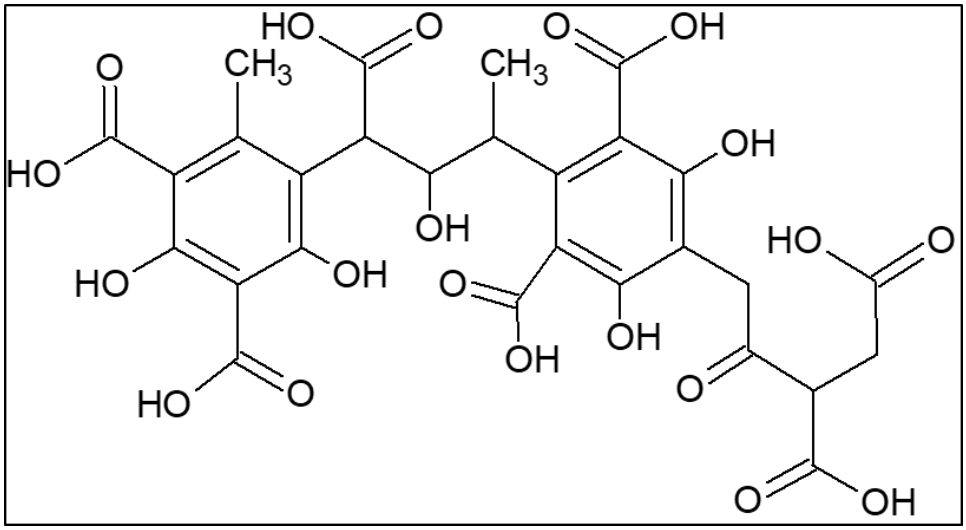


**Figure 2.2**: Proposed chemical structure of humic acid (Sîrbu et al., 2010).

Fulvic acids (FA) are found in any kind of soil. As shown in the model chemical structure depicted in **Figure 2.3**, FA consist of a combination of weak chains bearing both aliphatic and aromatic alcohols and organic acids. Relative to other HS fractions, FA contain less hydrogen and carbon (Klučáková, 2018). The molecular weight of FA ranges from 100 to 10 000 Da, which is much smaller than that of HA (Qin *et al*., 2019). For this reason, FA are described as low molecular weight HS (Qin *et al*., 2019). The smaller size of FA makes them easy to be absorbed by roots of many plants. FA are soluble at any pH levels and appear yellow brown in colour (Nkambule *et al*., 2012). The presence of FA in soil is beneficial since it stimulates the growth of roots and increase both uptake of water and nutrients. Moreover, FA prevent the growth of harmful microorganisms in crops (Zhao *et al*., 2019).

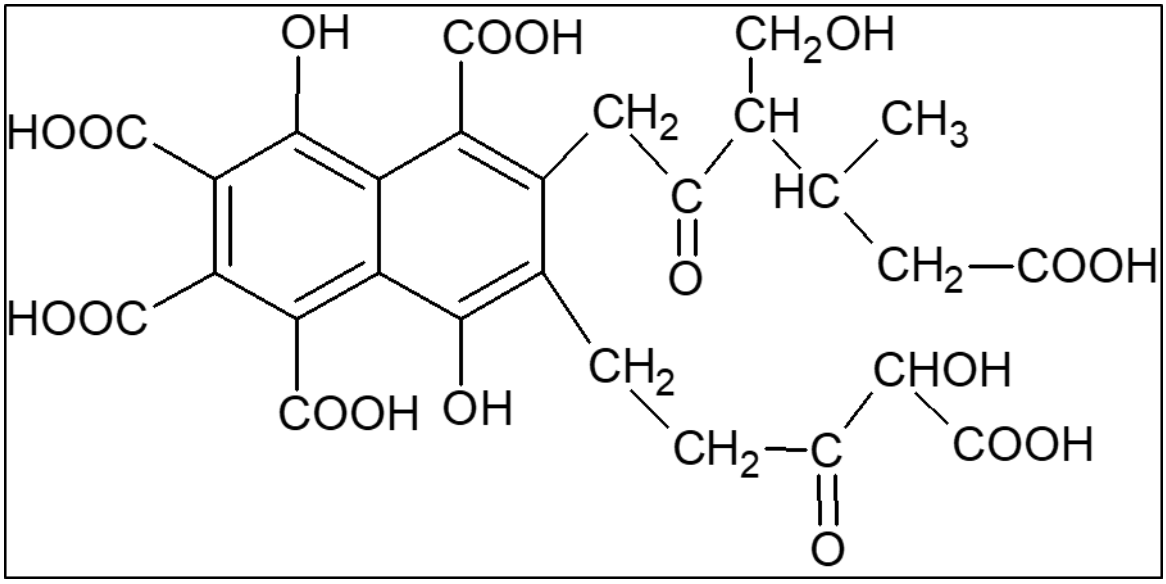


**Figure 2.3**: Molecular structure of fulvic acid (Rupiasih & Vidyasagar, 2005; permission granted by Research Gate).

Humin is a black coloured component of HS, which is soluble at low pH (Zandvoort *et al*., 2015). It is made up of aliphatic hydrocarbons such as lipids, cuticular materials and small components of peptides and carbohydrates (Hayes *et al*., 2017). The chemical properties of humin is like that of HA; humin is however more resistant to decomposition. As shown on **Figure 2.4**, humin consists of interlinked furanic rings, which in some instances are linked by short aliphatic linkers. Humin plays a major role in enhancing soil structure and richness (Goveia *et al*., 2013).

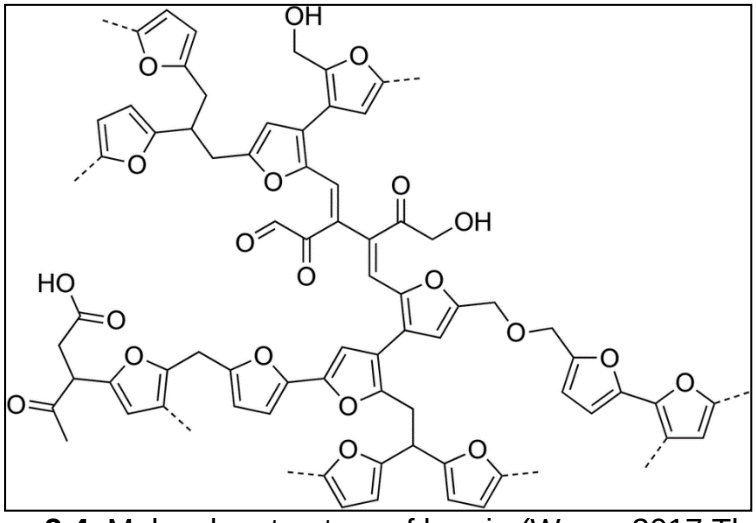


**Figure 2.4**: Molecular structure of humin (Wang, 2017 Thesis).

#### 2.2.1.2 Non-humic substances

Non-humic substances form part of the hydrophilic fraction of NOM. They are derived from easily decayed polysaccharides, carbohydrates and proteins. In terms of the chemical structure, non-humic substances are consisted mainly of aliphatic carbons and hydroxyl groups (Yamamura *et al*., 2014; Ghernaout, 2014). Soil organisms utilizes non-humic substances as their source of nutrients (Bot & Benites, 2005). The most found non-humic substances in soil are carbohydrates in the form of mainly glucose and sugars, which mostly comprises about 5-25 % of the soil organic matter (Ratnayake *et al*., 2013). Most researchers commonly use glucose as a model compound for non-humic substances in laboratories (Gerke, 2018).

## 2.3 Impacts of NOM in water treatment

Drinking water disinfection has been practiced over decades to protect public health from illnesses caused by microorganisms found in water. Chlorine is used by most water utilities as a disinfectant because of its reliability and cost effectiveness (Sun *et al*., 2019; Villanueva & Cordier, 2015; Beniwal *et al*., 2018: Wang *et al*., 2015). However, chlorine react with NOM to form carcinogenic disinfection by-products (DBPs) (Stefán *et al*., 2019; Ding *et al*., 2019). In the form of biodegradable organic carbon (BDOC), NOM serves as a substrate for microbial re-growth and biofilm formation in water supply pipelines, which result in health problems associated with gastrointestinal diseases (Thayanukul *et al*., 2013; Lin *et al*., 2016; Liu *et al*., 2019). In addition, the re-growth of bacteria in distribution networks causes organoleptic problems that gives water bad taste and odour thus making it unpleasant to consumers (Li *et al*., 2018; Zhang *et al*., 2019). Geosmin and 2-methylisoborneol (MIB) are regarded as principal organoleptic compounds (Doederer *et al*., 2019). Colour in water is an indication of poor quality and it makes it unacceptable to consumers. The appearance of yellow-brownish colour of water is an indication of the presence of humic substances; however, even though water may appear clear, it may still contain organic substances (Ibrahim & Aziz, 2014; Perkins *et al*., 2019).

The South African National standards (SANS 241: 2015) specifies acceptable limits of < 15 Pt-Co for colour in drinking water.

High levels of NOM in raw water requires increased amounts or dosages of the coagulant, which in turn leads to increased treatment costs (Rathnayake *et al*., 2017; Krzeminski *et al*., 2019; Ferna *et al.*, 2013). Moreover, NOM leads to poor flocs formed during the coagulation-flocculation stage thus resulting in poor settling during the sedimentation process (Ibrahim & Aziz, 2014). Poorly formed flocs tend to block the filters and this result in shorter filter run and more frequent backwashing (Chaulk & Sheppard, 2011). This basically means that more treated water will be required to clean the filters which also increases treatment cost. Furthermore, in membrane technology, NOM is known to be the major membrane foulant due to deposition either on the membrane surface or within the membrane matrix (Baghbanzadeh *et al*., 2016; Vatanpour *et al*., 2011; Moslehyani *et al*., 2019). For these reasons, there is a need for the reduction or complete removal of NOM from water.

## 2.4 Current processes used for NOM removal

Due to the enduring problems in relation to the presence of NOM in drinking water, it is therefore vital to remove or reduce NOM and its components from water during or prior to treatment. Although several methods have been used for NOM removal from water, a number of these processes are costly and not environmentally friendly.

### 2.4.1 Enhanced Coagulation-flocculation

Surface water is the foremost water source for drinking water. Most surface waters consist of negatively charged colloidal particles of NOM molecular architecture. These particles can be destabilized by positively charged chemical coagulants such as polymers, aluminium salts and many other chemicals in a rapid mix form during the coagulation stage (Zhang *et al*., 2015; The *et al*., 2016; Su *et al*., 2017). Thereafter, small flocs aggregate during flocculation to form bigger flocs that can settle during the sedimentation stage (Chekli *et al*., 2019). Generally, conventional coagulation does not completely remove NOM from water. Therefore, enhanced coagulation has been implemented by optimising the dosage of the coagulants and

pH adjustment to improve NOM removal efficiency (Dlamini *et al*., 2013; Lobanga *et al*., 2014). However, the removal efficacy depends on the character, nature and geographical area of NOM (Tshindane *et al*., 2019; Özdemir, 2016).

Moreover, increasing coagulant dosage is accompanied by setbacks relating to increased treatment costs and the production of large quantities of sludge (Krzeminski *et al*., 2019). The working conditions (e.g. pH and coagulant dosage) should be considered when improving coagulation (Sillanpää *et al*., 2018; Hussain *et al*., 2019). In a study conducted by Awad *et al*. (2016), dissolved organic matter from sandy soil measured as dissolved organic carbon (DOC) was found to be lower (21.1 mg/L) than found in clay soil (38.6 mg/L) when a jar testing system with alum dosage of 8.0 mg/L was used. An increase in the dosage of alum to 10 mg/L decreased the DOC concentration by 0.15 mg/L. A comparative analysis of the performance of titanium chloride and salts of aluminium and iron in the removal of NOM by coagulation process was also undertaken by Wan *et al*. (2019). Results generated from the optimization of the coagulant dosage and pH by Wan *et al*. (2019) were in agreement with those of Awad *et al*. (2016). These results confirmed that the removal of NOM is dependent on the type of coagulant used, the nature of NOM and seasonal changes.

### 2.4.2 Adsorption processes

Research on innovative and reliable treatment methods for purposes of improving water quality and compliance with stringent water quality standards is continuously being conducted. Adsorption processes such as activated carbon and ion exchange have been used as polishing processes to optimize the conventional water treatments for the removal of NOM (Shimizu *et al*., 2018; Lee *et al*., 2018). Adsorption processes have specific advantages such as easy to design and operate processes; however, the cost of treatment is high due to expensive and environmentally unfriendly adsorbents such as powdered activated carbon (PAC), granular activated carbon (GAC) and ion exchange resins (Kaleta *et al*., 2017; Bertone *et al*., 2018).

As already mentioned, taste and odour problems in water treatment are caused by NOM compounds. Activated carbon is used for the removal of taste and odour

causing compounds such as geosmin and 2-methylisoborneol (MIB) from water (Menya *et al*., 2018; Kaleta *et al*., 2017). It can be added in powder (PAC) or granular (GAC) form (Zhang *et al*., 2019; Park *et al*., 2019; Jamil *et al*., 2019). In a conventional water treatment, PAC is usually used as a pre-treatment step while GAC is used in the post-treatment stage because of its effectiveness in the removal of heavy metals and organic substances (Marais *et al*., 2018). Ion-exchange (IEX) is widely used as an alternate method for the removal of NOM, especially the low molecular weight fraction that cannot be removed by coagulation from water (Vaudevire *et al*., 2019; Winter *et al*., 2018). Ion-exchange involves the exchange of specific ionic species that are present in a solution with similarly charged species (Levchuk *et al*., 2018). In IEX, non-desirable charged compounds (either negatively or positively charged) considered to be impurities are removed from a solution by exchanging them with a similarly charged ions anchored in the resin (Arias-Paic *et al*., 2016; Finkbeiner *et al*., 2019). Since NOM is mainly negatively charged, an anionic exchange resin is used for its removal in a typical conventional water treatment plant (Finkbeiner *et al*., 2018; Amini *et al*., 2018; Chen *et al*., 2018).

### 2.4.3 Advanced oxidation processes

In respects of the persisting related problems that NOM pose during water treatment, advanced oxidation processes (AOPs) has attracted many researchers to study AOPs as an additional method for NOM removal. This involves the use of oxidants such as ozone ($O_3$), hydrogen peroxide ($H_2O_2$) and ultraviolet (UV) light and many others (Sillanpää *et al*., 2018). Given the complex structure of NOM fractions, highly effective hydroxyl radicals are formed in high quantities from AOPs, especially when a combination of the oxidants are used (Ike *et al*., 2019). The produced hydroxyl radicals degrade NOM compounds into simpler products such as easily biodegradable carboxylic acids (Miklos *et al*., 2018; Ahn *et al*., 2017). However, a huge concern was expressed on the operational costs of AOPs and the generation of oxidation by-products, which poses adverse health impacts when AOPs are used for the removal of NOM (Cai & Lin, 2016; Ike *et al*., 2019). Complete oxidation of NOM by AOPs has apparently not yet been achieved and research on new and cost-effective technologies is still continuing (Ike *et al*., 2019).

Chlorine is one of the most used disinfectant for the deactivation of pathogens in water, due to its cost effectiveness and prolonged disinfection in distribution networks arising from residual chlorine. Nonetheless, the production of disinfection by-products caused by the reaction of NOM with chlorine is a concern (Nakada *et al*., 2019). For this reason, the removal of NOM prior to chlorination is critical. Ozone, a strong oxidizing agent is used in the pre-treatment step in conventional water treatment plants to improve NOM removal in the coagulation stage (Bu *et al*., 2019). Nevertheless, the production of hydroxyl radicals by ozone has been reported to be very low, and many researchers opt for some type of a combination process involving the use of ozone and other oxidants (Lamsal *et al*., 2011; Lue *et al*., 2018; Wang *et al*., 2019). However, the cost that is associated with a combined oxidation process is relatively high.

### 2.4.4 Membrane Technology

A membrane is a thin film of semi-permeable material that allows specific substances to pass through under pressure while rejecting others (Giwa *et al*., 2019; Zahid *et al*., 2018). Membranes are made of polymeric or ceramic materials (Alenazi *et al*., 2017; Vera *et al.*, 2017). Membranes are increasingly used for the removal of micro-organisms, particulate organic matter, organic substances and many other pollutants (Madhura *et al*., 2018; Nqombolo *et al*., 2018). Membrane processes (e.g. reverse osmosis, nanofiltration, ultrafiltration and microfiltration) provide an alternative method for the removal of organic and inorganic contaminants from water and wastewater (Motsa *et al.*, 2018; Sakarinen, 2016). In the past, membrane technology was used as a refining step to remove pathogens from water. However, increasing concerns regarding the presence of NOM in raw water has led to this technology being considered as a treatment option for NOM removal from drinking water (Chang *et al*., 2019; Shao *et al*., 2019). Nevertheless, NOM is a major foulant that causes a massive permeate flux reduction during membrane filtration processes, especially for denser membranes such as ultrafiltration and nanofiltration (Yu *et al*., 2018). NOM and other low molecular weight compounds tend to accumulate either on the membrane surface to form a cake layer or inside the membrane pores resulting in clogging of the membrane (Deng *et al*., 2019) (see **Figure 2.5**).

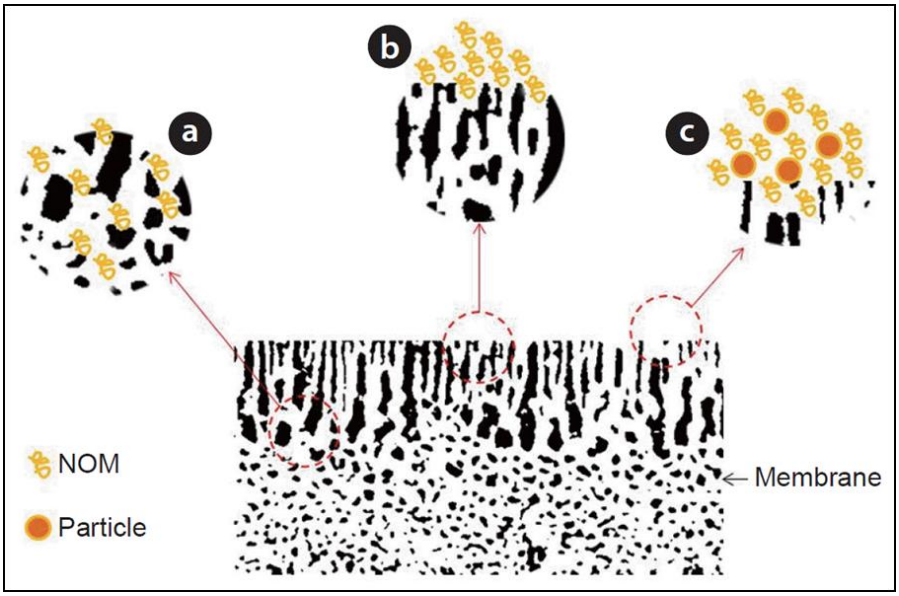


**Figure 2.5**: A schematic illustration of membrane fouling mechanism caused by NOM (Cui & Choo, 2014): (a) NOM particles inside the membrane pores; (b) Accumulating of NOM particles on the surface of the membrane; and (c) NOM bridging other particles on the membrane surface.

Any fouling or clogging of the membrane would require frequent cleaning either chemically or through backwashing. The cleaning results in increased operational costs and shortening of the lifespan of the membranes (Yu *et al*., 2019). The hydrophilic fraction of NOM is reported to be a major membrane foulant due to its low molecular weight, as it easily accumulates on the membrane pores (Yamamura *et al*., 2014; Alresheedi *et al*., 2019). Therefore, pre-treatment of NOM containing water is necessary prior to membrane filtration to mitigate fouling (Jepsen *et al*., 2018). Such a pre-treatment step may include the addition of chlorine or activated carbon to reduce NOM fractions in raw water (Xing *et al*., 2019; Yu *et al*., 2019).
Ceramic membranes are types of membranes which are gaining interest in the water industry for NOM removal. Although ceramic membranes have been successfully used for NOM removal, the high costs generation from ceramic components (Urbanowska & Kabsch-Korbutowicz, 2014) and the ease with which they break limit their full-scale application (Iorhemen *et al.*, 2016; Lee & Kim, 2014). Therefore, a need exists for membrane surface modification strategies targeted towards the

improvement of anti-fouling properties of these membranes while retaining good separation capacity.

Graphene oxide (GO) modified membranes have attracted attention as an alternative method for NOM removal. You *et al*. (2018) have obtained a 100 % NOM rejection while maintaining a high-water flux in GO-membrane based laboratory scale set-up. Although no fouling of the membranes was found to occur in the short-term, further studies to determine the long-term fouling of the membranes still needs to be carried out. Moreover, the high cost of GO materials, which are known to increase the overall water treatment cost have led to GO-modified membranes not being commercially available (Zhao *et al*., 2019). Such limitations suggest the research and development of advanced techniques for the removal of NOM still need to be undertaken. To this end, attempts at the development of membranes modified with multi-walled carbon nanotubes have successfully led to 79 % NOM removal from water (Hudaib *et al*., 2018). Membrane modification using microorganisms to improve the removal of pollutants from water has drawn attention by many researchers in the water industry.

The incorporation of biocatalytic molecules such as fungal enzymes on the membrane surface to fabricate biocatalytic membranes for high and improved pollutants removal efficiency is increasingly gaining the interest of researchers (Vitola *et al*., 2016). Biocatalytic membranes offer high permeate flux, high removal of pollutants and can tolerate wide ranges of pH and temperature conditions. Enzymes incorporated on or into the membrane matrix are apparently more stable than free enzymes (Li *et al*., 2018). Most importantly, biocatalytic membranes provide high chances of reusability (Ren *et al*., 2018). The production of lignolytic enzymes such as laccase, manganese peroxidase, lignin peroxidase and many others by white rot fungi (WRF) species offers a potential solution for the removal of NOM. WRF has been reported efficient in the degradation of organic substances in water and wastewater (Solarska *et al*., 2009; Zahmatkesh *et al*., 2016; Zahmatkesh *et al*., 2017). WRF are the most promising biological agent that can be used for improving the quality of water laden with NOM.

## 2.5 White rot fungi (WRF)

WRF are organisms that occur naturally and belong to the Basidiomycetes group of fungi that completely degrade wood components such as lignin through their secondary metabolism (Asif *et al*., 2017). As a result, WRF offers a potential environmentally friendly and cost-effective solution for NOM biodegradation and removal (Zhang *et al*., 2017). Lignin is a complex polymer that gives plants their structural support. Lignin has different structural components consisting of a mixture of aromatic alcohols, monolignols and hydroxycinnamyl alcohols (**Figure 2.6**) obtained mostly from wood (Detta *et al*., 2017).

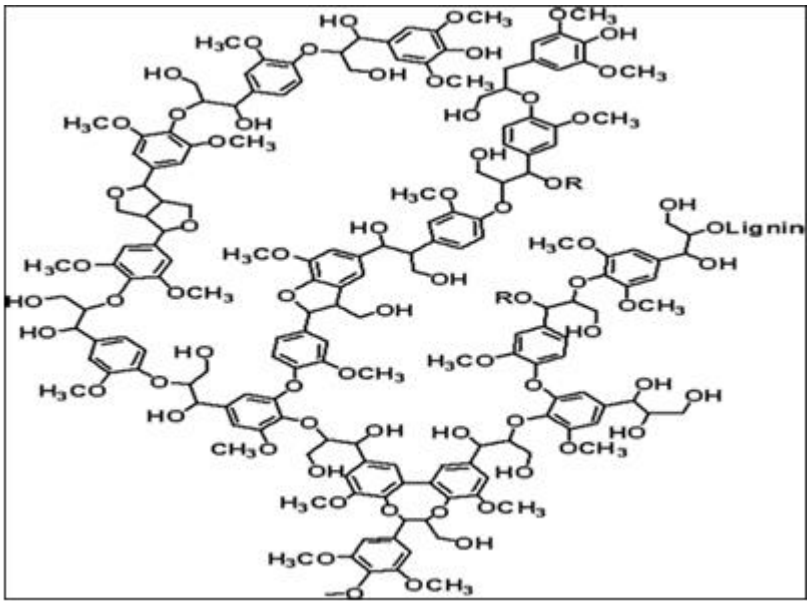


**Figure 2.6**: Structure of lignin (Pollegioni *et al*., 2015).

Lignin structure is similar to that of organic matter. Moreover, lignin serves as a second source of NOM found in terrestrial ecosystems as it contributes about 20 % of soil organic matter (Khatami *et al*., 2019). As shown on **Figure 2.7**, the change of wood from brownish to white colour is ascribed to the degradation of lignin by WRF such as *Phanerochaete Chrysosporium*, a WRF that grows by forming flat attached reproductive fruiting bodies instead of a mushroom structure (Hervé *et al*., 2016; Rekik *et al*., 2019). WRF occur mostly in *Eucalyptus* trees under moist conditions and can withstand a variety of temperature and pH conditions (Negrão *et al*., 2014).

**Figure 2.7**: A picture of WRF *Phanerochaete chrysosporium* growing on rotting wood.

### 2.5.1 White rot fungi species and conditions for enzymes production

WRF species are widely used for the biodegradation of a wide array of pollutants in water and concentrated wastes. These species are preferred over other organisms such as bacteria since they can withstand high levels of contaminants during degradation (Rodríguez-Couto, 2017; Mir-Tutusaua *et al*., 2018). In addition, they are not dependent on climatic condition and do not require preconditioning to a pollutant (Rodríguez-Couto, 2017; Mir-Tutusaua *et al*., 2018). WRF species tolerate broad range of ecological conditions and use available lignocellulosic materials as nutrient source (Rodríguez-Couto, 2017; Mir-Tutusaua *et al*., 2018). Moreover, during their secondary metabolism, they can produce lignolytic enzymes, mainly lignin peroxidase (LiP), manganese-dependent peroxidase (MnP) and laccase (Hu *et al*., 2017). Lignolytic enzymes are oxidative enzymes produced by fungi and bacteria, and they catalyse the breakdown of lignin (Bugg *et al*., 2011). These enzymes can breakdown a wide range of contaminants to carbon dioxide and water (Grinhut *et al*., 2011). The production of the enzymes by WRF depends on the growth conditions provided such as temperature, pH, humidity and the availability of nutrients such as carbon and nitrogen (Collado *et al*., 2019). **Table 2.1** indicates the production conditions of lignolytic enzymes by WRF species. Amongst WRF species, *Phanerochaete chrysosporium, Trametes versicolor, Pleurotus eryngil,*

*Phlebia suserialis, Phanerochaete sordida and Bjerkandera adusta* are mostly studied for bioremediation of organic pollutants (Senthilkumar *et al*., 2014; Voběrková *et al*., 2018; Lee, 2005; Solarska *et al*., 2009).

**Table 2.1**: WRF species, growth conditions and enzyme produced

| WRF species | Temperature (℃) | pH | Carbon source | Enzyme produced | Enzyme activity | Incubation period (days) | Reference |
|---|---|---|---|---|---|---|---|
| *Pleurotus ostreatus* | 26 | 5.0 | Potato peel waste | Laccase | 6708.3 ± 75 U/L | 17 | Ergun & Urek (2017) |
| | | | | MnP | 2503.6 ± 50 U/L | | |
| | | | | LiP | 231.2 ± 9 U/L | | |
| *Lentinula boryana* | 20 | 5.3 | Corn cob meal | MnP | 20 U/L | 25 | Hermann *et al*. (2013) |
| *Bjerkandera adusta* | 30 | 5.6 | Potato dextrose broth | MnP | 0.31 U/mg | 5 | Bouacen *et al*. (2018) |
| | | | | LiP | 0.19 U/mg | | |
| *Pleurotus pulmonarius* | 30 | - | Corn cob | Laccase | 270 U/L | 20 | Tychanowicz *et al*. (2008) |
| *Pleurotus eryngii* (DC) *gillet* (MCC58) | 29 | 6.0 | Grape waste | Laccase | 2247 ± 75 U/L | 10 | Akpinar & Urek (2012) |
| | | | | MnP | 2198.44 ± 65 U/L | 15 | |
| *Phanerochaete chrysosporium* (ATTC 20696) | 30 | 4.5 | Dextrose | MnP | 88.5 U/L | 8 | Wang *et al*. (2008) |
| | | | | LiP | 541.0 U/L | | |
| *Ganoderma Leucidum* | 35 | 4.5 | Corn cob | LiP | 2807 U/mL | 4 | Mehboob *et al*. (2011) |
| *Pleurotus sajor-caju* | 26 | - | Rice husk | Laccase | 45 U/L | 3 | Ang, 2013 |
| *Trametes versicolor* | 30 | 4.5 | Wet apple residues | Laccase | 4.12 ± 0.36 U/g | 3 | Landolo *et al*. (2011) |
| | | | | MnP | 0.89 ± 0.06 U/g | 5 | |

### 2.5.2 Application of WRF enzymes for the biodegradation of organic matter

The degradation of NOM in wastes using WRF was investigated by Lee, (2005) using two types of WRF species (*Phanerochaete chrysosporium*, *Trametes versicolor)* and yeast *Saccharomyces* in laboratory cultured strains. NOM degradation ranged from 37 %-73 %, which was attributed to the activity of enzyme laccase and manganese-dependent peroxidase produced by the two WRF species, was observed Lee, (2005). A very poor NOM degradation efficiency of 12 % was observed from the yeast *Saccharomyces*, which agreed with findings by Solarska *et al*. (2009), was achieved (Lee, 2005). Using experiment involving potable water contained in shake flasks culture without supplements, Solarska *et al*. (2009) have studied the potential of WRF species to degrade NOM in potable water. To this end, high NOM removal efficiency rates amounting to 65 %, which were ascribed to the activity of the *Bjerkandera adusta* species, were reported (Solarska *et al*., 2009).

Enzyme laccase produced by WRF species have been reported to be the most effective enzyme in the degradation of humic acid (HA) in liquid and solid media (Zahmatkesh *et al.*, 2016). The potential of laccase produced by different WRF strains was investigated to remove HA by monitoring the change in HA concentration and molecular size distribution (Zahmatkesh *et al.*, 2016). Degradation of HA was reported to be 80 %, due to the action of the laccase enzyme (Zahmatkesh *et al.*, 2016). The presence of other constituents in WRF growth media reduce the production of enzymes. The impact of heavy metals such as copper, manganese and cobalt on the growth and enzymes activity for the bioremediation and removal of organic contaminants was investigated by Asif *et al.* (2018). When present in high concentrations, these heavy metals hinder the growth of WRF thus impacting its potential to produce lignolytic enzymes, which are able to degrade organic compounds found in water and wastes.

It is clear from the studies mentioned above that there is great potential in using the appropriate WRF species for the degradation and removal of organic compounds such as NOM.

### 2.5.3 Mechanism of lignin-degrading enzymes

Lignolytic enzymes are profoundly oxidative in nature and degrade lignin by the one-electron oxidation reaction due to the production of free radicals, which experience further natural reactions (Karigar & Rao, 2011; Ijoma, 2016). The availability of limiting nutrients such as carbon and nitrogen source enhances the production of lignolytic enzymes by WRF (Ma *et al*., 2018). Lignin decomposition permit the fungal species to use cellulose and hemicellulose as their carbon and energy sources (Wen & Li, 2009). Lignin degradation results in the formation of water-soluble compounds which are then mineralized to form carbon dioxide (Singh & Chen, 2008).

#### 2.5.3.1 Lignin peroxidase (LiP)

Lignin peroxidase (EC 1.11.1.14) is a heme containing peroxidase enzyme that utilizes hydrogen peroxide ($H_2O_2$) to oxidize non-phenolic aromatic compounds such as veratryl alcohol (VA) to produce cation radicals (Bilal & Iqbal, 2019). Since this type of enzyme is more powerful than other peroxidases, it oxidizes not only phenols but a wide range of non-phenolic and aromatic compounds such as methoxylated benzenes and benzyl alcohols, which have similar structures as lignin (Falade *et al*., 2017). The activity of LiP is usually assayed by the addition of $H_2O_2$ which oxidizes veratryl alcohol (3,4-dimethoxybenzyl alcohol) to veratraldehyde (Rubilar *et al*., 2008). The ultraviolet (UV) absorbance of LiP is usually determined at 310 nm.

As indicated by **Figure 2.8**, the oxidation mechanism of LiP occurs in a cyclic process whereby the transfer of electrons comprises the use of $H_2O_2$ to oxide Fe (III) enzyme to LiP compound (Mester & Tien, 2000). The oxidation process begins with the production of two-electrons in compound I, which then results in the reduction of one-electron of VA. Thereafter, compound I eliminates one electron from VA, which serves as the donating substrate, thus causing the production of reduced compound II and intermediate cation radical. Compound II is then oxidized by the second molecule of VA through one electron transfer resulting in the production of another cation radical intermediate and the resting state of LiP. The produced cation radical naturally breaks into smaller components. With excess $H_2O_2$ and VA, compound II can then be oxidized to compound III, which can be oxidized

further into the natural state of LiP (Alneyadi *et al*., 2018). Furthermore, compound III can be inactivated if there is any excess $H_2O_2$. However, any presence of VA inhibits the inactivation process by giving out VA+ intermediate, which results in the reduction of compound III to its natural state (Alneyadi *et al*., 2018).

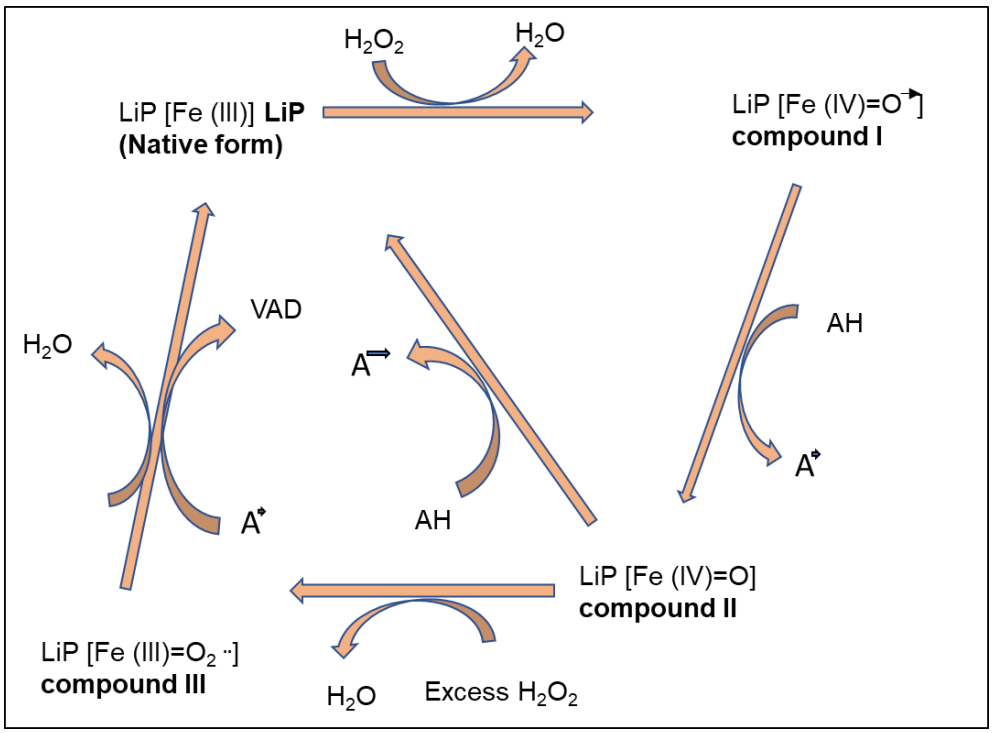


**Figure 2.8**: Represent the oxidation mechanism of lignin peroxidase (LiP) whereby AH represent an electron-donor substrate, A+ represents a cation radical and VA+ represents VA radical cation (Wan & Li, 2013).

### 2.5.3.2 Manganese-dependent peroxidase (MnP)

Manganese-dependent peroxidase (EC 1.11.1.13) is also a heme-containing peroxidase, and the oxidation process involving this enzyme is similar to that of LiP, with the presence of $Mn^{2+}$ being a crucial substrate (Bansal & Kanwar, 2013; Li *et al*., 2019). MnP utilizes $H_2O_2$ as an oxidant to oxidize $Mn^{2+}$ to $Mn^{3+}$, which then oxidize many phenolic compounds to phenoxyl radicals (Wang *et al*., 2018). The UV absorbance of MnP in a reaction mixture using $H_2O_2$ as an oxidant is recorded at a wavelength of 350 nm (Duan *et al*., 2018).

The oxidation cycle of MnP involves the binding of $H_2O_2$ to the natural state of ferric enzyme and the production of iron peroxidase compound as illustrated in **Figure 2.9** (Xu *et al*., 2017). In this cycle-step, two electrons are transported from heme to bind with oxygen-oxygen bond in the peroxide to produce MnP compound I (Nousiainen *et al*., 2012). Mn compound II is then formed when MnP compound I is reduced together with $Mn^{3+}$ from $Mn^{2+}$ thus resulting in the reproduction of natural enzyme when water molecules are released (Wang *et al*., 2018). Inactivation of MnP can be reserved together with the production of compound III when the concentrations of $H_2O_2$ is high. $Mn^{3+}$ is then released from the surface of the enzyme into the nearby environment (Nousiainen *et al*., 2012). The released $Mn^{3+}$ then oxidizes lignin and many other compounds; the $Mn^{3+}$ serves as a low molecular mediator for phenolic compounds degradation (Datta *et al*., 2017; Kuhar *et al*., 2016).

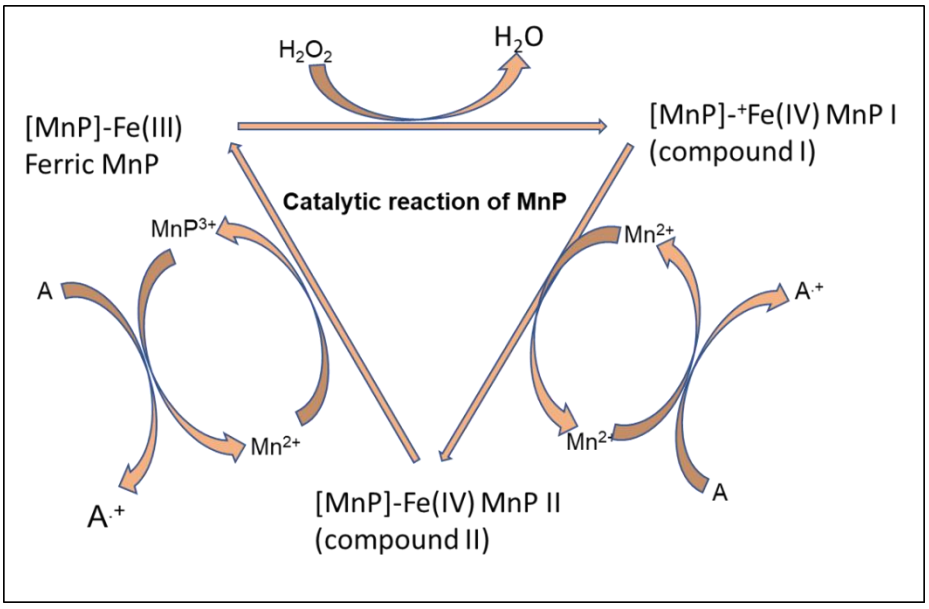


**Figure 2.9**: Oxidation cycle of MnP (Datta *et al.*, 2017).

The incubation conditions of WRF to produce MnP enzymes differ from species to species. MnP enzymes produced by *Trametes pubescens* strain i8 isolated from camphor wood was investigated for its ability to decolourize dyes (Rekik *et al*., 2019). The enzyme was found to have a molecular mass of 55.2 kDa, at optimised incubation conditions of pH 5 and 40 ℃. The catalytic efficiency of MnP produced by *Trametes pubescens* strain i8 was compared with that of the MnP produced by other WRF. Results generated by Rekik *et al*. (2019) have shown that MnP

produced by *Trametes pubescens* strain i8 has higher catalytic efficacy than MnP produced by other WRF species. Kong *et al*. (2016) have reported a higher efficacy of MnP produced by *Echinodontium taxodii* 2538 at an optimised incubation of pH 3.5 and 55 ℃. This proves that the type of species producing the enzyme and their growth conditions differ.

#### 2.5.3.3 Laccase

Laccase (EC 1.10.3.2) is an enzyme consisting of blue copper atoms that can only catalyse the oxidation of phenolic compounds to phenoxyl radicals due to its low redox potential (Vivekanandam *et al*., 2014). Laccase is the most widely studied WRF enzyme for the biomineralization of phenolics and non-phenolic compounds due to its eco-friendly benefits (Yang *et al*., 2015; Vršanská *et al*., 2017; Ren *et al*., 2018; Unuofin *et al*., 2019).The production of Laccase differ from fungus to fungus especially those related with wood rot (Asadgol *et al*., 2014; Allard-Massicotte *et al*., 2017). The oxidation of complex substrates by laccase can be increased through the addition of mediators such as 1-hydroxybenzotriazole (HBT) and 2.2-azino-bis 3-ethylbenzothiadine-6-sufunic acid (ABTs) (Moilanen *et al*., 2014; Christopher & Ji, 2014; Perna *et al*., 2018).

Laccase contain four or more copper atoms that are responsible for the oxidation of phenolic substrates through the reduction of oxygen to water as the final product (Kumar *et al*., 2018; Monssef *et al*., 2016). Oxygen is used as an electron acceptor for the conversion of phenolic compounds to phenoxy radicals (Batal *et al*., 2015). The four copper sites can be categorized into three types namely; type 1 (T1), type 2 (T2) and type 3 (T3) (Jones & Solomon, 2015). Laccase is only able to oxidize phenolic compounds, which are much smaller and therefore able to access the active site at the centre of the enzyme (Bagewadi *et al*., 2017). The blue colour of the enzyme is due to T1 where the substrate oxidation occurs and can be characterized using UV absorbance of 610 nm (Agrawal *et al*., 2018). T2 is colourless and it does not have strong absorption elements. For this reason, T2 is closely positioned to T3 copper site forming a trinuclear centre-like shape where oxygen molecules are reduced to water molecules (Wang *et al*., 2015). T3 copper sites are usually in pairs (T3 and T3´), which are not easily detectable in the visible

regions of the spectrum. However, in some cases T3 can be detected at a wavelength of 33 nm (Agrawal *et al*., 2018).

Generally, the oxidation of substrates occurs at the T1 copper site and the oxygen reduction into water molecules take place at T2 and T3 copper sites (Wang *et al*., 2015). The cycle of laccase substrate oxidation is depicted in **Figure 2.10.** The substrate is oxidized such that Cu1 lose one electron to form free radicals, which can further perform oxidation. The lost electron from Cu1 is transferred via His-cys-His motif to Cu2/Cu3 sites where oxygen molecules are reduced to water molecules. One oxygen molecule to two water molecules is escorted by the oxidation of four molecules of substrate (Mate & Alcalde, 2017).

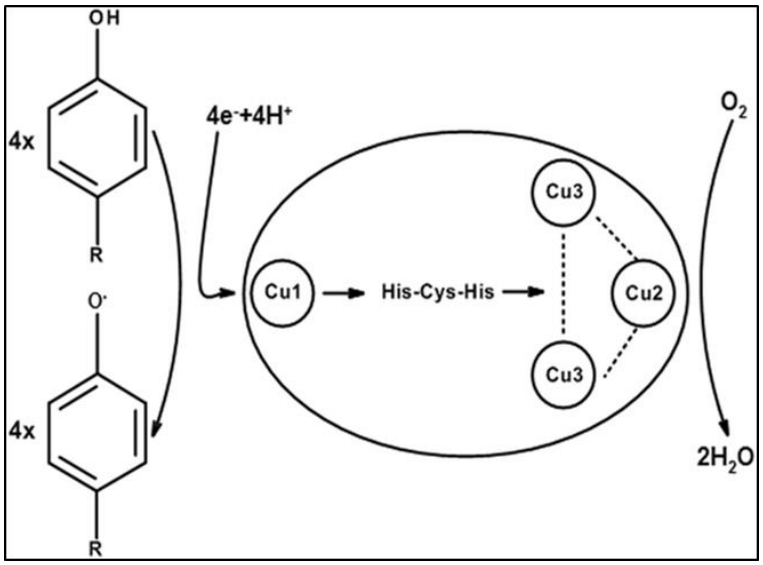


**Figure 2.10**: Reaction mechanism of enzyme laccase (Wang *et al*., 2015).

## 2.6 Immobilisation of lignin-degrading enzymes on membrane surface

It is vital to ensure the stability of enzymes that are used for degradation purposes. Free enzymes are not stable at high temperatures and pH conditions (Jochem *et al*., 2011). Therefore, immobilisation of enzymes onto a support offers the best way for ensuring enzyme stability and reusability. Immobilisation of the enzyme is achieved by introducing the enzymes on or inside a suitable support material (Deska & Konczak, 2019). However, proper use of support materials, techniques and

operational conditions is essential. As indicated by **Figure 2.11**, immobilisation can be divided into three main methods namely:

i. Binding of enzymes into a support or carrier. This type of immobilisation can occur physically through interactions of van der Waals forces, ionic or the binding of the support and enzymes covalently (Taheran *et al*., 2017). When enzymes are physically attached to a support, the interaction is weak. Therefore, escape of the enzymes can easily occur whereas ionic and covalent binding of the enzyme on the support material is much stronger because the enzymes are kept on the support under severe conditions (Sheldon & Pelt, 2013).

ii. Entrapment involves encapsulating the enzyme inside the matrices of a material or support such as inorganic or organic polymers (Sirisha *et al*., 2016). This type of immobilisation involves preparing the polymer with the enzymes.

iii. Cross-linking involves the use of bifunctional reagent to form cross-linking bonds between the enzymes. For instance, Li *et al*. (2015) cross-linked Ca-alginate particle with peroxidases produced from WRF species *Trametes versicolor*. However, high loading of enzymes should be avoided as it would results in the loss of enzyme activity (Sheldon & Pelt, 2013).

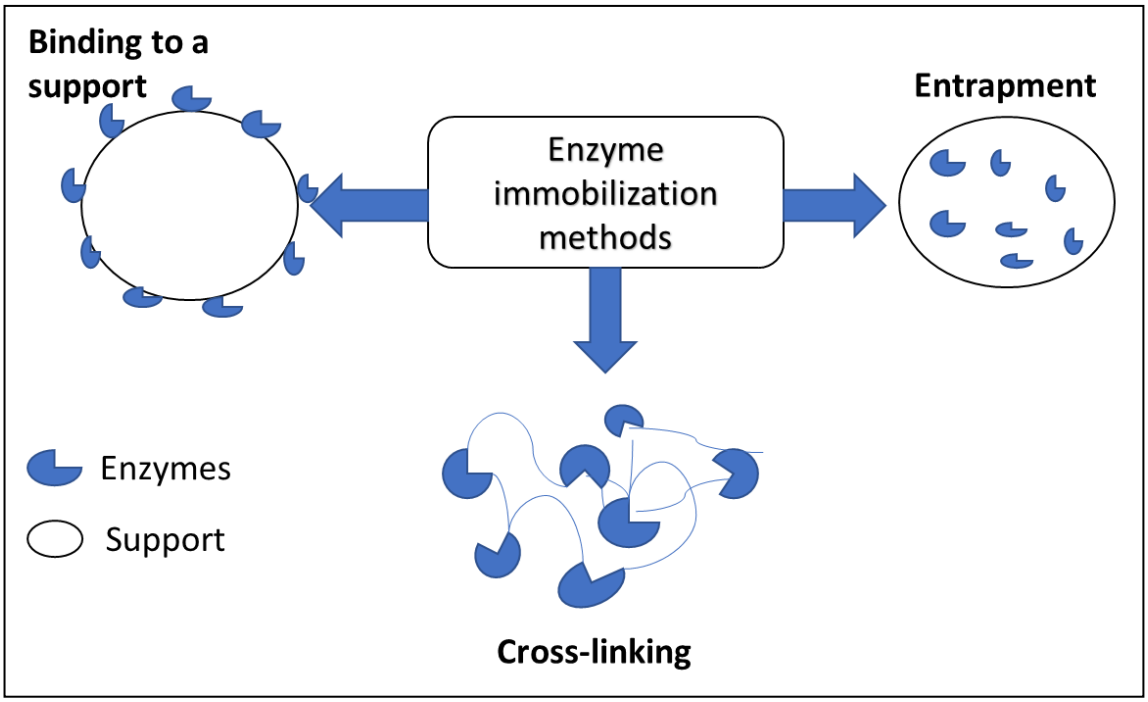


**Figure 2.11**: Methods of enzyme immobilisation on a support material adapted from Sheldon & Pelt, (2013).

The support material for enzyme immobilisation can be resins, biopolymers, inorganic or organic membranes (Jun *et al*., 2019). Bilal *et al*. (2018) reviewed different materials such as nanofibers, nanoparticles, polymeric membranes and many others for the immobilisation of peroxidase enzymes. Simón-Herrero *et al*. (2019) immobilised laccase enzyme on polyamide aerogels for the removal of pharmaceuticals compounds from wastewater. Most researchers prefer to use polymeric materials independently or incorporated with nanoparticles because they provide a variety of barrier structures and properties, the energy requirement is low and the operational scale-up can be easily changed (Zdarta *et al*., 2019; Qiu *et al*., 2019; Xu *et al*., 2018; Costa *et al*., 2019). It should however be noted that the resultant membranes should be strong enough to withstand high mechanical forces as well as high temperature conditions and pH. The active site of the membranes should be modified using certain functional groups to allow the binding of enzymes on the membrane surface (Sarma *et al*., 2018; Barrios-Estrada *et al*., 2017). Moreover, the functional groups introduced on the membrane surface should be controlled in such a way that the activity of the enzymes is maintained (Jochems *et al*., 2011). The immobilised enzyme on the membrane can be used in an enzymatic membrane reactor (EMR) whereby the feed is transferred across the membrane

whereas the enzymes are retained on the surface of the membrane with the product being produced.

## 2.7 Membrane bioreactors (MBR) in water treatment

Membrane bioreactors (MBR) are systems that combine membrane filtration processes such as microfiltration or ultrafiltration with a biological water or wastewater treatment (Xiao *et al*., 2019; Ma *et al*., 2018). MBR systems are applied according to two main configurations namely:

1) Submerged **(Figure 2.12)**, which involves placing the membrane modules inside the reactor. This type has several benefits such as being less costly due to low energy and low operational pressure, good permeability, less sensitive to variations in wastewater characteristics (chemically stable) and minimal flow instabilities. However, it suffers from some drawbacks such as low membrane flux, more membrane area requirement, difficult to extend and more frequent backwashing for membrane cleaning (Mutamim *et al*., 2012).

2) External **(Figure 2.12)**, whereby the membrane modules are located outside the reactor and feed recirculation occurs in the reactor. Advantages associated with this set-up includes high membrane flux, easy to extend, less area requirement and less frequent cleaning of the membranes. The disadvantages include high sensitivity to variations in wastewater characteristics, increased power consumption, high membrane pressure and more expensive (Aslam *et al*., 2017).

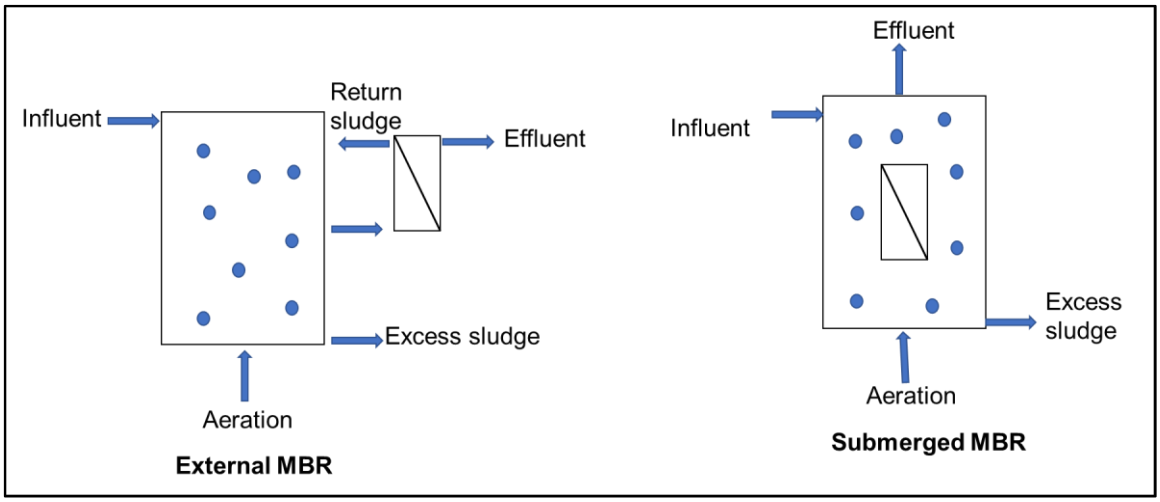


**Figure 2.12**: Typical MBR process configuration.

### 2.7.1 Applications of MBR

MBR have been widely used and have proven effective in removing pollutants from drinking water and wastewaters of (e.g. domestic, industrial and agricultural origin) (Tian *et al*., 2008; Bernal *et al*., 2017; Arriaga *et al*., 2016; Quist-Jensen *et al*., 2015).

Main industrial wastewater emanates from chemical, textile, tannery, food and paper industries (Fazal *et al*., 2015; Alighardashi *et al*., 2017). These activities lead to the generation of unsaturated fatty acids and chlorinated resin acids, which cause undesirable aesthetic problems such as colour (Erkan *et al*., 2017; Ashrafi *et al*., 2015; Johansson *et al*., 2012). Wastewater generated from textile industry contributes to pollution of water sources as large amounts of toxic and polluted wastewater containing inorganic and organic pollutants are generated from the use of dyes and finishing of agents (Badani *et al*., 2005; Lorena *et al*., 2011; Jegatheesan *et al*., 2016). MBR systems have been found effective in the treatment of textile wastewater (Niren & Jigisha, 2011). The food production industry utilizes large quantities of water for irrigation, livestock operation and food processing. Water reclamation methods from agricultural waste such as forward osmosis and membrane distillation was reviewed by Quist-Jensen *et al*. (2015).

Domestic wastewater is also reported to be rich in micro pollutants, which are released into surface water sources thus resulting in water pollution (Assayie *et al*., 2017; Arriage *et al*., 2016; Özkan *et al*., 2017). Therefore, the development of

alternative methods that can remove pollutants from domestic wastewater prior to discharge is required. Over the years, potential application of MBR, at pilot or large scale, for municipal wastewater treatment have increased tremendously, (Bernal *et al*., 2017; Ma *et al*., 2018; Besha *et al*., 2017). Although most water treatment companies rely on conventional water treatment processes to remove specific types of pollutants found in drinking water sources, these processes are not efficient to remove total organic content of the pollutants found in water (Tian *et al*., 2008; Khan *et al*., 2018). MBR technology is currently being implemented as an alternate to traditional water treatment processes due to its several benefits over traditional treatment processes.

### 2.7.2 MBR studies

The use of MBR coupled with WRF species have previously been used for the bioremediation of a wide array of organic contaminants (other than NOM) present in wastewater (Wang *et al.*, 2014). Bioreactors have found application in different sectors of the industry such as bioremediation of industrial waste, food wastes, trace organic compounds (TrOCs) and dyes (Burton *et al.*, 2004; Thorulsley, 2015; Agtas *et al*., 2016). The effectiveness of membrane distillation coupled with enzymatic membrane bioreactor for the degradation of selected TrOCs in synthetic wastewater was studied by Asif *et al.* (2017) using two separate and combined catalysts (viduric acid and syringaldehyde). Findings indicated that high removal efficiency was due to dosing the catalysts separate compared to when combined (Asif *et al.,* 2017). The coupling of the two systems (membrane distillation and enzymatic membrane bioreactor) improved the removal of the organic compounds under investigation.

Nguyen *et al.* (2013) has also investigated the degradation and removal of TrOCs two MBRs operated under the same experimental conditions, namely: one with enzymes produced by WRF species *Trametes versicolor* and activated sludge, and another with just activated sludge. An increase in biodegradability was only observed for the mixed MBR because of the added redox-mediator 1-hydroxybenzotriazole (HBT) (Nguyen *et al.,* 2013). Fungal MBRs were also investigated by Yang *et al.* (2013) by comparing the removal of bisphenol A and diclofenac with pure culture of WRF *Trametes versicolor* in batch and continuous

systems operated under non-sterile conditions. High removal of the organic compounds was observed in a batch system due to degradation by WRF enzymes when compared with continuous addition of conventional bacteria to the MBR system. However, poor removal of diclofenac was observed in batch tests; this could be due to diclofenac not adsorbing onto the biomass and insufficient retention time that allows biodegradation. A case study comparing the performance of fungal MBR and photocatalytic membrane reactor in the removal of carbon oxygen demand (COD) and colour from industrial textile wastewater was investigated by Deveci *et al*. (2016). The fungal MBR contained WRF *Phanerochaete Chrysosporium* and the photocatalytic membrane reactor was exposed to ultra-violet light using titanium dioxide and zinc oxide as photo-catalysts. The two systems were operated single or as a combined use system. Overall, the combined systems achieved high removal percentages of COD and colour compared to the single use system.

The degradation of NOM present in surface water was also investigated using a photocatalytic reactor in the presence of nanocomposites such as titanium oxide (Sun *et al.*, 2014). Whereas high degradation of hydrophobic fraction of NOM was reported, very little degradation of the hydrophilic fraction was achieved.

It is apparent from the studies reported above that most of the studies were carried out on degradation of TrOCs in MBR systems using different types of WRF species. However, very little has been reported on the direct use of enzymes for NOM degradation, and knowledge on the behaviour and performance of these enzymes in the degradation of NOM is limited. Furthermore, the performance of these enzymes when infused in polymeric membranes has not been sufficiently studied. For this reason, this work seeks to study the biodegradation of NOM in water using an enzyme-modified membrane.

### 2.7.3 Factors affecting MBR performance

#### *2.7.3.1 Feed composition*

The organic load in the feed tank affects the removal efficiency, growth and activity of micro-organisms; therefore, organics compounds are consumed by the organisms as a source of food (Boonyungyuen *et al*., 2014). In this regard, the food to micro-organism ratio is a critical factor in MBR operation and should be calculated accordingly whether in a submerged or side stream system (Wei *et al*., 2014).

#### *2.7.3.2 Hydraulic retention time (HRT)*

Another important factor in MBR operation is HRT, which is the average period taken by a compound to remain in the feed tank or reactor before it leaves the tank (Tavana *et al*., 2019). Studies suggest that less HRT would result in low removal efficiency due to less contact time that the pollutants have with the micro-organisms (Sambusiti *et al*., 2019). It is therefore vital to note the HRT for the removal of contaminants in the feed. This would allow the organisms to have enough time to adsorb the organics before leaving the reactor. Moreover, the volume of the feed tank directly influences HRT. For instance, a bigger tank volume would have a higher HRT. Other researchers recommend an HRT of 5 to 10 hours (Judd, 2011); however, as already mentioned, HRT depends on the volume of the reactor. Hemmati *et al*. (2012) investigated the effect of different HRT on membrane fouling and the removal of phenols and chemical oxygen demand (COD) from wastewater. Increasing HRT from 8 h to 12 h led to a reduction in fouling and a high phenols and COD removal efficiencies of 99 % and 96 %, respectively.

#### *2.7.3.3 Aeration rate*

The supply of oxygen in the feed tank in MBR by aeration is important as some micro-organisms require oxygen for them to survive especially aerobic organisms. Iorhmen *et al*. (2016) have reported that an increase in the rate of aeration reduces membrane fouling since it allows the disruption of cake layer formed on the

membrane surface; however, increasing the rate of aeration results in high operational costs due to high energy usage. Makisha & Nesterenko (2018) have suggested an aeration rate of between 0.2 to 1.3 $m^3$ /h for a 1 $m^2$ area of membrane.

*2.7.3.4 Temperature*

As already mentioned, the growth of micro-organisms depends on temperature conditions and the availability of nutrients. Therefore, the activity and growth of micro-organisms is greatly influenced by the temperature (Calderón *et al*., 2012). In MBR, it has been reported that low temperature was responsible for a reduction in permeate flux, which in turn affected the transmembrane pressure (Arévalo *et al*., 2014).

## 2.8 Conclusion

NOM in water has persisted over decades and is responsible for the formation of various undesirable compounds produced upon reaction with disinfectants. A review of literature presented herein has highlighted several ways of characterizing the nature of NOM, its impact on the drinking water treatment process and several removal methods. The currently available methods for NOM removal have been reported to be time consuming and not cost effective. Amongst conventional treatment processes, coagulation-flocculation have been recognised as the most promising process for NOM removal. However, in order to achieve complete NOM removal from water, optimisation of the process such as coagulant dose and pH is often required. Biocatalytic processes implemented in bioreactors have presented promising alternatives for the effective degradation of NOM with improved properties such as NOM removal efficiency. Therefore, this work seeks the use of biocatalytic membrane for the degradation of NOM in water.

## 2.9 References

Adusei-Gyamfi, J., Ouddane, B., Rietveld, L., Cornard, J.P. and Criquet, J., 2019. Natural organic matter-cations complexation and its impact on water treatment: A critical review. *Water Research*, 160, pp.130-147.

Agrawal, K., Chaturvedi, V. and Verma, P., 2018. Fungal laccase discovered but yet undiscovered. *Bioresources and Bioprocessing*, *5*(1), pp.4.

Agtas, M., Ersahin, M.E., Ozgun, H. and Koyuncu, I., 2016. Impact of module design on the performance of membrane bioreactors treating municipal wastewater. *Separation Science and Technology*, *51*(5), pp.836-844.

Ahn, Y., Lee, D., Kwon, M., Choi, I.H., Nam, S.N. and Kang, J.W., 2017. Characteristics and fate of natural organic matter during UV oxidation processes. *Chemosphere*, *184*, pp.960-968.

Akpinar, M. and Urek, R.O., 2012. Production of ligninolytic enzymes by solid-state fermentation using *Pleurotus* eryngii. *Preparative Biochemistry and Biotechnology*, *42*(6), pp.582-597.

Alenazi, N.A., Hussein, M.A., Alamry, K.A. and Asiri, A.M., 2017. Modified polyether-sulfone membrane: a mini review. *Designed Monomers and Polymers*, *20*(1), pp.532-546.

Allard-Massicotte, R., Chadjaa, H. and Marinova, M., 2017. Phenols Removal from Hemicelluloses Pre-Hydrolysate by Laccase to Improve Butanol Production. *Fermentation*, *3*(3), p.31.

Alneyadi, A.H., Rauf, M.A. and Ashraf, S.S., 2018. Oxidoreductases for the remediation of organic pollutants in water–a critical review. *Critical reviews in Biotechnology*, *38*(7), pp.971-988.

Alresheedi, M.T., Barbeau, B. and Basu, O.D., 2019. Comparisons of NOM fouling and cleaning of ceramic and polymeric membranes during water treatment. *Separation and Purification Technology*, *209*, pp.452-460.

Amini, N., Papineau, I., Storck, V., Bérubé, P.R., Mohseni, M. and Barbeau, B., 2018. Long-term performance of biological ion exchange for the removal of natural organic matter and ammonia from surface waters. *Water research*, *146*, pp.1-9.

Ang, T.N., 2013. *Production of laccase enzyme using rice husk as substrate in fungal solid-state fermentation* (Doctoral dissertation, Jabatan Kejuruteraan Kimia, Fakulti Kejuruteraan, Universiti Malaya).

Arévalo, J., Ruiz, L.M., Pérez, J. and Gómez, M.A., 2014. Effect of temperature on membrane bioreactor performance working with high hydraulic and sludge retention time. *Biochemical Engineering Journal*, *88*, pp.42-49.

Arias-Paic, M., Cawley, K.M., Byg, S. and Rosario-Ortiz, F.L., 2016. Enhanced DOC removal using anion and cation ion exchange resins. *Water Research*, *88*, pp.981-989.

Arriaga, S., de Jonge, N., Nielsen, M.L., Andersen, H.R., Borregaard, V., Jewel, K., Ternes, T.A. and Nielsen, J.L., 2016. Evaluation of a membrane bioreactor system as post-

treatment in wastewater treatment for better removal of micropollutants. *Water Research*, *107*, pp. 37-46.

Asadgol, Z., Forootanfar, H., Rezaei, S., Mahvi, A.H. and Faramarzi, M.A., 2014. Removal of phenol and bisphenol-A catalyzed by laccase in aqueous solution. *Journal of Environmental Health Science and Engineering*, *12*(1), p.93.

Ashrafi, O., Yerushalmi, L. and Haghighat, F., 2015. Wastewater treatment in the pulp and paper industry: A review of treatment processes and the associated greenhouse gas emission. *Journal of Environmental Management*, *158*, pp. 146-157.

Asif, M.B., Hai, F.I., Dhar, B.R., Ngo, H.H., Guo, W., Jegatheesan, V., Price, W.E., Nghiem, L.D. and Yamamoto, K., 2018. Impact of simultaneous retention of micropollutants and laccase on micropollutant degradation in enzymatic membrane bioreactor. *Bioresource Technology*, *267*, pp. 473-480.

Asif, M.B., Hai, F.I., Hou, J., Price, W.E. and Nghiem, L.D., 2017. Impact of wastewater derived dissolved interfering compounds on growth, enzymatic activity and trace organic contaminant removal of white rot fungi–a critical review. *Journal of Environmental Management*, *201*, pp. 89-109.

Asif, M.B., Hai, F.I., Kang, J., Van De Merwe, J.P., Leusch, F.D., Price, W.E. and Nghiem, L.D., 2018. Biocatalytic degradation of pharmaceuticals, personal care products, industrial chemicals, steroid hormones and pesticides in a membrane distillation enzymatic bioreactor. *Bioresource Technology*, *247*, pp. 528-536.

Asif, M.B., Hai, F.I., Singh, L., Price, W.E. and Nghiem, L.D., 2017. Degradation of pharmaceuticals and personal care products by white-rot fungi—A critical review. *Current Pollution Reports*, *3*(2), pp. 88-103.

Aslam, M., Charfi, A., Lesage, G., Heran, M. and Kim, J., 2017. Membrane bioreactors for wastewater treatment: a review of mechanical cleaning by scouring agents to control membrane fouling. *Chemical Engineering Journal*, *307*, pp. 897-913.

Assayie, A.A., Gebreyohannes, A.Y. and Giorno, L., 2017. Municipal Wastewater Treatment by Membrane Bioreactors. In *Sustainable Membrane Technology for Water and Wastewater Treatment* (pp. 265-294). Springer, Singapore.

Awad, J., van Leeuwen, J., Liffner, J., Chow, C. and Drikas, M., 2016. Treatability of organic matter derived from surface and subsurface waters of drinking water catchments. *Chemosphere*, *144*, pp.1193-1200.

Badani, Z., Ait-Amar, H., Si-Salah, A., Brik, M. and Fuchs, W., 2005. Treatment of textile wastewater by membrane bioreactor and reuse. *Desalination*, *185*(1-3), pp.411-417.

Bagewadi, Z.K., Mulla, S.I. and Ninnekar, H.Z., 2017. Purification and immobilization of laccase from Trichoderma harzianum strain HZN10 and its application in dye decolorization. *Journal of Genetic Engineering and Biotechnology*, *15*(1), pp.139-150.

Baghbanzadeh, M., Rana, D., Lan, C.Q. and Matsuura, T., 2016. Effects of inorganic nano-additives on properties and performance of polymeric membranes in water treatment. *Separation & Purification Reviews*, *45*(2), pp.141-167.

Bansal, N. and Kanwar, S.S., 2013. Peroxidase (s) in environment protection. *The Scientific World Journal*, *2013*.

Barrios-Estrada, C., de Jesús Rostro-Alanis, M., Parra, A.L., Belleville, M.P., Sanchez Marcano, J., Iqbal, H.M. and Parra-Saldívar, R., 2018. Potentialities of active membranes with immobilized laccase for Bisphenol A degradation. *International Journal of Biological Macromolecules*, *108*, pp. 837-844.

Basumallick, S. and Santra, S., 2017. Monitoring of ppm level humic acid in surface water using ZnO–chitosan nanocomposite as fluorescence probe. *Applied Water Science*, *7*(2), pp.1025-1031.

Beniwal, D., Taylor-Edmonds, L., Armour, J. and Andrews, R.C., 2018. Ozone/peroxide advanced oxidation in combination with biofiltration for taste and odour control and organics removal. *Chemosphere*, *212*, pp. 272-281.

Bernal, R., von Gottberg, A. and Mack, B., 2017. using membrane bioreactors for wastewater treatment in small communities. *Technical paper, Suez SA, Water Technologies & Solutions*, pp.1-6.

Bertone, E., Chang, C., Thiel, P. and O'Halloran, K., 2018. Analysis and modelling of powdered activated carbon dosing for taste and odour removal. *Water Research*, *139*, pp. 321-328.

Besha, A.T., Gebreyohannes, A.Y., Tufa, R.A., Bekele, D.N., Curcio, E. and Giorno, L., 2017. Removal of emerging micropollutants by activated sludge process and membrane bioreactors and the effects of micropollutants on membrane fouling: a review. *Journal of Environmental Chemical Engineering*, *5*(3), pp.2395-2414.

Bilal, M. and Iqbal, H.M., 2019. Lignin peroxidase immobilization on Ca-alginate beads and its dye degradation performance in a packed bed reactor system. *Biocatalysis and Agricultural Biotechnology*, p.101205.

Bilal, M., Rasheed, T., Zhao, Y., Iqbal, H.M. and Cui, J., 2018. "Smart" chemistry and its application in peroxidase immobilization using different support materials. *International Journal of Biological Macromolecules*, *119*, pp.278-290.

Boguta, P., D'Orazio, V., Senesi, N., Sokołowska, Z. and Szewczuk-Karpisz, K., 2019. Insight into the interaction mechanism of iron ions with soil humic acids. The effect of the pH and chemical properties of humic acids. *Journal of Environmental Management*, *245*, pp.367-374.

Boonyungyuen, W., Wonglertarak, W. and Wichitsathian, B., 2014, September. Effect of organic loading rate on the performance of a membrane bioreactor (MBR) treating textile wastewater. In *International Conference on Chemical, Environment & Biological Sciences (CEBS-2014)* (pp. 17-18).

Bot, A. and Benites, J., 2005. *The importance of soil organic matter: Key to drought resistant soil and sustained food production* (No. 80). Food & Agriculture Org.

Bouacem, K., Rekik, H., Jaouadi, N.Z., Zenati, B., Kourdali, S., El Hattab, M., Badis, A., Annane, R., Bejar, S., Hacene, H. and Bouanane-Darenfed, A., 2018. Purification and characterization of two novel peroxidases from the dye-decolorizing fungus

Bjerkandera adusta strain CX-9. *International Journal of Biological Macromolecules*, *106*, pp.636-646.

Bu, F., Gao, B., Shen, X., Wang, W. and Yue, Q., 2019. The combination of coagulation and ozonation as a pre-treatment of ultrafiltration in water treatment. *Chemosphere*, *231*, pp.349-356.

Bugg, T.D., Ahmad, M., Hardiman, E.M. and Rahmanpour, R., 2011. Pathways for degradation of lignin in bacteria and fungi. *Natural Product Reports*, *28*(12), pp.1883-1896.

Burton, S.G., Ryan, D.R. and Van Wyk, L., 2004. Bioreactor Systems Using the White Rot Fungus Trametes for Bioremediation of Industrial Wastewater. *Water Research Commission.*

Cai, M.J. and Lin, Y.P., 2016. Effects of effluent organic matter (EfOM) on the removal of emerging contaminants by ozonation. *Chemosphere*, *151*, pp.332-338.

Calderón, K., González-Martínez, A., Montero-Puente, C., Reboleiro-Rivas, P., Poyatos, J.M., Juárez-Jiménez, B., Martínez-Toledo, M.V. and Rodelas, B., 2012. Bacterial community structure and enzyme activities in a membrane bioreactor (MBR) using pure oxygen as an aeration source. *Bioresource Technology*, *103*(1), pp.87-94.

Chang, Y.R., Lee, Y.J. and Lee, D.J., 2019. Membrane fouling during water or wastewater treatments: Current research updated. *Journal of the Taiwan Institute of Chemical Engineers*, *94*, pp.88-96.

Chaulk, M. and Sheppard, G., 2011. Study on Characteristics and Removal of Natural Organic Matter in Drinking Water Systems in Newfoundland and Labrador. Newfoundland Labrador Department of Environment and Conservation Division WM; August. Report No. *Contract*, (103047.00).

Chekli, L., Galloux, J., Zhao, Y.X., Gao, B.Y. and Shon, H.K., 2015. Coagulation performance and floc characteristics of polytitanium tetrachloride (PTC) compared with titanium tetrachloride ($TiCl_4$) and iron salts in humic acid–kaolin synthetic water treatment. *Separation and Purification Technology*, *142*, pp.155-161.

Chen, Y., Xu, W., Zhu, H., Wei, D., Wang, N. and Li, M., 2018. Comparison of organic matter removals in single-component and bi-component systems using enhanced coagulation and magnetic ion exchange (MIEX) adsorption. *Chemosphere*, *210*, pp.672-682.

Christopher, L.P., Yao, B. and Ji, Y., 2014. Lignin biodegradation with laccase-mediator systems. *Frontiers in Energy Research*, *2*, p.12.

Collado, S., Oulego, P., Suárez-Iglesias, O. and Díaz, M., 2019. Leachates and natural organic matter. A review of their biotreatment using fungi. *Waste Management*, *96*, pp.108-120.

Costa, J.B., Lima, M.J., Sampaio, M.J., Neves, M.C., Faria, J.L., Morales-Torres, S., Tavares, A.P. and Silva, C.G., 2019. Enhanced biocatalytic sustainability of laccase by immobilization on functionalized carbon nanotubes/polysulfone membranes. *Chemical Engineering Journal*, *355*, pp.974-985.

Cui, X. and Choo, K.H., 2014. Natural organic matter removal and fouling control in low pressure membrane filtration for water treatment. *Environmental Engineering Research*, *19*(1), pp.1-8.

Datta, R., Kelkar, A., Baraniya, D., Molaei, A., Moulick, A., Meena, R. and Formanek, P., 2017. Enzymatic degradation of lignin in soil: a review. *Sustainability*, *9*(7), p.1163.

de Abreu Domingos, R. and da Fonseca, F.V., 2018. Evaluation of adsorbent and ion exchange resins for removal of organic matter from petroleum refinery wastewaters aiming to increase water reuse. *Journal of Environmental Management*, *214*, pp.362-369.

Deng, L., Ngo, H.H., Guo, W. and Zhang, H., 2019. Pre-coagulation coupled with sponge membrane filtration for organic matter removal and membrane fouling control during drinking water treatment. *Water Research*, *157*, pp.155-166.

Deska, M. and Kończak, B., 2019. Immobilized fungal laccase as" green catalyst" for the decolourization process–state of the art. *Process Biochemistry*, 84, pp.112-123.

Deveci, E.Ü., Dizge, N., Yatmaz, H.C. and Aytepe, Y., 2016. Integrated process of fungal membrane bioreactor and photocatalytic membrane reactor for the treatment of industrial textile wastewater. *Biochemical Engineering Journal*, *105*, pp.420-427.

Ding, S., Deng, Y., Bond, T., Fang, C., Cao, Z. and Chu, W., 2019. Disinfection by-product formation during drinking water treatment and distribution: A review of unintended effects of engineering agents and materials. *Water Research*, 160, pp. 313-329.

Dlamini, S.P., Haarhoff, J., Mamba, B.B. and Van Staden, S., 2013. The response of typical South African raw waters to enhanced coagulation. *Water Science and Technology: Water Supply*, *13*(1), pp.20-28.

Doederer, K., Gale, D. and Keller, J., 2019. Effective removal of MIB and geosmin using MBBR for drinking water treatment. *Water Research*, *149*, pp.440-447.

Duan, Z., Shen, R., Liu, B., Yao, M. and Jia, R., 2018. Comprehensive investigation of a dye-decolorizing peroxidase and a manganese peroxidase from Irpex lacteus F17, a lignin-degrading basidiomycete. *AMB Express*, *8*(1), p.119.

El Monssef, R.A.A., Hassan, E.A. and Ramadan, E.M., 2016. Production of laccase enzyme for their potential application to decolorize fungal pigments on aging paper and parchment. *Annals of Agricultural Sciences*, *61*(1), pp.145-154.

El-Batal, A.I., ElKenawy, N.M., Yassin, A.S. and Amin, M.A., 2015. Laccase production by Pleurotus ostreatus and its application in synthesis of gold nanoparticles. *Biotechnology Reports*, *5*, pp.31-39.

Ergun, S.O. and Urek, R.O., 2017. Production of ligninolytic enzymes by solid state fermentation using Pleurotus ostreatus. *Annals of Agrarian Science*, *15*(2), pp.273-277.

Erkan, H.S. and Engin, G.O., 2017. The investigation of paper mill industry wastewater treatment and activated sludge properties in a submerged membrane bioreactor. *Water Science and Technology*, *76*(7), pp.1715-1725.

Falade, A.O., Nwodo, U.U., Iweriebor, B.C., Green, E., Mabinya, L.V. and Okoh, A.I., 2017. Lignin peroxidase functionalities and prospective applications. *Microbiology Open*, *6*(1), p.e00394.

Finkbeiner, P., Moore, G., Pereira, R., Jefferson, B. and Jarvis, P., 2019. The combined influence of hydrophobicity, charge and molecular weight on natural organic matter removal by ion exchange and coagulation. *Chemosphere*, p.124633.

Finkbeiner, P., Redman, J., Patriarca, V., Moore, G., Jefferson, B. and Jarvis, P., 2018. Understanding the potential for selective natural organic matter removal by ion exchange. *Water Research*, *146*, pp.256-263.

Gerke, J., 2018. Concepts and misconceptions of humic substances as the stable part of soil organic matter: A review. *Agronomy*, *8*(5), p.76.

Giwa, A., Ahmed, M. and Hasan, S.W., 2019. Polymers for Membrane Filtration in Water Purification. In *Polymeric Materials for Clean Water* (pp. 167-190). Springer, Cham.

Goveia, D., Melo, C.D.A., Oliveira, L.K.D., Fraceto, L.F., Rocha, J.C., Dias Filho, N.L. and Rosa, A.H., 2013. Adsorption and release of micronutrients by humin extracted from peat samples. *Journal of the Brazilian Chemical Society*, *24*(5), pp.721-730.

Grinhut, T., Hertkorn, N., Schmitt-Kopplin, P., Hadar, Y. and Chen, Y., 2011. Mechanisms of humic acids degradation by white rot fungi explored using 1H NMR spectroscopy and FTICR mass spectrometry. *Environmental science & technology*, *45*(7), pp.2748-2754.

Hai, F., Riley, T., Shawkat, S., Magram, S. and Yamamoto, K., 2014. Removal of pathogens by membrane bioreactors: a review of the mechanisms, influencing factors and reduction in chemical disinfectant dosing. *Water*, *6*(12), pp.3603-3630.

Hayes, M.H., Mylotte, R. and Swift, R.S., 2017. Humin: Its composition and importance in soil organic matter. In *Advances in agronomy* (Vol. 143, pp. 47-138). Academic Press.

Hemmati, A., Dolatabad, M.M., Naeimpoor, F., Pak, A. and Mohammdi, T., 2012. Effect of hydraulic retention time and temperature on submerged membrane bioreactor (SMBR) performance. *Korean Journal of Chemical Engineering*, *29*(3), pp.369-376.

Hermann, K.L., Costa, A., Helm, C.V., LIMA, E.A. and Tavares, L.B., 2013. Expression of manganese peroxidase by Lentinula edodes and Lentinula boryana in solid state and submerged system fermentation. *Anais da Academia Brasileira de Ciências*, *85*(3), pp.965-973.

Hervé, V., Ketter, E., Pierrat, J.C., Gelhaye, E. and Frey-Klett, P., 2016. Impact of Phanerochaete chrysosporium on the functional diversity of bacterial communities associated with decaying wood. *PloS one*, *11*(1), p.e0147100.

Hu, L., Liu, Y., Zeng, G., Chen, G., Wan, J., Zeng, Y., Wang, L., Wu, H., Xu, P., Zhang, C. and Cheng, M., 2017. Organic matters removal from landfill leachate by immobilized Phanerochaete chrysosporium loaded with graphitic carbon nitride under visible light irradiation. *Chemosphere*, *184*, pp.1071-1079.

Hudaib, B., Gomes, V., Shi, J., Zhou, C. and Liu, Z., 2018. Poly (vinylidene fluoride)/polyaniline/MWCNT nanocomposite ultrafiltration membrane for natural organic matter removal. *Separation and Purification Technology*, *190*, pp.143-155.

Hussain, S., Awad, J., Sarkar, B., Chow, C.W., Duan, J. and van Leeuwen, J., 2019. Coagulation of dissolved organic matter in surface water by novel titanium (III) chloride: Mechanistic surface chemical and spectroscopic characterisation. *Separation and Purification Technology*, *213*, pp.213-223.

Iandolo, D., Amore, A., Birolo, L., Leo, G., Olivieri, G. and Faraco, V., 2011. Fungal solid-state fermentation on agro-industrial wastes for acid wastewater decolorization in a continuous flow packed-bed bioreactor. *Bioresource Technology*, *102*(16), pp.7603-7607.

Ibrahim, N. and Aziz, H.A., 2014. Trends on natural organic matter in drinking water sources and its treatment. *International Journal of Scientific Research in Environmental Sciences*, *2*(3), p.94.

Ijoma, G.N., 2016. Enzyme production and activities of lignocellulolytic fungi cultivated on agricultural residues (Doctoral dissertation, University of South Africa).

Ike, I.A., Karanfil, T., Cho, J. and Hur, J., 2019. Oxidation by-products from the degradation of dissolved organic matter by advanced oxidation processes–A critical review. *Water Research*, p.114929.

Ike, I.A., Lee, Y. and Hur, J., 2019. Impacts of advanced oxidation processes on disinfection by-products from dissolved organic matter upon post-chlor (am) ination: A critical review. *Chemical Engineering Journal*, p.121929.

Iorhemen, O., Hamza, R. and Tay, J., 2016. Membrane bioreactor (MBR) technology for wastewater treatment and reclamation: membrane fouling. *Membranes*, *6*(2), p.33.

Jamil, S., Loganathan, P., Listowski, A., Kandasamy, J., Khourshed, C. and Vigneswaran, S., 2019. Simultaneous removal of natural organic matter and micro-organic pollutants from reverse osmosis concentrate using granular activated carbon. *Water Research*, *155*, pp.106-114.

Jegatheesan, V., Pramanik, B.K., Chen, J., Navaratna, D., Chang, C.Y. and Shu, L., 2016. Treatment of textile wastewater with membrane bioreactor: a critical review. *Bioresource Technology*, *204*, pp.202-212.

Jepsen, K., Bram, M., Pedersen, S. and Yang, Z., 2018. Membrane fouling for produced water treatment: A review study from a process control perspective. *Water*, *10*(7), p.847.

Jochems, P., Satyawali, Y., Diels, L. and Dejonghe, W., 2011. Enzyme immobilization on/in polymeric membranes: status, challenges and perspectives in biocatalytic membrane reactors (BMRs). *Green Chemistry*, *13*(7), pp.1609-1623.

Jones, S.M. and Solomon, E.I., 2015. Electron transfer and reaction mechanism of laccases. *Cellular and Molecular Life Sciences*, *72*(5), pp.869-883.

Jun, L.Y., Yon, L.S., Mubarak, N.M., Bing, C.H., Pan, S., Danquah, M.K., Abdullah, E.C. and Khalid, M., 2019. An Overview of Immobilized Enzyme Technologies for Dye,

Phaenolic Removal from Wastewater. *Journal of Environmental Chemical Engineering*, p.102961.

Kaleta, J., Kida, M., Koszelnik, P., Papciak, D., Puszkarewicz, A. and Tchórzewska Cieślak, B., 2017. The use of activated carbons for removing organic matter from groundwater. *Archives of Environmental Protection*, *43*(3), pp.32-41.

Karigar, C.S. and Rao, S.S., 2011. Role of microbial enzymes in the bioremediation of pollutants: a review. *Enzyme Research*, p.805187.

Khan, M.A., Ngo, H.H., Guo, W., Liu, Y., Chang, S.W., Nguyen, D.D., Nghiem, L.D. and Liang, H., 2018. Can membrane bioreactor be a smart option for water treatment?. *Bioresource Technology Reports*, *4*, pp.80-87.

Khatami, S., Deng, Y., Tien, M. and Hatcher, P.G., 2019. Formation of Water-Soluble Organic Matter Through Fungal Degradation of Lignin. *Organic Geochemistry*, 135, pp.64-70.

Klučáková, M., 2018. Conductometric study of the dissociation behavior of humic and fulvic acids. *Reactive and Functional Polymers*, *128*, pp.24-28.

Kong, W., Chen, H., Lyu, S., Ma, F., Yu, H. and Zhang, X., 2016. Characterization of a novel manganese peroxidase from white-rot fungus Echinodontium taxodii 2538, and its use for the degradation of lignin-related compounds. *Process Biochemistry*, *51*(11), pp.1776-1783.

Kraemer, J.T., Menniti, A.L., Erdal, Z.K., Constantine, T.A., Johnson, B.R., Daigger, G.T. and Crawford, G.V., 2012. A practitioner's perspective on the application and research needs of membrane bioreactors for municipal wastewater treatment. *Bioresource Technology*, *122*, pp.2-10.

Krzeminski, P., Vogelsang, C., Meyn, T., Köhler, S.J., Poutanen, H., de Wit, H.A. and Uhl, W., 2019. Natural organic matter fractions and their removal in full-scale drinking water treatment under cold climate conditions in Nordic capitals. *Journal of Environmental Management*, *241*, pp.427-438.

Kuhar, F., Castiglia, V.C. and Zamora, J.C., 2016. Detection of manganese peroxidase and other exoenzymes in four isolates of Geastrum (Geastrales) in pure culture. *Revista Argentina de Microbiologia*, *48*(4), pp.274-278.

Kumar, R., Raizner, Y., Kruh, L.I., Menashe, O., Azaizeh, H., Kapur, S. and Kurzbaum, E., 2018. Extracellular laccase production and phenolic degradation by an olive mill wastewater isolate. *Grasas y Aceites*, *69*(1), p.231.

Lamsal, R., Walsh, M.E. and Gagnon, G.A., 2011. Comparison of advanced oxidation processes for the removal of natural organic matter. *Water Research*, *45*(10), pp.3263-3269.

Lee, D.J., Cheng, Y.L., Wong, R.J. and Wang, X.D., 2018. Adsorption removal of natural organic matters in waters using biochar. *Bioresource Technology*, *260*, pp.413-416.

Lee, M., 2005. Application of White-rot Fungi for the biodegradation of natural organic matter in wastes. Degree Thesis.

Lee, S.J. and Kim, J.H., 2014. Differential natural organic matter fouling of ceramic versus polymeric ultrafiltration membranes. *Water Research*, *48*, pp.43-51.

Levchuk, I., Màrquez, J.J.R. and Sillanpää, M., 2018. Removal of natural organic matter (NOM) from water by ion exchange–A review. *Chemosphere*, *192*, pp.90-104.

Li, L., Liu, B., Yang, J., Zhang, Q., He, C. and Jia, R., 2019. Catalytic properties of a short manganese peroxidase from Irpex lacteus F17 and the role of Glu166 in the $Mn^{2+}$ independent activity. *International Journal of Biological Macromolecules*, 136, pp.859-869.

Li, S., Luo, J. and Wan, Y., 2018. Regenerable biocatalytic nanofiltration membrane for aquatic micropollutants removal. *Journal of Membrane Science*, *549*, pp.120-128.

Li, W., Zhang, J., Wang, F., Qian, L., Zhou, Y., Qi, W. and Chen, J., 2018. Effect of disinfectant residual on the interaction between bacterial growth and assimilable organic carbon in a drinking water distribution system. *Chemosphere*, *202*, pp.586-597.

Li, Y., Wang, Z., Xu, X. and Jin, L., 2015. A Ca-alginate particle co-immobilized with Phanerochaete chrysosporium cells and the combined cross-linked enzyme aggregates from Trametes versicolor. *Bioresource Technology*, *198*, pp.464-469.

Lin, Y.W., Li, D., Gu, A.Z., Zeng, S.Y. and He, M., 2016. Bacterial regrowth in water reclamation and distribution systems revealed by viable bacterial detection assays. *Chemosphere*, *144*, pp.2165-2174.

Liu, L., Xing, X., Hu, C. and Wang, H., 2019. O3-BAC-Cl2: A multi-barrier process controlling the regrowth of opportunistic waterborne pathogens in drinking water distribution systems. *Journal of Environmental Sciences*, *76*, pp.142-153.

Liu, M., Wang, C., Wang, F. and Xie, Y., 2019. Maize (Zea mays) growth and nutrient uptake following integrated improvement of vermicompost and humic acid fertilizer on coastal saline soil. *Applied Soil Ecology*, 142, pp.147-154.

Lobanga, K.P., Haarhoff, J. and Van Staden, S.J., 2014. Treatability of South African surface waters by enhanced coagulation. *Water SA*, *40*(3), pp.529-534.

Lorena, S., Martì, C. and Roberto, S., 2011. Comparative study between activated sludge versus membrane bioreactor for textile wastewater. *Desalination and Water Treatment*, *35*(1-3), pp.101-109.

Lu, L.W., Peng, Y.P. and Chang, C.N., 2018. Catalytic ozonation by palladium manganese for the decomposition of natural organic matter. *Separation and Purification Technology*, *194*, pp.396-403.

Ma, J., Dai, R., Chen, M., Khan, S.J. and Wang, Z., 2018. Applications of membrane bioreactors for water reclamation: Micropollutant removal, mechanisms and perspectives. *Bioresource Technology*, *269*, pp.532-543.

Ma, R., Guo, M. and Zhang, X., 2018. Recent advances in oxidative valorization of lignin. *Catalysis Today*, *302*, pp.50-60.

Madhura, L., Kanchi, S., Sabela, M.I., Singh, S. and Bisetty, K., 2018. Membrane technology for water purification. *Environmental Chemistry Letters*, *16*(2), pp.343-365.

Makisha, N. and Nesterenko, A., 2018, June. Wastewater treatment in membrane bioreactors. Features and application. In *IOP Conference Series: Materials Science and Engineering* (Vol. 365, No. 2, p. 022046). IOP Publishing.

Mamba, B.B., Krause, R.W., Malefetse, T.J., Sithole, S.P. and Nkambule, T.I., 2009. Humic acid as a model for natural organic matter (NOM) in the removal of odorants from water by cyclodextrin polyurethanes. *Water SA*, *35*(1).

Marais, S.S., Ncube, E.J., Msagati, T.A.M., Mamba, B.B. and Nkambule, T.T., 2018. Comparison of natural organic matter removal by ultrafiltration, granular activated carbon filtration and full-scale conventional water treatment. *Journal of Environmental Chemical Engineering*, *6*(5), pp.6282-6289.

Mate, D.M. and Alcalde, M., 2017. Laccase: a multi-purpose biocatalyst at the forefront of biotechnology. *Microbial Biotechnology*, *10*(6), pp.1457-1467.

Mehboob, N., Asad, M.J., Imran, M., Gulfraz, M., Wattoo, F.H., Hadri, S.H. and Asghar, M., 2011. Production of lignin peroxidase by Ganoderma leucidum using solid state fermentation. *African Journal of Biotechnology*, *10*(48), pp.9880-9887.

Menya, E., Olupot, P.W., Storz, H., Lubwama, M. and Kiros, Y., 2018. Production and performance of activated carbon from rice husks for removal of natural organic matter from water: a review. *Chemical Engineering Research and Design*, *129*, pp.271-296.

Mester, T. and Tien, M., 2000. Oxidation mechanism of ligninolytic enzymes involved in the degradation of environmental pollutants. *International Biodeterioration & Biodegradation*, *46*(1), pp.51-59.

Miklos, D.B., Remy, C., Jekel, M., Linden, K.G., Drewes, J.E. and Hübner, U., 2018. Evaluation of advanced oxidation processes for water and wastewater treatment–a critical review. *Water Research*, *139*, pp.118-131.

Mir-Tutusaus, J.A., Baccar, R., Caminal, G. and Sarrà, M., 2018. Can white-rot fungi be a real wastewater treatment alternative for organic micropollutants removal? A review. *Water Research*, *138*, pp.137-151.

Moilanen, U., Kellock, M., Várnai, A., Andberg, M. and Viikari, L., 2014. Mechanisms of laccase-mediator treatments improving the enzymatic hydrolysis of pre-treated spruce. *Biotechnology for Biofuels*, *7*(1), p.177.

Moslehyani, A., Ismail, A.F., Matsuura, T., Rahman, M.A. and Goh, P.S., 2019. Recent Progresses of Ultrafiltration (UF) Membranes and Processes in Water Treatment. In *Membrane Separation Principles and Applications* (pp. 85-110).

Motsa, M.M., Mamba, B.B. and Verliefde, A.R., 2018. Forward osmosis membrane performance during simulated wastewater reclamation: Fouling mechanisms and fouling layer properties. *Journal of Water Process Engineering*, *23*, pp.109-118.

Mutamim, N.S.A., Noor, Z.Z., Hassan, M.A.A. and Olsson, G., 2012. Application of membrane bioreactor technology in treating high strength industrial wastewater: a performance review. *Desalination*, *305*, pp.1-11.

Nakada, L.Y.K., Franco, R.M.B., da Silva Fiuza, V.R., dos Santos, L.U., Branco, N. and Guimarães, J.R., 2019. Pre-ozonation of source water: Assessment of efficacy against Giardia duodenalis cysts and effects on natural organic matter. *Chemosphere*, *214*, pp.764-770.

Negrão, D.R., da Silva Júnior, T.A.F., de Souza Passos, J.R., Sansígolo, C.A., de Almeida Minhoni, M.T. and Furtado, E.L., 2014. Biodegradation of eucalyptus urograndis wood by fungi. *International Biodeterioration & Biodegradation*, *89*, pp.95-102.

Nguyen, L.N., Hai, F.I., Yang, S., Kang, J., Leusch, F.D., Roddick, F., Price, W.E. and Nghiem, L.D., 2013. Removal of trace organic contaminants by an MBR comprising a mixed culture of bacteria and white-rot fungi. *Bioresource Technology*, *148*, pp.234-241.

Niren, P. and Jigisha, P., 2011. Textile wastewater treatment using a UF hollow-fibre submerged membrane bioreactor (SMBR). *Environmental Technology*, *32*(11), pp.1247-1257.

Nousiainen, P., Kontro, J., Manner, H., Hatakka, A. and Sipilä, J., 2014. Phenolic mediators enhance the manganese peroxidase catalyzed oxidation of recalcitrant lignin model compounds and synthetic lignin. *Fungal Genetics and Biology*, *72*, pp.137-149.

Nousiainen, P.A., Kontro, J.H.S., Manner, M.H., Mäkelä, M.R., Hilden, S.K., Maijala, P.M., Lundell, T.K., Hatakka, A.I. and Sipilä, A.J., 2012. Phenolic mediators enhance the manganese peroxidase catalyzed oxidation of recalcitrant lignin model compounds. In *OxiZymes 16.-19.9. 2012, Marseille, France* (pp. 123-123).

Nqombolo, A., Mpupa, A., Moutloali, R.M. and Nomngongo, P.N., 2018. Wastewater Treatment Using Membrane Technology. *Wastewater and Water Quality*, p.29.

Özdemir, K., 2016. The use of carbon nanomaterials for removing natural organic matter in drinking water sources by a combined coagulation process. *Nanomaterials and Nanotechnology*, *6*, p.1847980416663680.

Özkan, O. and Uyanık, İ., 2017. Effect of Membrane Type for the Treatment of Organized Industrial Zone (OIZ) Wastewater with a Membrane Bioreactor (MBR): Batch Experiments. *Water*, *9*(8), p.582.

Park, K.Y., Yu, Y.J., Yun, S.J. and Kweon, J.H., 2019. Natural organic matter removal from algal-rich water and disinfection by-products formation potential reduction by powdered activated carbon adsorption. *Journal of Environmental Management*, *235*, pp.310-318.

Perkins, R.G., Slavin, E.I., Andrade, T.M.C., Blenkinsopp, C., Pearson, P., Froggatt, T., Godwin, G., Parslow, J., Hurley, S., Luckwell, R. and Wain, D.J., 2019. Managing taste and odour metabolite production in drinking water reservoirs: The importance of ammonium as a key nutrient trigger. *Journal of Environmental Management*, *244*, pp.276-284.

Perna, V., Agger, J.W., Holck, J. and Meyer, A.S., 2018. Multiple Reaction Monitoring for quantitative laccase kinetics by LC-MS. *Scientific Reports*, *8*(1), p.8114.

Pollegioni, L., Tonin, F. and Rosini, E., 2015. Lignin-degrading enzymes. *The FEBS Journal*, *282*(7), pp.1190-1213.

Qin, Y., Zhang, M., Dai, W., Xiang, C., Li, B. and Jia, Q., 2019. Antidiarrhoeal mechanism study of fulvic acids based on molecular weight fractionation. *Fitoterapia*, p.104270.

Qiu, X., Qin, J., Xu, M., Kang, L. and Hu, Y., 2019. Organic-inorganic nanocomposites fabricated via functional ionic liquid as the bridging agent for Laccase immobilization and its application in 2, 4-dichlorophenol removal. *Colloids and Surfaces B: Biointerfaces*, *179*, pp.260-269.

Quist-Jensen, C.A., Macedonio, F. and Drioli, E., 2015. Membrane technology for water production in agriculture: Desalination and wastewater reuse. *Desalination*, *364*, pp.17-32.

Rathnayake, D.N., Korotta-Gamage, S.M., Kastl, G. and Sathasivan, A., 2017. Effect of KMnO4 treatment of granular activated carbon on the removal of natural organic matter. *Desalination and Water Treatment*, *71*, pp.201-206.

Ratnayake, R.R., Seneviratne, G. and Kulasooriya, S.A., 2013. Effect of soil carbohydrates on nutrient availability in natural forests and cultivated lands in Sri Lanka. *Eurasian Soil Science*, *46*(5), pp.579-586.

Rekik, H., Jaouadi, N.Z., Bouacem, K., Zenati, B., Kourdali, S., Badis, A., Annane, R., Bouanane-Darenfed, A., Bejar, S. and Jaouadi, B., 2019. Physical and enzymatic properties of a new manganese peroxidase from the white-rot fungus Trametes pubescens strain i8 for lignin biodegradation and textile-dyes biodecolorization. *International Journal of Biological Macromolecules*, *125*, pp.514-525.

Ren, D., He, X., Wang, C. and Zhang, S., 2018. Biodegradation of phenol by pleurotus laccase in the direct current electric field. *Biomedical Research (0970-938X)*.

Ren, Z., Luo, J. and Wan, Y., 2018. Highly permeable biocatalytic membrane prepared by 3D modification: Metal-organic frameworks ameliorate its stability for micropollutants removal. *Chemical Engineering Journal*, *348*, pp.389-398.

Rodrigues-Couto, S., 2017. Industrial and environmental applications of white-rot fungi. *Mycosphere*, *8*, pp.456-466.

Rubilar, O., Diez, M.C. and Gianfreda, L., 2008. Transformation of chlorinated phenolic compounds by white rot fungi. *Critical Reviews in Environmental Science and Technology*, *38*(4), pp.227-268.

Rupiasih, N.N. and Vidyasagar, P., 2005 A Review: Compositions, Structures, Properties and Applications of Humic Substances. *Journal of Advances in Science and Technology*, *8*, pp.16-25.

Sakarinen, E., 2016. Humic acid removal by chemical coagulation , electrocoagulation and ultrafiltration. Degree Thesis, Plastic Technology.

Sambusiti, C., Saadouni, M., Gauchou, V., Segues, B., Leca, M.A., Baldoni-Andrey, P. and Jacob, M., 2019. Influence of HRT reduction on pilot scale flat sheet submerged

membrane bioreactor (sMBR) performances for Oil & Gas wastewater treatment. *Journal of Membrane Science*, p.117459.

Sarma, R., Islam, M., Running, M. and Bhattacharyya, D., 2018. Multienzyme immobilized polymeric membrane reactor for the transformation of a lignin model compound. *Polymers*, *10*(4), p.463.

Senthilkumar, S., Perumalsamy, M. and Prabhu, H.J., 2014. Decolourization potential of white-rot fungus Phanerochaete chrysosporium on synthetic dye bath effluent containing Amido black 10B. *Journal of Saudi Chemical Society*, *18*(6), pp.845-853.

Shao, S., Fu, W., Li, X., Shi, D., Jiang, Y., Li, J., Gong, T. and Li, X., 2019. Membrane fouling by the aggregations formed from oppositely charged organic foulants. *Water Research*, *159*, pp.95-101.

Sheldon, R.A. and van Pelt, S., 2013. Enzyme immobilisation in bio-catalysis: why, what and how. *Chemical Society Reviews*, *42*(15), pp.6223-6235.

Shimizu, Y., Ateia, M. and Yoshimura, C., 2018. Natural organic matter undergoes different molecular sieving by adsorption on activated carbon and carbon nanotubes. *Chemosphere*, *203*, pp.345-352.

Sillanpää, M., Ncibi, M.C. and Matilainen, A., 2018. Advanced oxidation processes for the removal of natural organic matter from drinking water sources: A comprehensive review. *Journal of Environmental Management*, *208*, pp.56-76.

Sillanpää, M., Ncibi, M.C., Matilainen, A. and Vepsäläinen, M., 2018. Removal of natural organic matter in drinking water treatment by coagulation: A comprehensive review. *Chemosphere*, *190*, pp.54-71.

Simón-Herrero, C., Naghdi, M., Taheran, M., Brar, S.K., Romero, A., Valverde, J.L., Ramirez, A.A. and Sánchez-Silva, L., 2019. Immobilized laccase on polyimide aerogels for removal of carbamazepine. *Journal of Hazardous Materials*, *376*, pp.83-90.

Singh, D. and Chen, S., 2008. The white-rot fungus Phanerochaete chrysosporium: conditions for the production of lignin-degrading enzymes. *Applied Microbiology and Biotechnology*, *81*(3), pp.399-417.

Sîrbu, C., Cioroianu, T. and Rotaru, P., 2010. About the humic acids and thermal behaviour of some humic acids. *Physics AUC*, *20*(part 1), pp.120-126.

Sirisha, V.L., Jain, A. and Jain, A., 2016. Enzyme immobilization: an overview on methods, support material, and applications of immobilized enzymes. In *Advances in Food and Nutrition Research* (Vol. 79, pp. 179-211). Academic Press.

Solarska, S., May, T., Roddick, F.A. and Lawrie, A.C., 2009. Isolation and screening of natural organic matter-degrading fungi. *Chemosphere*, *75*(6), pp.751-758.

Stefán, D., Erdélyi, N., Izsák, B., Záray, G. and Vargha, M., 2019. Formation of chlorination by-products in drinking water treatment plants using breakpoint chlorination. *Microchemical Journal*,149, pp.104008.

Su, Z., Liu, T., Yu, W., Li, X. and Graham, N.J., 2017. Coagulation of surface water: Observations on the significance of biopolymers. *Water Research*, *126*, pp.144-152.

Sun, W., Chu, H., Dong, B., Cao, D. and Zheng, S., 2014. The Degradation of Natural Organic Matter in Surface Water by a Nano-TiO2/Diatomite Photocatalytic Reactor. *CLEAN–Soil, Air, Water*, *42*(9), pp.1190-1198.

Sun, X., Chen, M., Wei, D. and Du, Y., 2019. Research progress of disinfection and disinfection by-products in China. *Journal of Environmental Sciences*. pp. 52-67.

Taheran, M., Naghdi, M., Brar, S.K., Knystautas, E.J., Verma, M. and Surampalli, R.Y., 2017. Covalent immobilization of laccase onto nanofibrous membrane for degradation of pharmaceutical residues in water. *ACS Sustainable Chemistry & Engineering*, *5*(11), pp.10430-10438.

Tavana, A., Pishgar, R. and Tay, J.H., 2019. Impact of hydraulic retention time and organic matter concentration on side-stream aerobic granular membrane bioreactor. *Science of The Total Environment*, *693*, p.133525.

Teh, C.Y., Budiman, P.M., Shak, K.P.Y. and Wu, T.Y., 2016. Recent advancement of coagulation–flocculation and its application in wastewater treatment. *Industrial & Engineering Chemistry Research*, *55*(16), pp.4363-4389.

Thayanukul, P., Kurisu, F., Kasuga, I. and Furumai, H., 2013. Evaluation of microbial regrowth potential by assimilable organic carbon in various reclaimed water and distribution systems. *Water Research*, *47*(1), pp.225-232.

Tian, J.Y., Liang, H., Li, X., You, S.J., Tian, S. and Li, G.B., 2008. Membrane coagulation bioreactor (MCBR) for drinking water treatment. *Water Research*, *42*(14), pp.3910-3920.

Tshindane, P., Mamba, P.P., Moss, L., Swana, U.U., Moyo, W., Motsa, M.M., Chaukura, N., Mamba, B.B. and Nkambule, T.T., 2019. The occurrence of natural organic matter in South African water treatment plants. *Journal of Water Process Engineering*, *31*, p.100809.

Tychanowicz, G.K., Souza, D.F.D., Souza, C.G., Kadowaki, M.K. and Peralta, R.M., 2006. Copper improves the production of laccase by the white-rot fungus Pleurotus pulmonarius in solid state fermentation. *Brazilian Archives of Biology and Technology*, *49*(5), pp.699-704.

Unuofin, J.O., Okoh, A.I. and Nwodo, U.U., 2019. Aptitude of Oxidative Enzymes for Treatment of Wastewater Pollutants: A Laccase Perspective. *Molecules*, *24*(11), p.2064.

Urbanowska, A. and Kabsch-Korbutowicz, M., 2014. Influence of operating conditions on performance of ceramic membrane used for water treatment. *Chemical Papers*, *68*(2), pp.190-196.

van Zandvoort, I., Koers, E.J., Weingarth, M., Bruijnincx, P.C., Baldus, M. and Weckhuysen, B.M., 2015. Structural characterization of 13 C-enriched humins and alkali-treated 13 C humins by 2D solid-state NMR. *Green Chemistry*, *17*(8), pp.4383-4392.

Vatanpour, V., Madaeni, S.S., Moradian, R., Zinadini, S. and Astinchap, B., 2011. Fabrication and characterization of novel antifouling nanofiltration membrane prepared from oxidized multiwalled carbon nanotube/polyethersulfone nanocomposite. *Journal of Membrane Science*, 375(1-2), pp.284-294.

Vaudevire, E., Radmanesh, F., Kolkman, A., Vughs, D., Cornelissen, E., Post, J. and van der Meer, W., 2019. Fate and removal of trace pollutants from an anion exchange spent brine during the recovery process of natural organic matter and salts. *Water Research*, *154*, pp.34-44.

Vera, M., Martín-Alonso, J., Mesa, J., Granados, M., Beltran, J.L., Casas, S., Gibert, O. and Cortina, J.L., 2017. Monitoring UF membrane performance treating surface groundwater blends: Limitations of FEEM-PARAFAC on the assessment of the organic matter role. *Chemical Engineering Journal*, *317*, pp.961-971.

Villanueva, C.M., Cordier, S., Font-Ribera, L., Salas, L.A. and Levallois, P., 2015. Overview of disinfection by-products and associated health effects. *Current Environmental Health Reports*, *2*(1), pp.107-115.

Vitola, G., Mazzei, R., Fontananova, E., Porzio, E., Manco, G., Gaeta, S.N. and Giorno, L., 2016. Polymeric biocatalytic membranes with immobilized thermostable phosphotriesterase. *Journal of Membrane Science*, *516*, pp.144-151.

Vivekanandan, K.E., Sivaraj, S. and Kumaresan, S., 2014. Characterization and purification of laccase enzyme from Aspergillus nidulans CASVK3 from vellar estuary south east coast of India. *International Journal Curr Microbiology Applied Sciences*, *3*, pp.213-227.

Voběrková, S., Solčány, V., Vršanská, M. and Adam, V., 2018. Immobilization of ligninolytic enzymes from white-rot fungi in cross-linked aggregates. *Chemosphere*, *202*, pp.694-707.

Vršanská, M., Voběrková, S., Jiménez, A., Strmiska, V. and Adam, V., 2017. Preparation and optimisation of cross-linked enzyme aggregates using native isolate white rot fungi trametes versicolor and fomes fomentarius for the decolourisation of synthetic dyes. *International Journal of Environmental Research and Public Health*, *15*(1), p.23.

Wan, C. and Li, Y., 2013. Solid-state biological pre-treatment of lignocellulosic biomass. In *Green Biomass Pre-treatment for Biofuels Production*. Springer, Dordrecht. pp. 67-86.

Wan, Y., Huang, X., Shi, B., Shi, J. and Hao, H., 2019. Reduction of organic matter and disinfection by-products formation potential by titanium, aluminum and ferric salts coagulation for micro-polluted source water treatment. *Chemosphere*, *219*, pp.28-35.

Wan, Y., Xie, P., Wang, Z., Ding, J., Wang, J., Wang, S. and Wiesner, M.R., 2019. Comparative study on the pre-treatment of algae-laden water by UV/persulfate, UV/chlorine, and UV/$H_2O_2$: Variation of characteristics and alleviation of ultrafiltration membrane fouling. *Water Research*, *158*, pp.213-226.

Wang, C., Yu, J., Guo, Q., Sun, D., Su, M., An, W., Zhang, Y. and Yang, M., 2019. Occurrence of swampy/septic odour and possible odorants in source and finished drinking water of major cities across China. *Environmental Pollution*, *249*, pp.305-310.

Wang, D., Bolton, J.R., Andrews, S.A. and Hofmann, R., 2015. UV/chlorine control of drinking water taste and odour at pilot and full-scale. *Chemosphere*, *136*, pp.239-244.

Wang, J., Feng, J., Jia, W., Chang, S., Li, S. and Li, Y., 2015. Lignin engineering through laccase modification: a promising field for energy plant improvement. *Biotechnology for Biofuels*, *8*(1), p.145.

Wang, N., Li, X., Yang, Y., Shang, Y., Zhuang, X., Li, H. and Zhou, Z., 2019. Combined process of visible light irradiation photocatalysis-coagulation enhances natural organic matter removal: Optimization of influencing factors and mechanism. *Chemical Engineering Journal*, 374, pp.748-759.

Wang, P., Hu, X., Cook, S., Begonia, M., Lee, K.S. and Hwang, H.M., 2008. Effect of culture conditions on the production of ligninolytic enzymes by white rot fungi Phanerochaete chrysosporium (ATCC 20696) and separation of its lignin peroxidase. *World Journal of Microbiology and Biotechnology*, *24*(10), pp.2205-2212.

Wang, X., Yao, B. and Su, X., 2018. Linking enzymatic oxidative degradation of lignin to organics detoxification. *International journal of molecular sciences*, *19*(11), p.3373.

Wang, Y., 2017. *Liquefaction of humins from C6-sugar conversions using heterogeneous catalysts* (Doctoral thesis. University of Groningen).

Wang, Z., Ma, J., Tang, C.Y., Kimura, K., Wang, Q. and Han, X., 2014. Membrane cleaning in membrane bioreactors: a review. *Journal of Membrane Science*, *468*, pp.276-307.

Wei, C.H., Harb, M., Amy, G., Hong, P.Y. and Leiknes, T., 2014. Sustainable organic loading rate and energy recovery potential of mesophilic anaerobic membrane bioreactor for municipal wastewater treatment. *Bioresource Technology*, *166*, pp.326-334.

Wen, X., Jia, Y. and Li, J., 2009. Degradation of tetracycline and oxytetracycline by crude lignin peroxidase prepared from Phanerochaete chrysosporium–a white rot fungus. *Chemosphere*, *75*(8), pp.1003-1007.

Winter, J., Wray, H.E., Schulz, M., Vortisch, R., Barbeau, B. and Bérubé, P.R., 2018. The impact of loading approach and biological activity on NOM removal by ion exchange resins. *Water Research*, *134*, pp.301-310.

Xiao, K., Liang, S., Wang, X., Chen, C. and Huang, X., 2019. Current state and challenges of full-scale membrane bioreactor applications: a critical review. *Bioresource Technology*, *271*, pp.473-481.

Xing, J., Liang, H., Xu, S., Chuah, C.J., Luo, X., Wang, T., Wang, J., Li, G. and Snyder, S.A., 2019. Organic matter removal and membrane fouling mitigation during algae rich surface water treatment by powdered activated carbon adsorption pre-treatment: Enhanced by UV and UV/chlorine oxidation. *Water Research*, *159*, pp.283-293.

Xu, H., Guo, M.Y., Gao, Y.H., Bai, X.H. and Zhou, X.W., 2017. Expression and characteristics of manganese peroxidase from Ganoderma lucidum in Pichia

pastoris and its application in the degradation of four dyes and phenol. *BMC Biotechnology*, *17*(1), p.19.

Xu, H.M., Sun, X.F., Wang, S.Y., Song, C. and Wang, S.G., 2018. Development of laccase/graphene oxide membrane for enhanced synthetic dyes separation and degradation. *Separation and Purification Technology*, *204*, pp.255-260.

Yamamura, H., Okimoto, K., Kimura, K. and Watanabe, Y., 2014. Hydrophilic fraction of natural organic matter causing irreversible fouling of microfiltration and ultrafiltration membranes. *Water Research*, *54*, pp.123-136.

Yang, J., Yang, X., Lin, Y., Ng, T.B., Lin, J. and Ye, X., 2015. Laccase-catalysed decolorization of malachite green: performance optimization and degradation mechanism. *PloS one*, *10*(5), p.e0127714.

Yang, S., Hai, F.I., Nghiem, L.D., Price, W.E., Roddick, F., Moreira, M.T. and Magram, S.F., 2013. Understanding the factors controlling the removal of trace organic contaminants by white-rot fungi and their lignin modifying enzymes: a critical review. *Bioresource Technology*, *141*, pp.97-108.

You, Y., Jin, X.H., Wen, X.Y., Sahajwalla, V., Chen, V., Bustamante, H. and Joshi, R.K., 2018. Application of graphene oxide membranes for removal of natural organic matter from water. *Carbon*, *129*, pp.415-419.

Yu, W., Graham, N. and Liu, T., 2019. Prevention of UF membrane fouling in drinking water treatment by addition of $H_2O_2$ during membrane backwashing. *Water Research*, *149*, pp.394-405.

Yu, W., Liu, T., Crawshaw, J., Liu, T. and Graham, N., 2018. Ultrafiltration and nanofiltration membrane fouling by natural organic matter: Mechanisms and mitigation by pre-ozonation and pH. *Water Research*, *139*, pp.353-362.

Zahid, M., Rashid, A., Akram, S., Rehan, Z.A. and Razzaq, W., 2018. A comprehensive review on polymeric nano-composite membranes for water treatment. *Journal of Membrane Science Technology*, *8*(1), pp.179-198.

Zahmatkesh, M., Spanjers, H. and van Lier, J.B., 2017. Fungal treatment of humic-rich industrial wastewater: application of white rot fungi in remediation of food processing wastewater. *Environmental Technology*, *38*(21), pp.2752-2762.

Zahmatkesh, M., Spanjers, H.L.F.M., Toran, M.J., Blánquez, P. and Van Lier, J.B., 2016. Bioremoval of humic acid from water by white rot fungi: exploring the removal mechanisms. *AMB Express*, *6*(1), p.118.

Zdarta, J., Meyer, A.S., Jesionowski, T. and Pinelo, M., 2019. Multi-faceted strategy based on enzyme immobilization with reactant adsorption and membrane technology for biocatalytic removal of pollutants: A critical review. *Biotechnology Advances*, 37(7), p.107401.

Zhang, D., Duan, D., Huang, Y., Yang, Y. and Ran, Y., 2017. Composition and structure of natural organic matter through advanced nuclear magnetic resonance techniques. *Chemical and Biological Technologies in Agriculture*, *4*(1), p.8.

Zhang, J., Li, W., Chen, J., Wang, F., Qi, W. and Li, Y., 2019. Impact of disinfectant on bacterial antibiotic resistance transfer between biofilm and tap water in a simulated distribution network. *Environmental Pollution*, *246*, pp.131-140.

Zhang, Y., Wang, X., Jia, H., Fu, B., Xu, R. and Fu, Q., 2019. Algal fouling and extracellular organic matter removal in powdered activated carbon-submerged hollow fiber ultrafiltration membrane systems. *Science of The Total Environment*, *671*, pp.351-361.

Zhang, Y., Zhao, X., Zhang, X. and Peng, S., 2015. A review of different drinking water treatments for natural organic matter removal. *Water Science and Technology: Water Supply*, *15*(3), pp.442-455.

Zhao, J., Yang, Y., Li, C. and Hou, L.A., 2019. Fabrication of GO modified PVDF membrane for dissolved organic matter removal: Removal mechanism and antifouling property. *Separation and Purification Technology*, *209*, pp.482-490.

Zhao, Y., Wei, Y., Zhang, Y., Wen, X., Xi, B., Zhao, X., Zhang, X. and Wei, Z., 2017. Roles of composts in soil based on the assessment of humification degree of fulvic acids. *Ecological Indicators*, *72*, pp.473-480.

Zhou, L., Monreal, C.M., Xu, S., McLaughlin, N.B., Zhang, H., Hao, G. and Liu, J., 2019. Effect of bentonite-humic acid application on the improvement of soil structure and maize yield in a sandy soil of a semi-arid region. *Geoderma*, *338*, pp.269-280.

# CHAPTER 3

# EXPERIMENTAL METHODOLOGY

## 3.1 Introduction

This chapter discusses the materials and methods used for the preparation of ultrafiltration polymeric membranes and methods on the collection of white rot fungi isolates, and preparation of fungal inoculum. In addition, water samples and analysis are also discussed in this chapter.

## 3.2 Reagents and Materials

All chemicals used in this study were used without any further purification. The following chemicals were purchased from Sigma-Aldrich (Johannesburg, South Africa): polyethersulfone (PES), polyethylene glycol (PEG) BioUltra 400 Da, 1-methyl-2-pyrrolidone (NMP) (≥99.5 vol %), were used as a polymer, poreformer and solvent respectively. Humic acid (HA), Bovine serum albumin (BSA) (>96 %) and acid blue dye (45 % dye content) were used as model compounds for membrane rejection experiments. Sabouraud Dextrose Broth (SDB) was used for the growth of fungal isolates for identification using Matrix Assisted Laser Desorption Ionisation- Time of Flight Mass Spectrometry (MALDI-TOF). Absolute ethanol (100 %), formic acid (70 %), acetonitrile (ACN) (50 %) and nitrilotriacetic acid (≥99.0 %) were used as reagents for sample preparation for fungal identification using MALDI-TOF biotyping. Guaiacol (≥98.0 %) was used as substrate for the screening of lignin-degrading enzymes. Hydrogen peroxide ($H_2O_2$) and veratryl alcohol or 3.4-Dimethoxybenzyl alcohol ($(CH3O)_2C_6H_3CH_2OH$) (≥99.0 %) were used for the determination of peroxidases activity. Potassium hydrogen phthalate ($C_8H_5KO_4$) (≥99.95 %), sodium hydroxide (NaOH) (≥98.0 %) and hydrochloric acid (HCl) (≥37.0 %) were used in preparation of HA stock solution. Potassium dihydrogen phosphate ($KH_2PO_4$)

(≥98 %), magnesium sulfate heptahydrate ($MgSO_4.7H_2O$) (≥99.0 %) , calcium chloride ($CaCl_2$) (≥93.0 %), ammonium sulfate ($(NH_4)_2SO_4$) (≥99.0 %), magnesium sulfate ($MgSO_4$), (≥99.5 %), manganese sulfate ($M_nSO_4$ )(≥ 99.0 %), sodium chloride (NaCl) (≥99.5 %), ferrous sulfate heptahydrate ($FeSO_4.7H_2O$), cobalt(II) sulfate ($CoSO_4$), zinc sulfate ($ZnSO_4$), copper(II) sulfate pentahydrate ($CuSO_4.5H_2O$), aluminium potassium sulfate (Alk ($SO_4$)2), boric acid ($H_3BO_3$), ammonium molybdate tetrahydrate ($(NH_4)_6Mo_7O_{24}$), biotic, folic acid ($C_{19}H_{19}N_7O_6$) (≥97.0 %), thiamine hydrochloride ($HC_{12}H_{17}ON_4SCl_2$), Riboflavin ($C_{17}H_{20}N_4O_6$), pyridoxine hydrochloride ($C_8H_{12}ClNO_3$), cyanocobalamine ($C_{63}H_{88}CoN_{14}O_{14}P$), nicotinic acid ($C_6H_5NO_2$), DL-calcium pantothenate ($C_{18}H_{32}CaN_2O_{10}$), p-aminobenzoic acid, thioctic acid ($C_8H_{14}O_2S_2$), hydrogen peroxide ($H_2O_2$), sodium acetate ($C_2H_3NaO_2$), sodium tartrate ($C_4H_4O_6Na_2$) and citric acid ($C_6H_8O_7$) were used to prepare basal medium for fungal growth. α-Cyano-4-hydroxycinnamic acid (HCCA) was supplied by Bruker (Sandton, South Africa) and used as matrix for MALDI-TOF biotyping. The following chemicals were supplied by Inqaba Biotechnical Industries (Pty) Ltd (Pretoria, South Africa): Sabouraud Dextrose Agar (SDA) was used as solid media for fungal growth and chloramphenicol was used as an antibiotic to prevent bacterial growth. Zymo fungal/bacterial research quick DNA extraction kit, forward and reverse primer internal transcript spacer (ITS1 and ITS4), master mix, water molecular biology reagent, ethidium bromide, agarose gel and Tris-acetate-EDTA (TAE) were used for fungal molecular identification. Sodium acetate (anhydrous, $C_2H_3NaO_2$) (≥99.0 %) was used as a buffer for maintaining the natural state of the enzymes and 4-hydroxybenzoic acid ($4\text{-}HOC_6H_4CO_2H$) (≥99 %) was used as a substrate for enzyme laccase in immobilisation studies. Purified crude laccase enzymes from identified isolates, namely D and R as *Perenniporia* sp. UOC KAUNP MK 65 and *Polyporaceae* sp. GMB-2014 voucher MEL: 2382662, were used for membrane immobilisation.

### 3.2.1 Membrane preparation

The membranes reported in this work were prepared through the phase inversion process depicted in **Figure 3.1**. Several factors that influence membrane morphology were investigated during membrane preparation. The dope solution compositions are presented in **Table 3.1**. The polymer PES was initially dried in an oven at 120 °C for 12 h to remove moisture. The dried polymer was then allowed to cool to room temperature, weighed and added to a previously weighed mixture of PEG and NMP. The solution was vigorously stirred at approximately 60 °C for at least 14 h to ensure complete dissolution of the polymer. The dope solution was then allowed to cool to room temperature and various amounts of ultra-pure water were added dropwise and under stirring conditions to the dope solution. The dropwise addition of the water was carried out to determine the influence of water as a non-solvent on the membrane structure. The resulting solution was stirred for a further 12 h to allow complete homogeneity to occur and thereafter kept at room temperature for the degassing processing to complete. Prior to immersion into a coagulation bath containing ultra-pure water, a manual casting knife and a glass plate was used to cast the solution. The prepared membranes were kept in ultra-pure water at 4 ºC prior to characterization and testing.

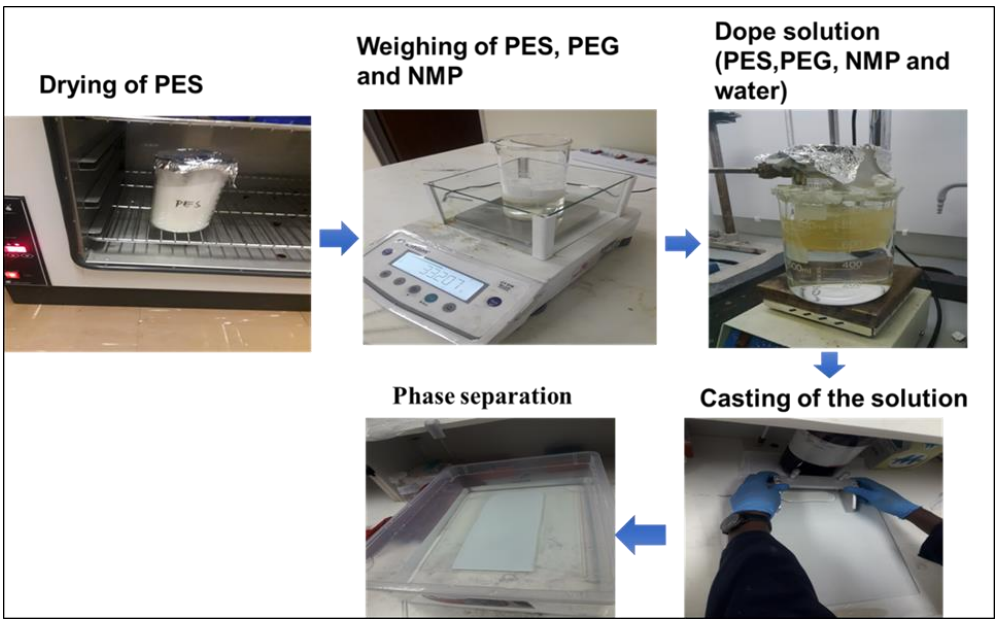


**Figure 3.1**: Graphical representation of polymeric membrane preparation via the phase inversion process.

**Table 3.1**: Casting solution compositions for the fabrication of membranes M.1-M.9.

| Membranes | PES wt.% | NMP wt.% | PEG wt.% | Water wt.% |
|---|---|---|---|---|
| M.1 | 20 | 60 | 20 | 0 |
| M.2 | 20 | 57.5 | 20 | 2.5 |
| M.3 | 20 | 56.5 | 20 | 3.5 |
| M.4 | 20 | 55 | 20 | 5 |
| M.5 | 20 | 44 | 36 | 0 |
| M.6 | 20 | 38.5 | 36 | 5.5 |
| M.7 | 20 | 37.7 | 36 | 6.5 |
| M.8 | 22 | 42 | 36 | 0 |
| M.9 | 22 | 39.5 | 36 | 2.5 |

The coagulation bath composition influences the structure of a membrane. Thus, its effect on membrane performance was determined. The highest performing membranes in terms of water flux were selected from the first set of prepared membranes and thus used to study the influence of the coagulation bath composition on the structure and the performance of the membranes. The concentration variations of the coagulation bath are presented in **Table 3.2**.

**Table 3.2**: Composition of the coagulation bath

| NMP v/v.% | Water v/v.% |
|---|---|
| 0 | 100 |
| 5 | 95 |
| 10 | 90 |
| 15 | 85 |

The third parameter that was studied is the membrane thickness. The following range of membrane thickness was studied: 150 µm, 120 µm, 90 µm and 60 µm.

### 3.2.2 Micro-organisms

#### 3.2.2.1 Sampling sites and sample collection

Fruiting bodies of 18 WRF isolates collected from decaying *Eucalyptus* trees in the following four pulp and paper farms were used in this study: (i) Mondi Farm in Piet Retief (South Africa) (27°06´05.9"S, 31°01´29.7"E); (ii) Montigny Farm near MR 9 in Nhlangano (Eswatini) (26°59´45.8"S, 31°15´38.0"E); (iii) Goodluck Farm, near Maseyisini, Nhlangano (Eswatini) (27°06´22.4"S, 31°09´27.0"E); (iv) J.P Robberts and Sons Plantations (Pty) Ltd Farm, near Nhlangano town (eSwatini) (27°01´06.0"S, 31°14´07.2"E). The locations of the above-mentioned sampling sites are shown as **A**, **B**, **C** and **D**, respectively, in **Figure 3.2**. The samples were collected in paper plates and thereafter placed and transported to the laboratories in cooler boxes at temperatures below 10 °C. The samples were kept overnight at 4 °C in the

laboratories of the University of South Africa, Science Campus, Florida, Johannesburg.

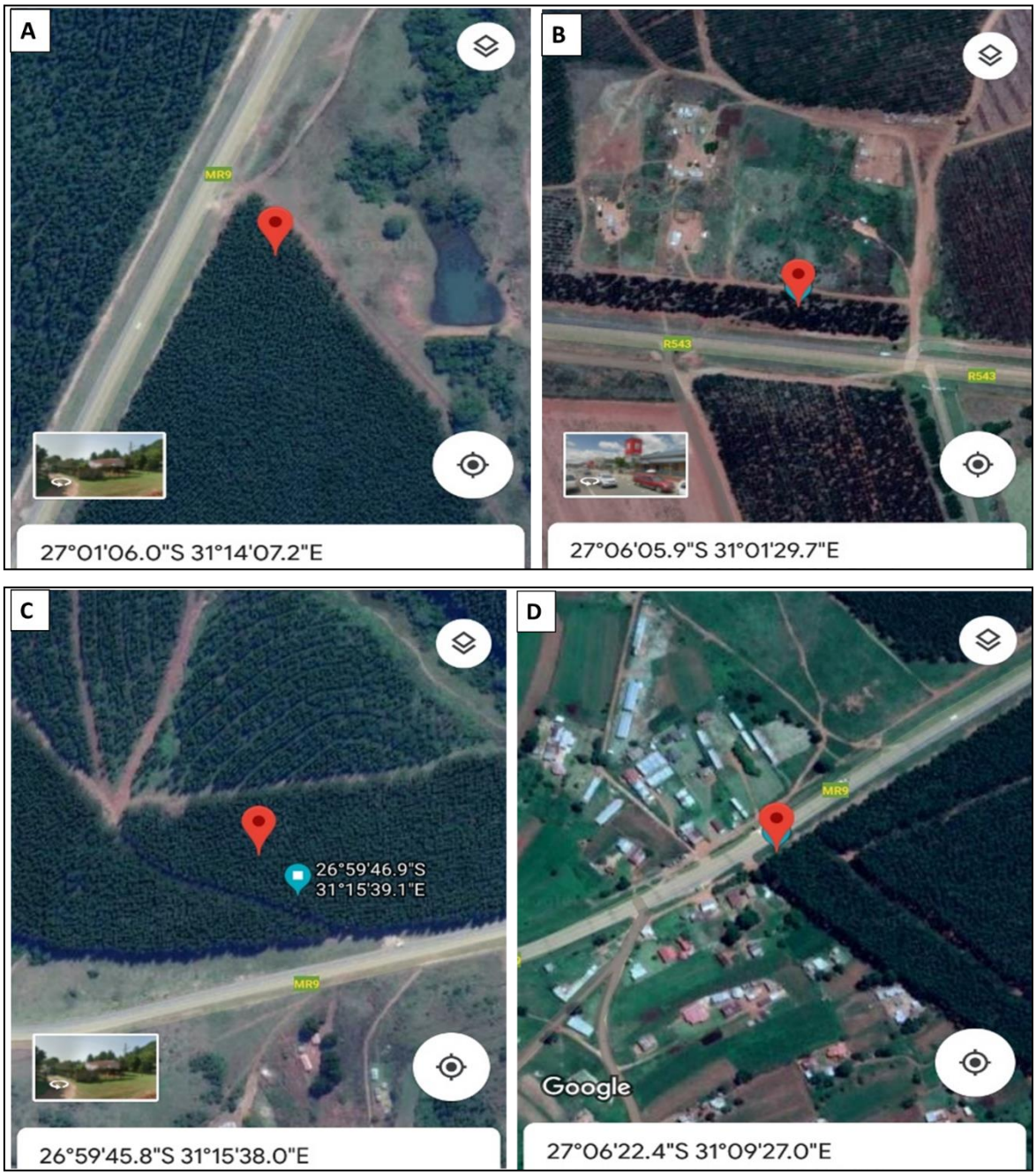


**Figure 3.2**: Satellite imagery showing locations of the four fungal sampling sites.

### 3.2.2.2 Media preparation, plating and sub-culturing

A selective culture media Sabouraud Dextrose Agar (SDA) was prepared by dissolving 63.5 g of SDA in 1 L of deionized water. Prior to autoclaving at 121 °C for

15 min, approximately 0.4 g of the chloramphenicol antibiotic was added to the media to prevent the growth of bacteria. The media was poured into sterile culture plates for solidification. Approximately 0.5 x 1 cm fruiting body was sliced using a sterilized scissor and transferred to the SDA solid media in triplicates and thereafter incubated at 28 °C for 7 days. The fungi were periodically sub-cultured into fresh culture media until pure cultures were obtained. The pure cultures were used for identification and screening of lignolytic enzymes and humic acid. Agar slants were prepared in 100 ml sterile polystyrene tubes, inoculated with pure cultures and stored at 4 °C for future use.

#### 3.2.2.3 Primary screening for ligninolytic enzyme activity

Screening was carried out by supplementing 0.1% guaiacol as a substrate for detecting laccase activity. This screening process was adopted based on the optimised concentration levels reported for the screening of the lignolytic enzymes (Ijoma, 2016; Masalu, 2016; Casceillo *et al*., 2017; Sharma *et al*., 2017). Actively growing mycelia was cut from each pure culture and plated into culture plates with guaiacol, and thereafter incubated at 28 °C for 7 days. Colour change of fungal colonies was observed around and below the colony surface as an indication of lignolytic enzymes activity and their ability to oxidize guaiacol. Culture plates that did not show any colour change were kept in the incubator for a period of 10 days and thereafter discarded when no colour change was observed.

### 3.2.3 Screening of fungal isolates for humic acid (HA) removal

#### 3.2.3.1 HA stock solution preparation

HA stock solution was prepared according to the method proposed by Zahmatkesh *et al*. (2016). After dissolving 4 g of powdered HA in 200 mL of 0.1 M NaOH, the resultant solution was stirred at room temperature for 30 min. Purification of HA solution was carried out by centrifugation for 20 min at 8 000 rpm. The supernatant liquid was withdrawn and approximately 100 mL of 0.5 M potassium hydrogen phthalate was added to the supernatant, and pH of the resultant solution was

adjusted to 4.5 using HCl. The solution supplemented with the buffer was centrifuged at 8000 rpm for 20 min to remove particulates, and the supernatant liquid was sucked using a sterile syringe and used as HA stock solution. The stock solution was filtered (0.45 µm) and used for all the experiments.

### 3.2.3.2 Solid media preparation

Solid media was used to estimate HA decolourization by all the fungal isolates. Mineral and vitamin solution were prepared with slight modifications according to the method reported by Kirk *et al*. (1978). Solution 1 (Mineral) and solution 2 (vitamin) were diluted 5 and 20 folds, respectively. A solution containing a mixture of (0.2 g of $KH_2PO_4$, 0.05 g of $MgSO_4 \cdot 7H_2O$ and 0.01 g of $CaCl_2$) dissolved in deionized water was used as major minerals. The solution was then supplemented with 100 µL solution 1 (mineral), 26 mM ammonium sulphate as nitrogen source, 100 mL HA stock solution as carbon source and 15 g agar for solidification. These were mixed in a 1 L bottle with deionized water and the pH of the resulting solution was adjusted to 4.5 using HCl prior to autoclaving for 15 min at 121 °C. The solution was left to cool down to room temperature and supplemented with 25 µL filtered (0.45 µm) vitamin solution. Finally, the media was poured into culture plates (20 x 100 mm) for solidification.

### 3.2.3.3 Liquid media preparation

To the liquid media containing major minerals (0.12 g of $KH_2PO_4$, 0.03 g of $MgSO_4 \cdot 7H_2O$ and 0.006 g of $CaCl_2$) and 2.064 g of ammonium sulphate, 30 mL of HA stock solution and 60 µL of the solution 1 (mineral) was added in 600 mL of deionized water, and the pH of the resultant solution was adjusted to 4.5 with HCl prior to autoclaving for 15 min at 121 °C. The culture media was then supplemented with 15 µL of solution 2 (vitamin) and the mixture was dispensed into 18 autoclaved 250 mL conical flasks and covered with aluminium foil.

### 3.2.4 Humic acid degradation experiments

#### 3.2.4.1 HA solid media pre-screening

Culture plates with solid agar were inoculated by plating using a sterile blade approximately 1 $cm^2$ of actively growing mycelium from pure fungal culture at the centre of duplicate plates. The plates were then incubated for 15 days at 28 °C in the absence of light and two uninoculated plates were used as controls. The diameter of the fungal growth and decolourization of HA on the plates (top, bottom and vertical) were observed after 4, 7, 10 and 15 days of incubation and were thereafter analysed for qualitative degradation of HA.

#### 3.2.4.2 HA removal in liquid media

All conical flasks with 30 mL liquid media were inoculated with one piece of mycelium growth, incubated in an orbital shaker for effective growth and shaken continuously for 15 days at 28 °C and 150 rpm. A control was uninoculated and incubated with the samples under similar conditions. After incubation, the content of the flasks was filtered through glass fiber filters (0.45µm) prior to conducting dissolved organic carbon analysis and ultraviolet visible absorbances to determine HA removal and degradation after fungal treatment.

### 3.2.5 Production of enzymes

#### 3.2.5.1 Solid state fermentation

Fungal isolates D and R were further studied for enzyme production in solid state fermentation (SSF) as they indicated high laccase activity in solid media and HA removal. SSF is a high enzyme production method whereby solid materials such as corn corb, corn husk or wheat straw are used as a carbon source for the growth of micro-organisms in the presence of little liquid media (Ergun & Urek, 2017). Fermentation was carried out in duplicate in 2 L (isolate R) and 1 L (isolate D) Erlenmeyer flasks (see **Figure 3.3**) using corn husks as a carbon source for fungal growth and little amount of basal media prepared as described by Kirk *et al*. (1978).

Firstly, freshly grown cultures of fungi was inoculated into 250 mL Erlenmeyer flasks containing 100 mL basal medium and incubated for 7 days in duplicates at 30 °C and 150 rpm. The fungal growth was homogenized by stirring at 2.8 rpm using an IKA, T25 digital ULTRA TURRAX mixer and poured into 70 g sterilized corn husks with little amount of basal media and incubated in complete darkness for 21 days at 30 °C. Samples were collected for enzyme assay after 4, 7, 10,15 and 21 days of incubation.

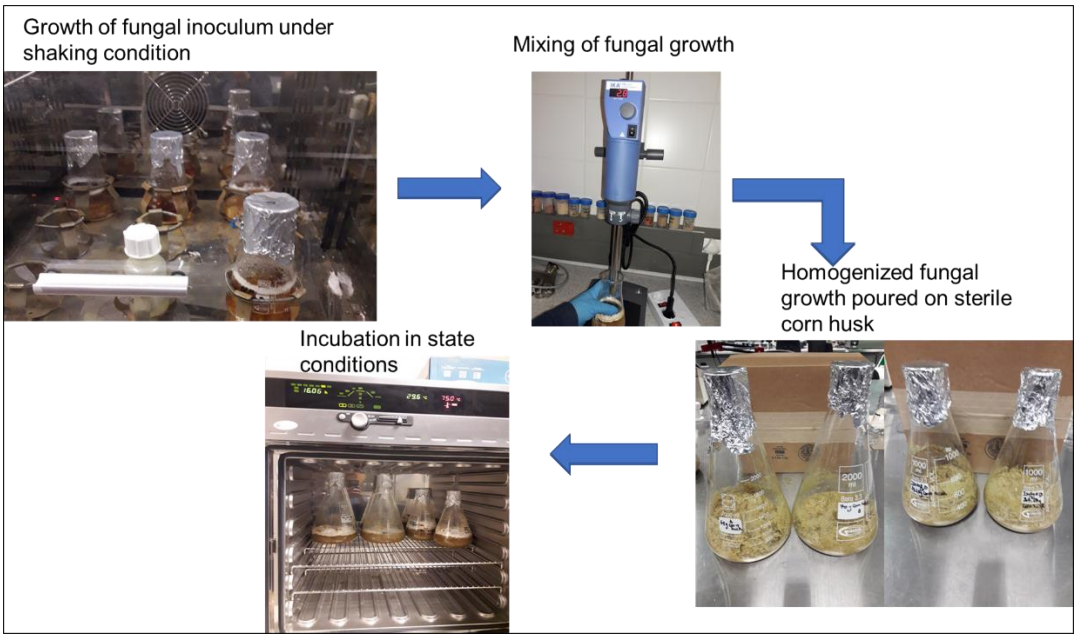


**Figure 3.3**: The solid-state fermentation set-up used in this study.

### 3.2.5.2 Enzyme Assays

The method for determining enzyme activity was adopted from Ijoma (2016) and used with slight modification.

#### 3.2.5.2.1 Laccase activity

Laccase activity was assayed using guaiacol as a substrate. The increase in ultraviolet (UV) absorbance at 470 nm was measured as laccase activity at 25 °C after incubation at 30 °C for 2 minutes. The reaction mixture contained 1.2 mL

guaiacol, 0.4 mL 100 mM sodium buffer at pH 5, and 0.4 mL crude enzymes. The reaction mixture was shaken by swirling and UV absorbances were measured.

#### 3.2.5.2.2. Manganese-dependent peroxidase (MnP) activity

MnP activity was determined in a mixture which consist of 0.4 mL of 0.1 M manganese sulphate, 0.4 mL of 50 mM sodium tartrate at pH 5, 0.6 mL autoclaved deionized water, 0.2 mL crude enzyme and the mixture was activated by adding 0.4 mL of 5 mM hydrogen peroxide ($H_2O_2$). The UV absorbances of the reaction mixture were immediately measured at 350 nm after 1 minute at room temperature.

#### 3.2.5.2.3 Lignin peroxidase (LiP) activity

LiP was assayed in a reaction mixture which contain 0.5 mL veratryl alcohol as a substrate, 0.4 mL of 0.3 M citrate/phosphate buffer at pH 4.5, 40 µL crude enzyme and 1.26 mL autoclaved deionized water. The mixture was activated by adding 250 µL of 5 mM $H_2O_2$ and UV absorbances were immediately measured at 310 nm at room temperature.

The activity for all enzymes were calculated using (**Equation 1**).

$$\boldsymbol{E.A} = \frac{\boldsymbol{A.V}}{\boldsymbol{t.\varepsilon.v}} \qquad \textbf{(1)}$$

where E.A is the enzyme activity (U/mL), A is the absorbance (a.u), V is the total volume of the reaction mixture (mL), t is the incubation time, ε is the enzyme extinction coefficient and v is the volume of crude enzyme (mL).

### 3.2.5.3 Extraction of enzymes

Crude enzymes extraction was carried out after 10 days of incubation by filtering the content of the SSF flasks using a clean cloth. The solid content was rinsed in 0.1 M citrate phosphate buffer (pH 5) and filtered .The filtered solution was centrifuged at 4400 rpm for 20 min to remove particulate and assayed for enzyme activity as previously discussed in **Section 3.2.5.2.** prior to purification.

### 3.2.5.4 Enzyme purification

The crude enzymes were purified using ammonium sulfate precipitation method (Othman *et al*., 2014). Approximately 80 % ammonium sulfate was dissolved in isolate R and D solution while stirring overnight at 0 °C. After centrifuging the mixture for 20 min at 4400 rpm, the supernatant was separated from the precipitate (pellet) by decanting into sterile 250 mL glass bottles and the supernatant liquid was kept at 4 ℃. The precipitate was homogenized in 30 mL of 0.05 M citrate-phosphate buffer (pH 6.0) and stored at 4 °C. Prior to being dialyzed, both solutions were determined for enzyme activity as previously discussed in **Section 3.2.5.2**.

## 3.3 NOM Synthetic solution preparation

Synthetic solutions of humic acid (HA) and bovine serum albumin (BSA) of concentrations of 30 mg/L were prepared by dissolving 0.03 g/L of the pure substance (HA and BSA) in deionized water and used as the feed for rejection studies.

## 3.4 Characterization techniques used in this study

### 3.4.1 Filtration systems

*Cross-flow system (membrane permeability tests)*

Pure water flux was measured in triplicates using a cross-flow filtration system at an operational pressure of 3 bars. The membranes were cut into 8.6 cm length and 3.9

cm width dimensions (effective membrane area = 0.00354 $m^2$) and assembled within the cross-flow cells. The membranes were first compacted at 7 bars for 1 hour to allow for the attainment of a steady flux before collecting the permeate. The water flux was calculated using (**Equation 2**) (Li *et al*., 2016).

$$\boldsymbol{J_w = \frac{V}{\Delta t \, .A}} \qquad \textbf{(2)}$$

where $J_w$ is water flux ($L.m^{-2}.h^{-1}$), V is the permeate volume (*L*), $\Delta t$ is the time taken to collect the permeate (h) and A is the effective membrane area ($m^2$).

*Dead-end cell*

Rejection studies were performed using a dead-end system at 3 bars. Only high performing membranes were selected for rejection studies. Solute percentage rejection for the membranes was calculated using (**Equation 3**) (Li *et al*., 2016).

$$\boldsymbol{R(\%) = \frac{C_f - C_p}{C_f} \times 100} \qquad \textbf{(3)}$$

where $R(\%)$ is the solute rejection, $C_f$ is the feed concentration (mg/L) and $C_p$ is the permeate concentration (mg/L).

### 3.4.2 Wettability

Contact angle measurements for all the prepared membranes were performed using DSA30 Kruss drop shape Analyzer, GmbH (Hamburg, Germany). The aim of measuring the contact angle was to determine the hydrophilicity of the membranes prepared. Membrane samples were initially dried for 12 h at 40 °C and thereafter cut into small pieces on a glass slide prior to analysis using the sessile drop method. The contact angle was measured by delivering a minimum of 10 water droplets at different spots or areas across each membrane surface. The average contact angle value was reported.

### 3.4.3 Mechanical strength

The mechanical properties of the membranes were determined using SAXSpace system (Anton Paar GmbH, Graz, Austria). The membranes were dried for 24 h at 40 °C and thereafter cut into smaller sized membrane samples of 40 x 10 mm dimensions. The membrane samples were then attached to the measuring stage. The cross-section area of the membranes was calculated by multiplying the width and the thickness of the membranes, which were measured using a micrometer. Each membrane sample was clamped on the sides with an aluminium tensile stage and stretched at a speed of 0.50 mm/min. Three samples were tested, and the average value of the tensile strength and elongation was reported.

### 3.4.4 Scanning Electron Microscopy (SEM)

The morphology of the prepared membranes was studied using scanning electron microscopy (SEM) (JSM-IT300 Joel, Tokyo, Japan). This microscope is used to produce 2 dimensional images of a sample by focusing an electron beam which then interact with the atoms of the samples thus resulting in the production of an image or composition of the sample (Akhtar *et al*., 2018). To study the cross-sectional morphology, the membranes were cut into smaller pieces and dipped in liquid nitrogen for fracturing. After being coated with gold, the fractured membrane pieces were analysed with SEM. SEM was also used to study the morphology of all the fungal isolates collected. Relatively small quantities of mycelium growth from fresh cultures were inoculated into glass plates mounted with double-sided tape. The samples were coated with an 8 nm gold layer prior to examination.

### 3.4.5 Water uptake measurements

Membrane samples were initially cut into a size 5.1 $cm^2$ and immersed in ultra-pure water for 24 h. The membrane samples were then dried by placing between two layers of paper towel and weighed immediately. The very same membrane sample was then dried in an oven at 45 ºC and weighed again. The water uptake (%) was calculated using the wet and dry weights of the membrane by (**Equation 4**) (Yee *et al*., 2013).

$$\textbf{Water uptake}\ (\%) = \left(\frac{\mathbf{Ww-Wd}}{\mathbf{Ww}}\right)\ \mathbf{X\ 100} \qquad \textbf{(4)}$$

Where: Ww is the wet membrane weight (g) and Wd is the dry membrane weight (g).

### 3.4.6 Matrix Assisted Laser Desorption Ionisation-Time of flight/ Time of flight Mass Spectrometry (MALDI) Biotyper

Fungal identification was carried out using MALDI Biotyper software. This technique uses a laser energy absorbing matrix that is used as a substrate to assists in the desorption and ionization of sample ions (Patel, 2019). Samples were prepared by standard operating procedure using the cultivation method for filamentous fungi. Mycelium growth from pure culture plates were inoculated in Sabouraud Dextrose Broth (SDB) media contained in 15 mL Falcone tubes and thereafter cultivated for 3 days in a rotator at 20 rpm. Fungi sediments was let to settle at the bottom of the tubes for 10 min, harvested and transferred to a 1.5 mL Eppendorf tube before being centrifuged for 2 minutes at 13 000 rpm. The resultant supernatant was removed, and 1 mL HPLC-grade water was added to the pellets and suspended by vortexing for 1 min. The mixture was centrifuged for the second time, and the supernatant was sucked out. HPLC-grade water (300 µL) and absolute ethanol (900 µL) was added to the pellets, vortexed and centrifuged for 2 min at 13 000 rpm. The supernatant was removed, and the pellets were dried at room temperature before adding 70% formic acid depending on the size of the pellets. An amount of acetonitrile similar to that of formic acid was added and the resultant solution as mixed prior to centrifugation for 2 min at 13 000 rpm. The supernatant (1 µL) was pipetted into a clean MALDI steel target plate and let to dry at room temperature before spotting HCCA solution (1 µL) on the dried samples and left to dry at room temperature prior to analysis.

### 3.4.7 Molecular characterization of fungal isolates

Genomic DNA extraction was carried out by harvesting fresh mycelium growth from 7-day old cultures grown on SDA media. The fungal DNA was extracted using a zymo fungal/bacterial research quick DNA extraction kit following the extraction protocol of the manufacture. Amplification of pure eluted DNA was performed with polymerase chain reaction (PCR) using primers ITS1 and ITS 4 with the following sequence: ITS1 (forward) 5'-TCC GTA GGT GAA CCT GCG G-3' and ITS4 (reverse) 5'-TCC TCC GCT TAT TGA TAT GC-3' (White *et al*., 1990). The amplification was carried out in a 25 µL reaction mixture, which contained 12.5 µL master mix, 0.5 µL primers, 10.5 µL water molecular biology reagent and 1 µL eluted pure fungal DNA. The PCR reaction was run using a BIO-RAD T100 Thermal Cycler. The PCR protocol began with 1 min denaturation at 95 °C, 35 X amplification cycles of denaturation at 95 °C for 1 min, annealing at 53 °C for 1 min and extension at 72 °C for 1 min. Additional extension was carried out at 72 °C for 10 min then maintained at 4 °C. Agarose gel of 0.7 % was prepared in 250 mL TAE and stained with 10 µL ethidium bromide. The final PCR product was sent to Inqaba Biotechnical Industries (Pty) Ltd for sequencing and a BLAST search was carried out using the National Centre for Biotechnology Information (NCBI) software.

### 3.4.8 Natural organic matter (NOM) characterization techniques

*Dissolved organic carbon*

Total organic carbon (TOC) is composed of particulate matter, which gets retained on a filter paper after filtration through a 0.45 µm filter and dissolved organic carbon (DOC), the portion that passes through the filter (Darrien *et al*., 2019). NOM is quantified as DOC using a TOC analyzer to oxidize organic carbon to carbon dioxide (Yoon *et al*., 2018). This technique can be used to determine concentrations of up to 30 000 mg/L for a variety of water samples such as drinking water, wastewater, sea water or grey water (Pan *et al*., 2016). The concentrations of real water samples and residual HA after fungal treatment was determined using a TOC torch analyzer, (Teledyne Tekmar, Mason, Ohio, USA). Residual HA concentration in inoculated and uninoculated flasks was measured as DOC after filtering the samples through

a 0.45µm glass fiber filters. It was also used to measure the concentration of the feed and permeate in membrane filtration.

*Ultra-violet visible (UV-Vis) spectroscopy*

UV-Vis spectrophotometer is a technique used for measuring absorbance of visible light beam by comparing visible light absorbance before and after it passes through a sample analyte (Kim *et al*., 2016). The absorbance of the analyte can be measured using a single wavelength or over a range of spectra. For example, NOM has been reported to absorb at wavelengths in the range of 220 to 280 nm (Matilainen *et al*., 2011). The most used wavelength that is representative of NOM measurements is $UV_{254}$; this range measures the aromatic components of NOM (Nkambule *et al*., 2012). The absorbance of the feed and permeate for BSA, acid blue dye and residual HA were determined using a UV-Vis Spectrometer (Lambda 650S PerkinElmer, USA) in a 1 cm quartz cuvette. The measurements were undertaken by running a full scan (200-400 nm) giving specific attention to 254 nm as the absorbing wavelength for humic substances (Nkambule *et al*., 2012).

## 3.5 References


Akhtar, K., Khan, S.A., Khan, S.B. and Asiri, A.M., 2018. Scanning Electron Microscopy: Principle and Applications in Nanomaterials Characterization. In: *Handbook of Materials Characterization* (pp. 113-145). Springer, Cham.

Casciello, C., Tonin, F., Berini, F., Fasoli, E., Marinelli, F., Pollegioni, L. and Rosini, E., 2017. A valuable peroxidase activity from the novel species Nonomuraea gerenzanensis growing on alkali lignin. *Biotechnology Reports*, *13*, pp.49-57.

Derrien, M., Brogi, S.R. and Gonçalves-Araujo, R., 2019. Characterization of aquatic organic matter: Assessment, perspectives and priorities of research. *Water Research*, p.114908.

Ergun, S.O. and Urek, R.O., 2017. Production of ligninolytic enzymes by solid state fermentation using Pleurotus ostreatus. *Annals of Agrarian Science*, *15*(2), pp.273-277.

Ijoma, G.N., 2016. *Enzyme production and activities of lignocellulolytic fungi cultivated on agricultural residues* (Doctoral dissertation, University of South Africa).

Kim, C., Eom, J., Jung, S. and Ji, T., 2016. Detection of organic compounds in water by an optical absorbance method. *Sensors*, *16*(1), p.61.

Kirk, T.K., Schultz, E., Connors, W.J., Lorenz, L.F. and Zeikus, J.G., 1978. Influence of culture parameters on lignin metabolism by Phanerochaete chrysosporium. *Archives of Microbiology*, *117*(3), pp.277-285.

Li, S., Cui, Z., Zhang, L., He, B. and Li, J., 2016. The effect of sulfonated polysulfone on the compatibility and structure of polyethersulfone-based blend membranes. *Journal of Membrane science*, *513*, pp.1-11.

Masalu, R., 2016. Ligninolytic enzymes of the fungus isolated from soil contaminated with cow dung. *Tanzania Journal of Science*, *42*(1), pp.85-93.

Matilainen, A., Gjessing, E.T., Lahtinen, T., Hed, L., Bhatnagar, A. and Sillanpää, M., 2011. An overview of the methods used in the characterisation of natural organic matter (NOM) in relation to drinking water treatment. *Chemosphere*, *83*(11), pp.1431-1442.

Nkambule, T.I., Krause, R.W.M., Haarhoff, J., & Mamba, B.B., 2012. Natural organic matter (NOM ) in South African waters : NOM characterisation using combined assessment techniques. *Water SA Vol*. 38(5), pp.697-706.

Othman, A.M., Elshafei, A.M., Hassan, M.M., Haroun, B.M., Elsayed, M.A. and Farrag, A.A., 2014. Purification, biochemical characterization and applications of Pleurotus ostreatus ARC280 laccase. *British Microbiology Research Journal*, *4*(12), pp.1418-1439.

Pan, Y., Li, H., Zhang, X. and Li, A., 2016. Characterization of natural organic matter in drinking water: Sample preparation and analytical approaches. *Trends in Environmental Analytical Chemistry*, *12*, pp.23-30.

Patel, R., 2019. A moldy application of MALDI: MALDI-ToF mass spectrometry for fungal identification. *Journal of Fungi*, *5*(1), p.4.

Sharma, A., Aggarwal, N. and Yadav, A., 2017. Isolation and screening of lignolytic fungi from various ecological niches. *Journal of Microbiology Research*, *5*, pp.25-34.

White, T.J., Bruns, T., Lee, S.J.W.T. and Taylor, J., 1990. Amplification and direct sequencing of fungal ribosomal RNA genes for phylogenetics. *PCR protocols: A guide to methods and Applications*, *18*(1), pp.315-322.

Yee, R., Zhang, K. and Ladewig, B., 2013. The effects of sulfonated poly (ether ether ketone) ion exchange preparation conditions on membrane properties. *Membranes*, *3*(3), pp.182-195.

Yoon, G., Park, S.M., Yang, H., Tsang, D.C., Alessi, D.S. and Baek, K., 2018. Selection criteria for oxidation method in total organic carbon measurement. *Chemosphere*, *199*, pp.453-458.

Zahmatkesh, M., Spanjers, H. and van Lier, J.B., 2017. Fungal treatment of humic-rich industrial wastewater: application of white rot fungi in remediation of food-processing wastewater. *Environmental Technology*, *38*(21), pp.2752-2762.

Zahmatkesh, M., Spanjers, H., Toran, M.J., Blánquez, P. and Van Lier, J.B., 2016. Bioremoval of humic acid from water by white rot fungi: exploring the removal mechanisms. *AMB Express*, *6*(1), p.118.

# CHAPTER 4

# IDEAL MEMBRANE STRUCTURE FOR HIGH FLUX AND DOM REMOVAL FROM WATER: INSIGHT INTO THE INFLUENCE OF PREPARATION CONDITIONS

## 4.1 Introduction

This chapter was aimed at preparing high flux polymeric ultrafiltration membrane using polyethersulfone (PES) as the polymer and polyethylene glycol (PEG) as the pore former. The effect of water as a non-solvent additive on the structure and performance of the fabricated membranes was studied. The membranes were prepared by altering influential phase inversion parameters and dope solution composition. In addition, the membranes performance in terms of high flux and dissolved organic matter (DOM) removal from water was optimised by varying the concentration of dope solution, composition of coagulation bath and membrane thickness. Results obtained from the application of PES membranes for high flux and DOM removal from water are discussed in detail in this chapter.

## 4.2 Results and Discussion

### 4.2.1 Membrane characterization

#### 4.2.1.1 Membrane morphology

The morphology of the prepared membranes was studied using scanning electron microscopy (SEM) as outlined in **Section 3.44**. As shown in **Figure 4.1**, the configuration of the resultant membrane structure is influenced by the addition of various amounts of water to the dope solution. Upon addition of water as a non-solvent (i.e. 5 wt.% water) **(Table 3.1)**, an evolution of the shape, orientation

*Part of this work has been submitted for publication to the Journal of Industrial & Engineering Chemistry Research, 10 January 2020.*

and size of macrovoids was observed at constant concentrations of polyethylene glycol (PEG) and polyethersulfone (PES) **(Figure 4.1a-d)**. A further addition of 7 wt.% resulted in phase separation. The phase separation, which resulted in the structure of the M.7 membrane depicted in **Figure 4.1g**, was particularly evident when 6.5 wt.% water was added to the dope solution. The spongy-like structure of the M.7 membrane terminated by large voids is indicative of a phase separation process that gives rise to mechanically poor membranes.

The next step for altering the membrane structure involve increasing the content of the pore former (PEG) from 20 to 36 wt.%. The macrovoids structure persisted until the water content was increased to 5.5 wt.% to form a completely sponge-like structure **(Figure 4.1f)**. Any further increases in the content of the polymer PES did not eradicate the macrovoids. From **Figure 4.1**, it can be concluded that the structural morphology of the membrane is dependent on the composition of the dope solution, which in turn influences physical properties such as viscosity and the solvent-non-solvent demixing rate (phase inversion). For the dope solution of PES/PEG, the optimized water content for achieving a spongy-like structure was found to be 5.5 wt.% (M.6) **(see Figure 4.1f)**, and any increases in the water content beyond 6.5 wt.% (M.7) failed to generate spongy-like structured membranes.

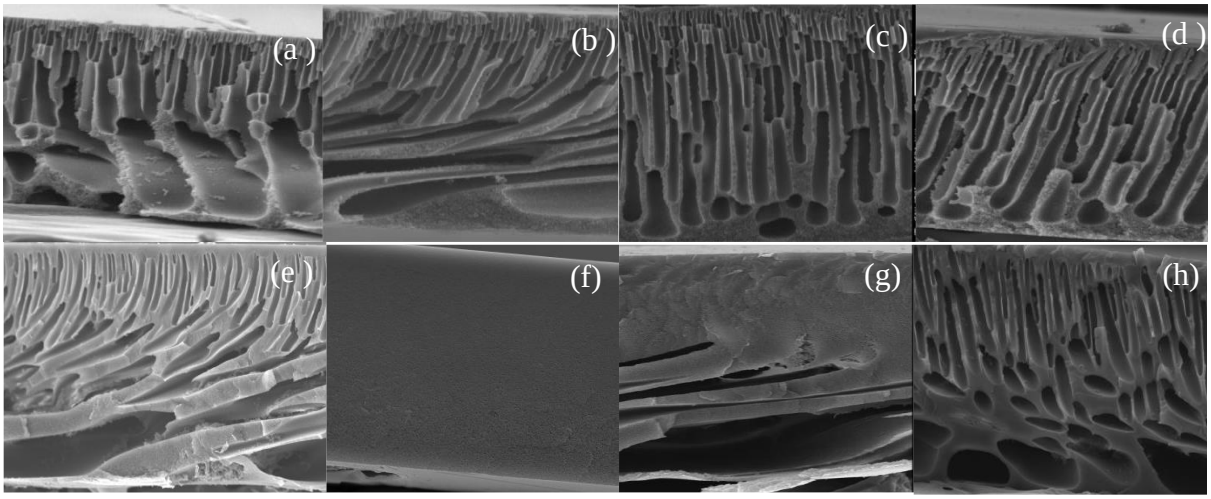


**Figure 4.1**: SEM images showing cross-section of the prepared membranes at x 800 magnification: (a) M.1, (b) M.2, (c) M.3, (d) M.4, (e) M.5, (f) M.6, (g) M.7 and (h) M.8 (membrane composition shown in Table 3.1).

#### 4.2.1.2 Membrane wettability

As previously discussed in **Section 3.4.2**, the wettability of the membranes was determined through contact angle measurements performed on dried membrane pieces. All the measured contact angles were above 60º and were as high as 80º for some of the membranes **(Figure 4.2a)**. In accordance with the basic definition of hydrophilicity, membranes produced in this study were classified as poorly hydrophilic and slightly hydrophobic. The sessile drop method requires that the water contact angle be measured on a dry membrane sample. This means that the angle is measured while the membrane surface is still wetting thus resulting in the actual contact angle being overestimated. **Figure 4.2b** shows the contact angle of M.5 (the most promising membrane in terms of high flux) measured over 10 minutes against that of the hydrophobic membrane under the same conditions. The stabilization of the contact angle at about 47° of polyethersulfone-ultrafiltration (PES-UF) **(see Figure 4.2b)** membrane provides proof that although the PES-UF membranes were hydrophilic, they took a bit of time to hydrate (the decline in water contact angle was attributed to membrane wetting instead of evaporation). It is clear from **Figure 4.2** that the use of water as a non-solvent additive in the dope solution plays no significant role on influencing the wettability of the membranes. This lack of correlation is ascribed to the weak interaction that exists between the water and the polymer. However, the manner in which surface wettability is measured using

the sessile drop method tends to overestimate the measured angles. It is possible that the dry membrane continues to hydrate during measurement of the contact angle. Huhtamäki *et al*. (2018) have suggested that the contact angle measured immediately after a drop is made will always be higher than the contact angle measured min after the drop has been made.

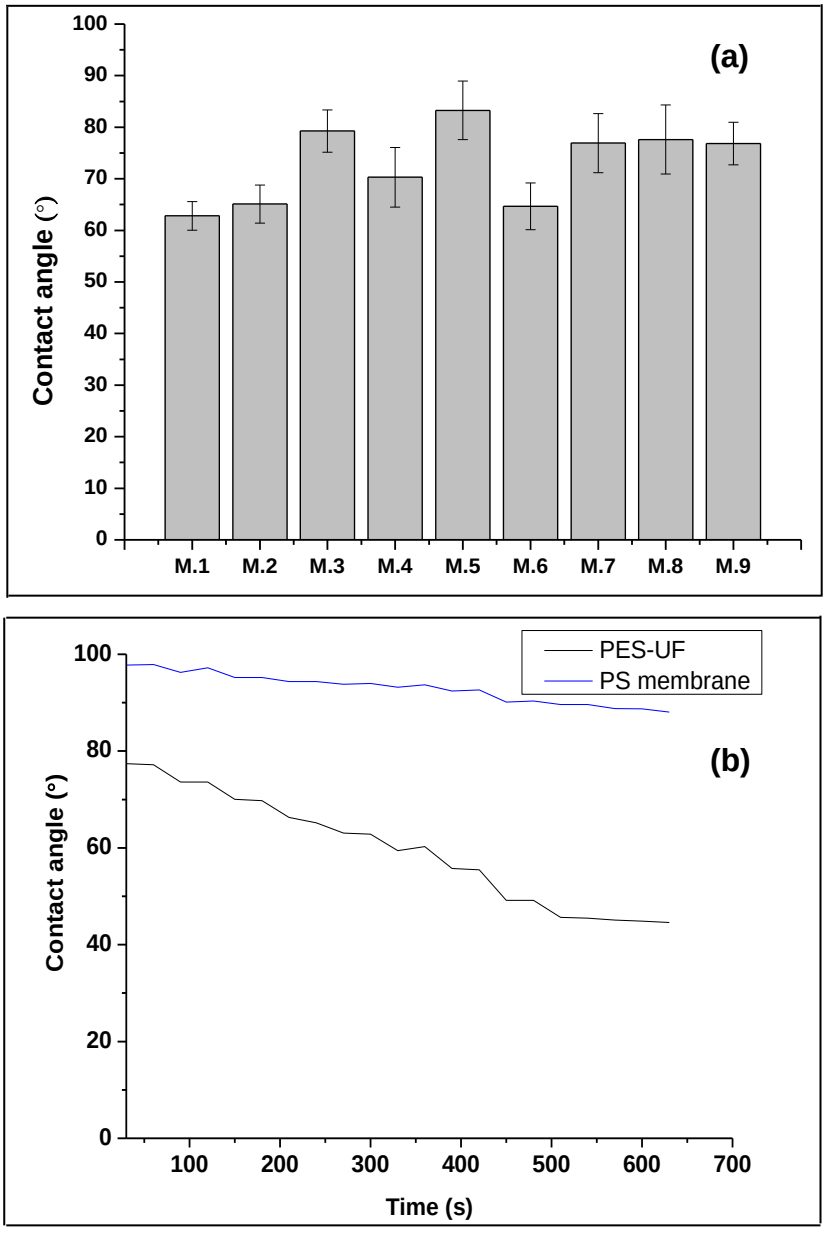


**Figure 4.2**: Wettability of prepared membranes derived from contact angle: (a) water contact angle of membrane variants, (b) water contact angle measured as a function of time for M.5 and a hydrophobic membrane.

### 4.2.1.3 Membrane water uptake measurements

The water uptake measurements of the membranes were accrued out as discussed in **Section 3.4.5** and undertaken using deionized water (see **Figure 4.3**). The equilibrium water content (uptake) of a membrane is used as an indirect measure of the hydrophilicity and flux patterns (Pandey *et al*., 2015). Upon exposure to water, the prepared membranes expanded more than twice their initial weight. When measured against the pristine PES membrane (M.1), a significant increase in the water uptake was recorded in all the membranes under investigation. A large interstitial volume for holding water was noticed in the structures of the membranes, thus confirming the hydrophilicity of the membranes. A correlation seems to exist between the evolution of macrovoids and the interstitial volume as well as the water uptake. A change of the morphology of the membranes from a finger-like to a sponge-like (M.6) gave rise to reduced uptake of the water **(Figure4.3)**. The reduced water uptake suggests that, in line with the results obtained for the water contact angles, the prepared membranes swell upon absorbing water and thus have a significantly large affinity for water. To this end, membranes that take up more water are more likely to possess a good passage for water during filtration.

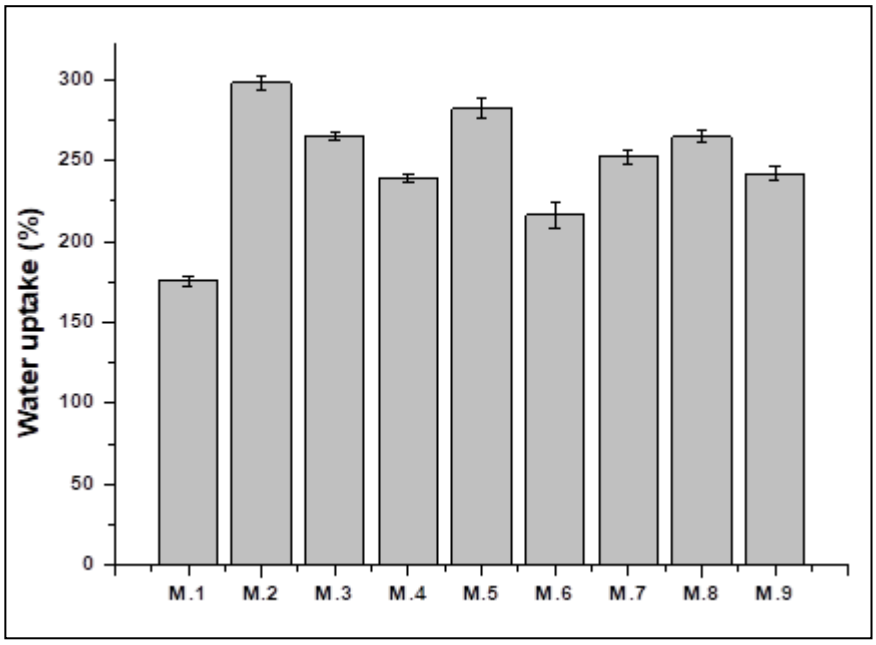


**Figure 4.3**: Water uptake capability of prepared ultrafiltration membranes.

#### 4.2.1.3 Tensile strength

The mechanical strength of the membranes was determined according to a procedure outlined in **Section 3.4.3**. In this work, an existence of a relationship amongst the mechanical properties, structural morphology and water uptake of the membranes was established. Results displayed in **Figure 4.4** demonstrates the lowest tensile strength associated with the M.5 membrane (high flux performing membrane). The weak mechanical strength of M.5 correlates well with its cross-sectional structure **(Figure 4.1e)**, which shows the presence of mixed orientations of the macrovoids. The different macrovoids serves as weak points (tear initiation points) in the membrane structure, thus resulting in an easy tear upon application of a force. However, the same weak points (macrovoids) are responsible for the high-water uptake as shown in **Figure 4.3**. The highest tensile strength and longest elongation was observed for the M.6 membrane. The applied pressure is well distributed throughout the structure of the membrane. Such a result can be attributed to the fully sponge-like structure of M.6 membrane. Furthermore, a high tensile strength and long elongation results from the uniform stretching of the membrane, which is in turn ascribed to the absence of voids (weak points). Therefore, results generated from this study confirm the high mechanical strength measurements reported for sponge-like morphologies (Feng *et al*., 2017; Zhu *et al*., 2017). The mechanical strength of the membranes has implications on the operational pressure and water transport.

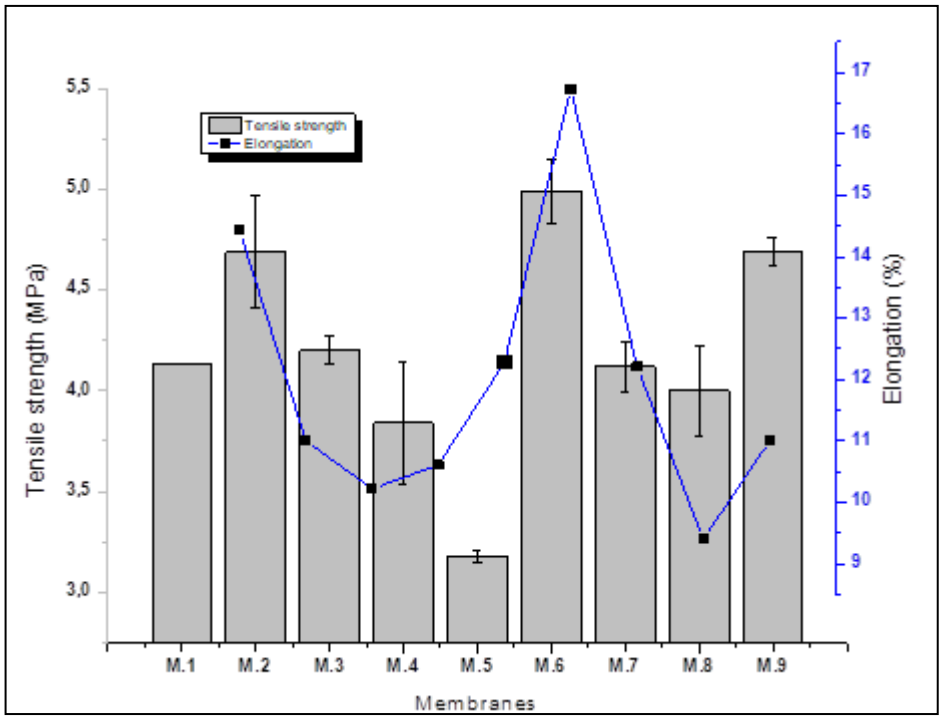


**Figure 4.4**: Tensile strength and elongation of the prepared membranes.

### 4.2.2 Membrane permeability

#### 4.2.2.1 Effect of water as a non-solvent additive in the dope solution

Permeate flux measurements were undertaken as reported in **Section 3.4.1**. Pure water flux tests revealed that the addition of water into the dope solution improved the water flux **(Figure 4.5)**. As previously highlighted in **Figure 4.1**, the optimum water content was 5.5 wt%, beyond which phase separation occurred thus leading to the production of structurally poor membranes. **Table A1** stipulate raw data of the prepared membranes. A water flux of 179.64 $L.m^{-2}.h^{-1}$ was achieved at 3 bars for water content of 5 wt.% **(Figure 4.5)**. To fabricate a membrane with a higher flux, the dope solution was altered by increasing the concentration of the pore former (PEG) from 20 wt.% to 36 wt.% **(Table 3.1)**. This resulted in an increase of the permeate flux from 17.61 (M.2) to 276.72 $L.m^{-2}.h^{-1}$ (M.5) **(Figure 4.5)**. To increase the flux further, an increased content of water (5.5 wt.% and 6.5 wt.%) was added to the dope solution. The membrane with a water content of 6.5 wt.% was found to possess a superior flux (134.33 $L.m^{-2}.h^{-1}$) than the membrane with 5.5 wt.% water

content (45.67 $L.m^{-2}.h^{-1}$). However, the flux obtained for the membrane with a water content of 6.5 wt.% (134.33 $L.m^{-2}.h^{-1}$) was not any higher than that of the M.5 water-free membrane (276.72 $L.m^{-2}.h^{-1}$) due to the dense sponge-like structure of the prepared membranes (M.6). The dense macrovoids-free structure of M.6 membrane was a result of the increased tortuosity (lengthened water path). Although high mass transfer through the membrane has been reported to be favoured by such a structure, this was observed mainly in nanoparticle bearing membranes (Daraei *et al*., 2013). In this study, water passage was contrastingly favoured by the macrovoids structure connected by the open cell structure. On the other hand, the macrovoids-free membrane offered resistance to water passage through the membrane. The low flux and resistance associated with the M.6 macrovoids-free membrane as compared to M.5 was corroborated by the second lowest water uptake results obtained for M.6 (see **Figure 4.3**). Additional attempts aimed at increasing the flux of the membranes were made by increasing the polymer (PES) concentration of the dope solution to 22 wt.% while maintaining the PEG at 36 wt.% (see **Table 3.1**). A flux of 181.43 $L.m^{-2}.h^{-1}$ (M.8) comparable to that of M.4 (179.64 $L.m^{-2}.h^{-1}$) was noticed. However, the addition of water (2.5 wt.%) increased M.8 flux to 264 $L.m^{-2}.h^{-1}$ (M.9). It can be concluded that increasing the concentration of PEG from 20 wt.% to 36 wt.% into the dope solution had an effect in increasing the performance of the membranes under investigation in terms of flux measurements.

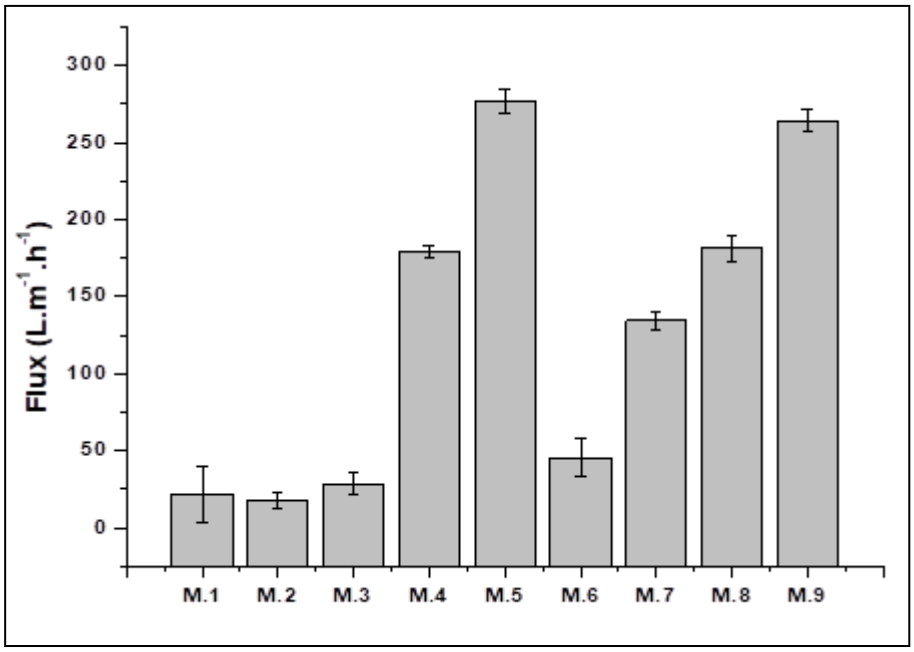


**Figure 4.5**: Recorded pure water fluxes for the prepared membranes operated at 3 bars.

### 4.2.2.2 Effect of coagulation bath composition

The effect of coagulation bath composition **(Table 3.2)** on the structure and performance of the membrane (M.1, M.4, M.5, M.8 and M.9) was studied by varying the concentration of the non-solvent in the coagulation bath. The presence of a solvent in a coagulation bath has been reported to lower the rate of phase inversion (i.e. rate of demixing between the solvent and the non-solvent such as water) (Rahimpour *et al*., 2010a). Such a decrease results to the production of a macrovoids-free structure and a uniform pore distribution such as the one depicted in **Figure 4.1**. In contrast, the morphology of the membranes being investigated in this study, was still dominated by macrovoids even after the concentration of the non-solvent was varied several times. Notwithstanding the domination of macrovoids, a reduction in the concentration of the non-solvent in the coagulation bath led to a modification of the macrovoids into elliptical and tear-like geometries and an interconnecting cell structure. The modification of the membrane morphology enhanced the water flux for the best performing membrane (M.5) **(Figure 4.6a)**. From **Figure 4.6b**, the addition and increment of the solvent in the coagulation bath

resulted in lower contact angles of the membranes. The increased water flux could be due to improved membrane hydrophilicity. The low contact angles can be explained by the slow phase inversion which led to slow PEG escape from the membrane matrix. Thus, resulting in slightly high concentration of PEG remaining in the membrane matrix after phase inversion, leading to increased hydrophilicity. More interestingly, the flux of membrane M.5 after the coagulation bath experiment is comparable to some of the flux obtained by nanoparticle bearing membranes **(Table 4.1)**. The highest flux was 580 $L.m^{-2}.h^{-1}$ recorded by the best performing membrane, M.5. Changing the coagulation bath improved the water flux of the selected membranes (M.1, M.4, M.5, M.8 and M.9) **(Figure 4.6a)**.

**Table 4.1**: Average flux of some nanoparticle bearing membranes.

| **Membrane type (UF)** | **Pressure (bar)** | **Flux ($L.m^{-2}.h^{-1}$)** | **Rejection (%)** | **Reference** |
|---|---|---|---|---|
| PES | 4.0 | 580 | >80 | this work |
| PES/SPSF/O-MWCNT | 1.5 | 560 | >99.9 (BSA) | Gumbi *et al*. (2018) |
| PES/PVP/HANTs | 1.0 | 439 | 90 (BSA) | Mu *et al*. (2019) |
| PSU/GO | 1.4 | 322 | - | Hwang *et al*. (2016) |
| PES/PANI/MWCNT | 1-2 | 490 | 80 (HA) | Lee *et al*. (2016) |
| PVDF/SGO | 1.0 | 450-740 | >95 (BSA) | Ayyaru & Ahn (2017) |
| PVDF/$TiO_2$/GO | 1.0 | 200 | 91 (BSA) | Xu *et al*. (2016) |
| PSF/CS/ $TiO_2$ | 5.0 | 350 | >90 (BSA) | Kumar *et al*. (2013) |
| PES/CuO-ZnO | 2.0 | 679 | >99 (BSA) | Nasrollahi *et al*. (2018) |
| PES/Ag | 2.0 | 520 | - | Teng *et al*. (2009) |

PES: Polyethersulfone; SPSF: Sulfonated polysulfone; O-MWCNT: Oxidized-multi wall carbon nanotube; PVP: Polyvinylpyrrolidone; HANTs: Hydroxyapatite nanotubes; PSU: Polysulfone; GO: Graphene oxide; PANI: Polyaniline; PVDF: Polyvinylidene fluoride; SGO: Sulfonated graphene oxide; $TiO_2$: Titanium dioxide; CS: Chitosan; ZnO: Zinc oxide; Ag: Silver.

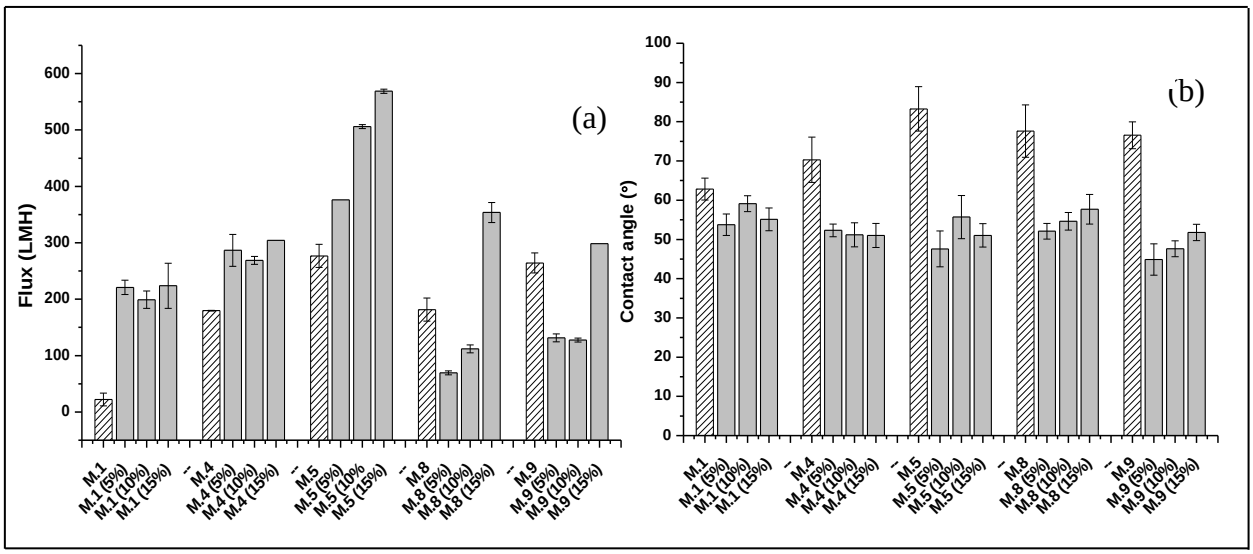


**Figure 4.6**: (a) Pure water flux and (b) wettability of selected prepared membranes.

### 4.2.2.3 Effect of membrane thickness on permeate flux

Membrane thickness has been reported to influence the performance of the membrane (Ahmad, 2005; Hamzah *et al*., 2014). Membrane thickness is inversely proportional to water passage through the membrane; thus, the effect of membrane thickness on the water permeation rates was investigated. After altering the membrane thickness by increasing the polymer concentration in dope solutions, Ahmad (2005) and Hamzah *et al*. (2014) reported that a high polymer concentration produces a thick membrane and a low membrane flux. In this study, the membrane (M.5) thickness was altered by reducing the gap of the casting knife. As depicted in **Figure 4.7** and in sharp contrast to the results reported by Ahmad (2005) and Hamzah *et al*. (2014), the reduction in the membrane thickness led to a corresponding reduction in the membrane flux. This anomaly casts serious doubt on the strategy adopted in this study for altering the thickness of the membrane through the reduction of the gap of the casting knife. It is quite evident that the casting knife approach is not favourable towards the alteration of the thickness of the membrane and ultimately the improvement of the membrane performance. Hence, the most stable thickness was 150 µm.

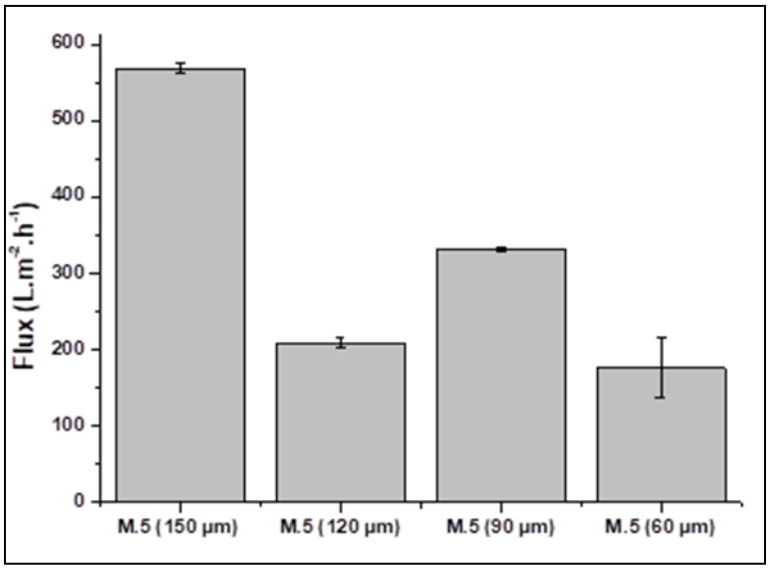


**Figure 4.7**: Effect of membrane thickness on water transport.

### 4.2.3 Rejection studies using model organic substances

Membranes prepared in this study can be classified as tight ultrafiltration membranes. That is, they have a pore size of 300 to 5000 Da (Aryanti *et al*., 2018). As described in **Section 3.4.1**, rejection studies were performed using high permeable membranes (M.1, M.4, M.5, M.8 and M.9) and model organic substances (acid blue dye, 416.4 Da; humic acid (HA), 2.0-1300 kDa (de Melo *et al*., 2016) and bovine serum albumin (BSA), 66.5 kDa). **Figure 4.8** shows that, for all the membranes evaluated, BSA is the most rejected pollutant due to its high molecular weight. Furthermore, all evaluated membranes achieved a rejection percentage of >60% for HA and <35% for acid blue dye **(Figure 4.8)**. From the low rejection rate associated with acid blue, the pore sizes of the prepared membranes were estimated to range between 2000 and 2500 Da. For both BSA and HA, the pristine PES membrane (M.1) achieved a higher rejection rate compared to the other membranes. These findings correlate well with the low water flux demonstrated by M.1 (see **Figure 4.5**). Furthermore, a clear or noticeable correlation between rejection of the pollutants and addition of the water to the dope solution could not be established. For this reason, it was deduced that the non-solvent does not significantly affect the rejection of the model pollutants that were investigated.

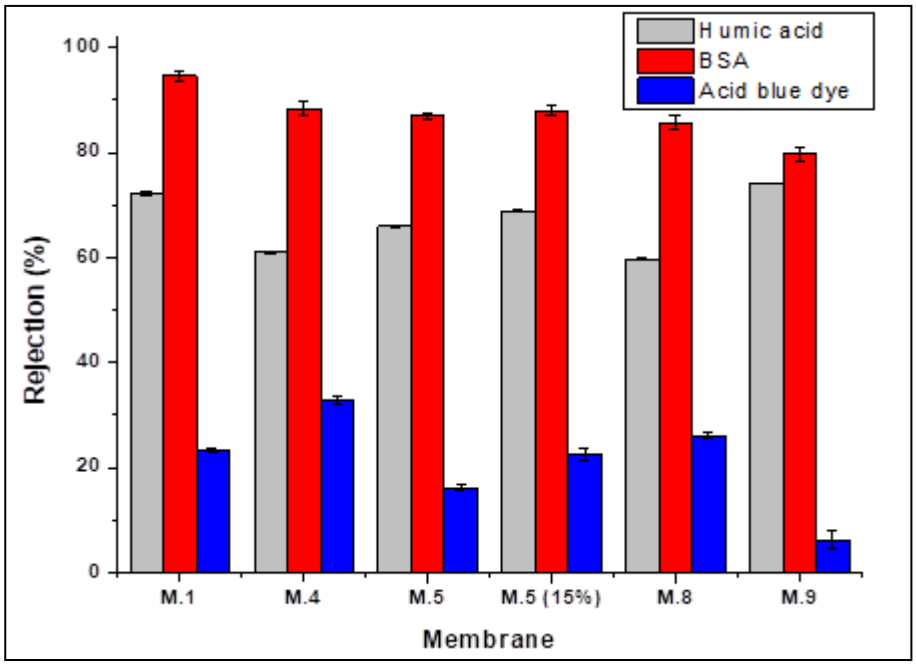


**Figure 4. 8**: Rejection of model organic substances by selected best performing membranes.

## 4.3 Conclusion

Although a sole addition of water to the dope solution of the fabricated ultrafiltration membranes failed to remove any of the macrovoids in the membrane structure except for M.6. An increase of both the water content and PEG from zero to 5.5 wt.% and 36 wt.%, respectively, led to the formation of a membrane possessing a spongy-like structure. Addition of water more than 5.5 wt.% resulted in phase separation and poorly formed membranes. Water permeability was favoured by the macrovoids structure connected by open-cell structures. The study has also revealed that an ideal membrane structure for water transport can be tailored through optimization of dope solution as well as physiochemical properties of the membranes studied. The coagulation bath composition was found to have a major effect on the hydrophilicity and water transport of the fabricated ultrafiltration membranes.

Alteration of membrane thickness had adverse effect on the water transport properties of the membranes. The fabricated membranes demonstrated high rejection rates towards NOM fractions (HA and BSA). For this reason, it is envisaged

that the next generation of membranes will be produced from new plain polymers or polymer prepared through the phase inversion process. It can therefore be concluded that the performance of polymeric membranes can be enhanced without the addition of nanoparticles. Instead, this performance enhancement can be achieved through the alteration of factors that control the phase inversion process, which ultimately dictates the morphology of the resultant membranes.

## 4.4 References

Ahmad, A.L., Sarif, M. and Ismail, S., 2005. Development of an integrally skinned ultrafiltration membrane for wastewater treatment: effect of different formulations of PSf/NMP/PVP on flux and rejection. *Desalination*, *179*(1-3), pp.257-263.

Aryanti, P.T.P., Hakim, A.N., Widodo, S., Widiasa, I.N. and Wenten, I.G., 2018, July. Prospect and Challenges of Tight Ultrafiltration Membrane in Drinking Water Treatment. In *IOP Conference Series: Materials Science and Engineering* (Vol. 395, No. 1, pp. 012012). IOP Publishing.

Ayyaru, S. and Ahn, Y.H., 2017. Application of sulfonic acid group functionalized graphene oxide to improve hydrophilicity, permeability, and antifouling of PVDF nanocomposite ultrafiltration membranes. *Journal of Membrane Science*, *525*, pp.210-219.

Daraei, P., Madaeni, S.S., Ghaemi, N., Monfared, H.A. and Khadivi, M.A., 2013. Fabrication of PES nanofiltration membrane by simultaneous use of multi-walled carbon nanotube and surface graft polymerization method: comparison of MWCNT and PAA modified MWCNT. *Separation and Purification Technology*, 104, pp.32-44.

de Melo, B.A.G., Motta, F.L. and Santana, M.H.A., 2016. Humic acids: Structural properties and multiple functionalities for novel technological developments. *Materials Science and Engineering: C*, *62*, pp.967-974.

Feng, B., Xu, K. and Huang, A., 2017. Synthesis of graphene oxide/polyimide mixed matrix membranes for desalination. *RSC Advances*, 7(4), pp.2211-2217.

Gumbi, N.N., Hu, M., Mamba, B.B., Li, J. and Nxumalo, E.N., 2018. Macrovoid-free PES/SPSf/O-MWCNT ultrafiltration membranes with improved mechanical strength, antifouling and antibacterial properties. *Journal of Membrane Science*, *566*, pp.288-300.

Hamzah, S., Ali, N., Ariffin, M.M., Ali, A. and Mohammad, A.W., 2014. High performance of polysulfone ultrafiltration membrane: Effect of polymer concentration. *Journal of Engineering and Applied Sciences*, 9(12), pp.2543-2550.

Huhtamäki, T., Tian, X., Korhonen, J.T. and Ras, R.H., 2018. Surface-wetting characterization using contact-angle measurements. *Nature Protocols*, 13(7), p.1521.

Hwang, T., Oh, J.S., Yim, W., Nam, J.D., Bae, C., Kim, H.I. and Kim, K.J., 2016. Ultrafiltration using graphene oxide surface-embedded polysulfone membranes. *Separation and Purification Technology*, 166, pp.41-47.

Kumar, R., Isloor, A.M., Ismail, A.F., Rashid, S.A. and Al Ahmed, A., 2013. Permeation, antifouling and desalination performance of TiO2 nanotube incorporated PSf/CS blend membranes. *Desalination*, 316, pp.76-84.

Lee, J., Jeong, S. and Liu, Z., 2016. Progress and challenges of carbon nanotube membrane in water treatment. *Critical Reviews in Environmental Science and Technology*, 46(11-12), pp.999-1046.

Mu, Y., Zhu, K., Luan, J., Zhang, S., Zhang, C., Na, R., Yang, Y., Zhang, X. and Wang, G., 2019. Fabrication of hybrid ultrafiltration membranes with improved water separation properties by incorporating environmentally friendly taurine modified hydroxyapatite nanotubes. *Journal of Membrane Science*, 577, pp.274-284.

Nasrollahi, N., Vatanpour, V., Aber, S. and Mahmoodi, N.M., 2018. Preparation and characterization of a novel polyethersulfone (PES) ultrafiltration membrane modified with a CuO/ZnO nanocomposite to improve permeability and antifouling properties. *Separation and Purification Technology*, 192, pp.369-382.

Pandey, T.P., Maes, A.M., Sarode, H.N., Peters, B.D., Lavina, S., Vezzu, K., Yang, Y., Poynton, S.D., Varcoe, J.R., Seifert, S. and Liberatore, M.W., 2015. Interplay between water uptake, ion interactions, and conductivity in an e-beam grafted poly (ethylene-co-tetrafluoroethylene) anion exchange membrane. *Physical Chemistry Chemical Physics*, 17(6), pp.4367-4378.

Rahimpour, A., Jahanshahi, M., Mortazavian, N., Madaeni, S.S. and Mansourpanah, Y., 2010. Preparation and characterization of asymmetric polyethersulfone and thin-film composite polyamide nanofiltration membranes for water softening. *Applied Surface Science*, 256(6), pp.1657-1663.

Silva, F.C., 2018. Fouling of Nanofiltration Membranes. *Nanofiltration*, p.119.

Teng, S.X., Wang, S.G., Gong, W.X., Liu, X.W. and Gao, B.Y., 2009. Removal of fluoride by hydrous manganese oxide-coated alumina: performance and mechanism. *Journal of Hazardous Materials*, 168(2-3), pp.1004-1011.

Xu, Z., Wu, T., Shi, J., Teng, K., Wang, W., Ma, M., Li, J., Qian, X., Li, C. and Fan, J., 2016. Photocatalytic antifouling PVDF ultrafiltration membranes based on synergy of graphene oxide and TiO2 for water treatment. *Journal of Membrane Science*, 520, pp.281-293.

Zhu, M., Han, J., Wang, F., Shao, W., Xiong, R., Zhang, Q., Pan, H., Yang, Y., Samal, S.K., Zhang, F. and Huang, C., 2017. Electrospun nanofibers membranes for effective air filtration. *Macromolecular Materials and Engineering*, *302*(1), p.1600353.

# CHAPTER 5

# SCREENING OF FUNGAL ISOLATES FOR HUMIC ACID REMOVAL AND DECOLOURIZATION

---

## 5.1 Introduction

Humic acid (HA) constitutes approximately > 70 % of natural organic matter (NOM) in surface water (Haarhoff *et al*., 2013; Nkambule *et al*., 2012), therefore in this chapter, HA was used as the closest model compound for NOM. The isolation and identification of white rot fungi (WRF) isolates using three well studied methods is also discussed in this chapter. Furthermore, the screening of isolated fungi for their ability to produce lignolytic enzymes and HA removal is discussed. Lastly, the production, purification and assay of the enzymes is also chronicled. The aim of this part of the study was to identify WRF isolates that would produce enzyme laccase in high quantities for immobilisation on the high flux performing membrane surface prepared in **Chapter 4**.

## 5.2 Results and discussion

### 5.2.1 Identification of fungal isolates

#### 5.2.1.1 Morphological examination

Identification of fungal isolates using morphological characterization techniques could be another useful method to identify fungi. In a study by Hopkins *et al*. (2007), morphological characterization techniques were successfully used for the identification of Australian wood decay fungal species based on their morphology and mycelium texture. The identification of the fungal isolates was also confirmed using the molecular method (Hopkins *et al*., 2007). In this work, the fungal isolates basidiocarps/fruiting bodies were initially identified based on morphological

characteristics and mycelium texture on dead decaying *Eucalyptus* wood, and colony growth characteristics on solid agar media as described by Hopkins *et al*. (2007). To determine the ultrastructural morphology differences in the fungal isolates, scanning electron microscopy (SEM) was used as discussed in **Section 3.4.4**. The identity of the fungal isolates was also confirmed by molecular methods, MALDI-TOF biotyping and sequencing of the internal transcribed spacer (ITS) region gene. **Figure 5.1** shows images of fruiting bodies of the fungal isolates growing on decaying wood of *Eucalyptus* trees, the fungal pure cultures on agar plates, and SEM images of the mycelium growth. A similar growth of the isolates on decaying wood has also been observed on solid media (see **Figure 5.1 (1** and **2)**). When comparing the morphology of the isolates, several similar physical features were observed. Based on the physiological features of the mycelium growth, the fungal isolates can be identified as fungal species classified under *Basidiomycota* and *Ascomycota* categories. Three of the isolates showed physical features of hyphae producing basidium such as isolates A, B and M. Similar features of aerial hyphae with clamp connections were shown in isolates D, F, and R. As observed for isolates L, N, P, Q and S, some of the isolates only displayed aerial hyphae. As indicated in **Figure 5.1**, isolates E and J displayed features of hyphae with chlamydocodia. Whereas isolate K showed production of conidia throughout the mycelium growth, isolate I showed a unique chain structure of arthroconidia.

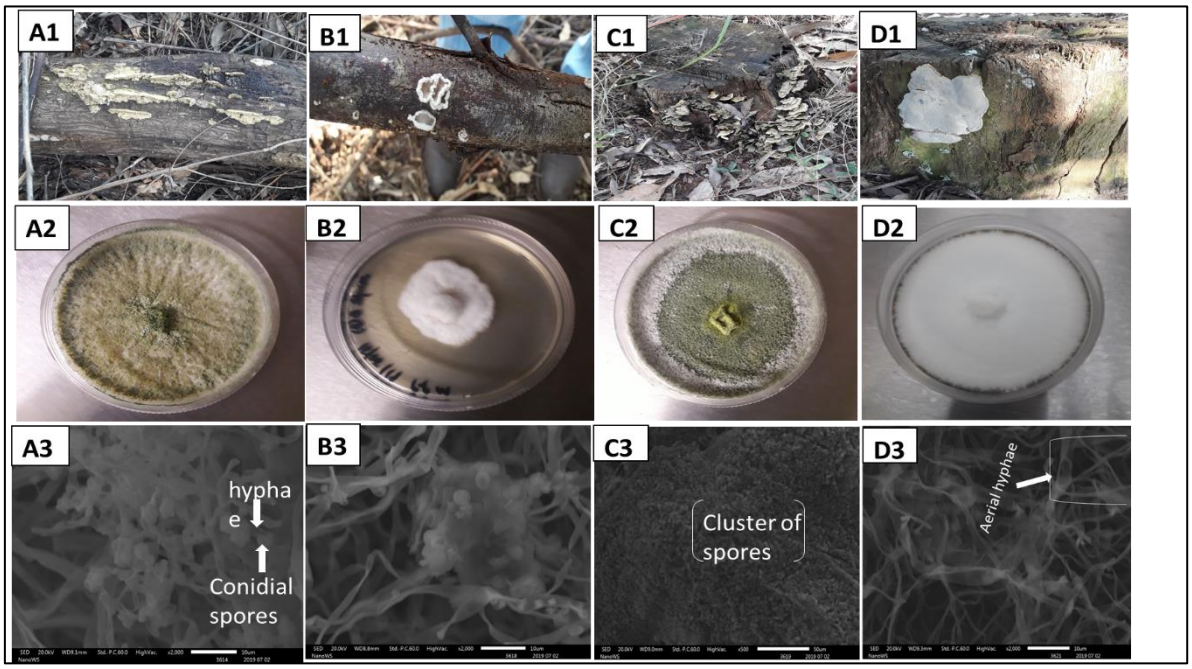

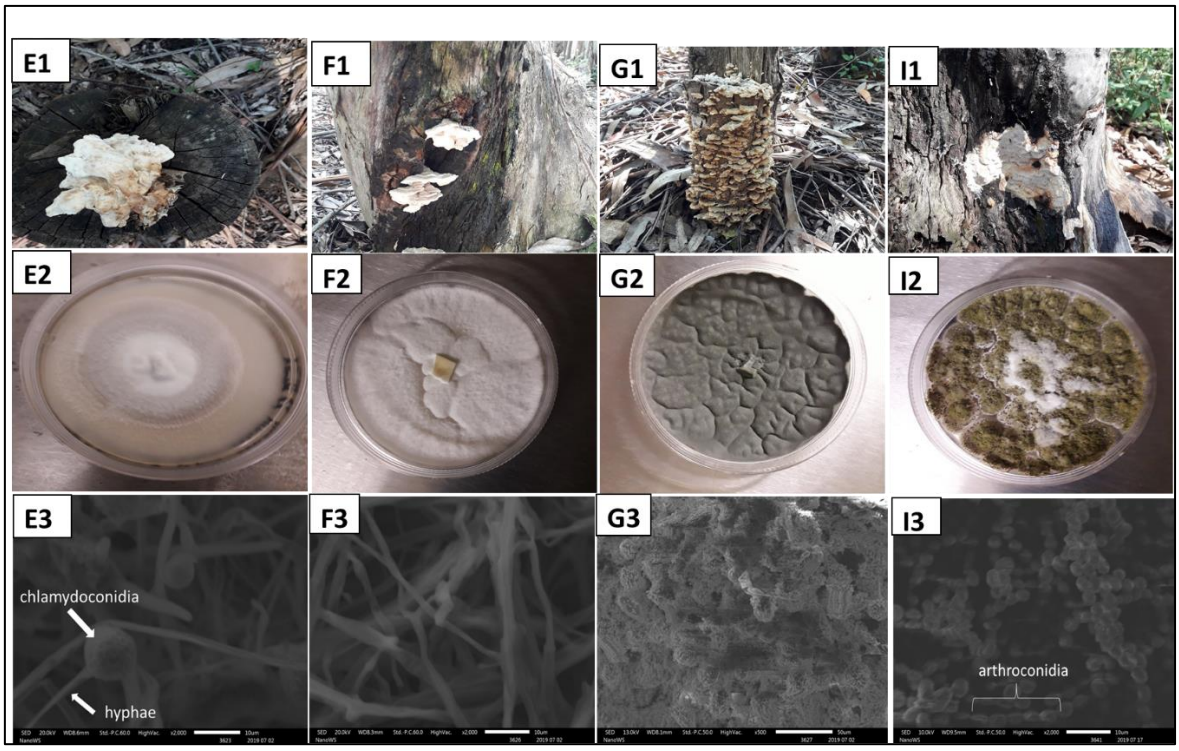
E1
F1
G1
I1
E2
F2
G2
I2
E3
chlamydoconidia
hyphae
F3
G3
I3
arthroconidia

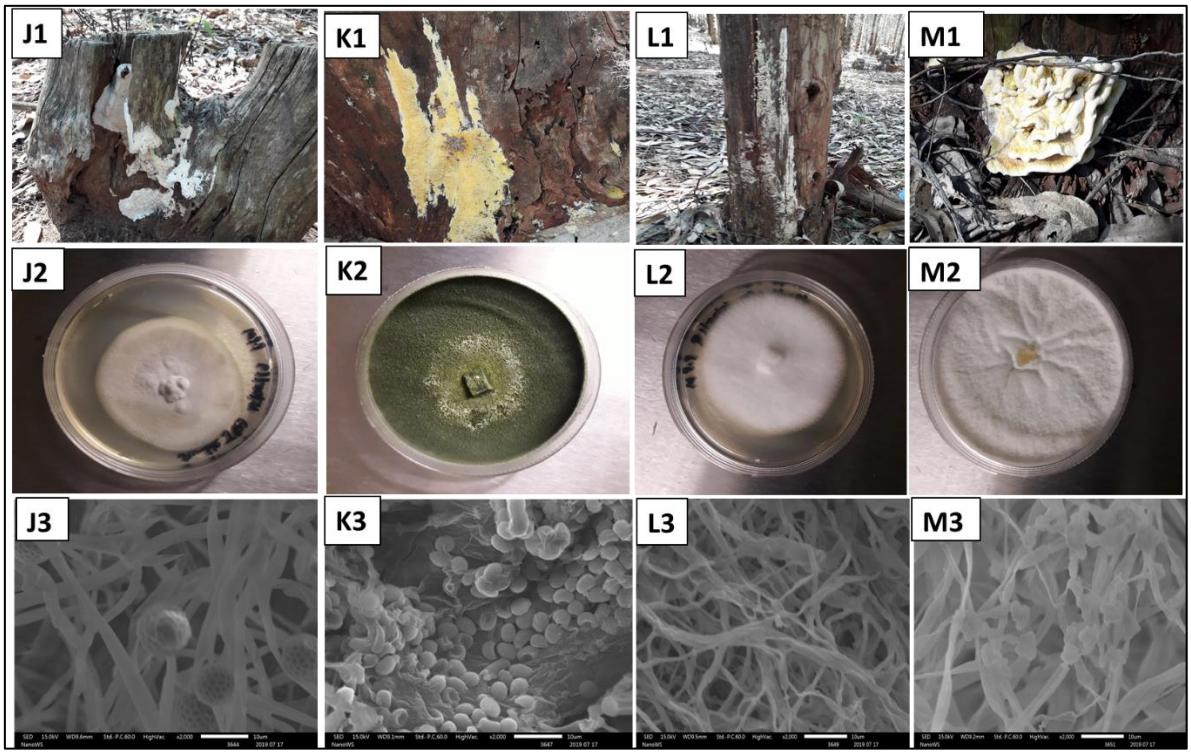
J1
K1
L1
M1
J2
K2
L2
M2
J3
K3
L3
M3

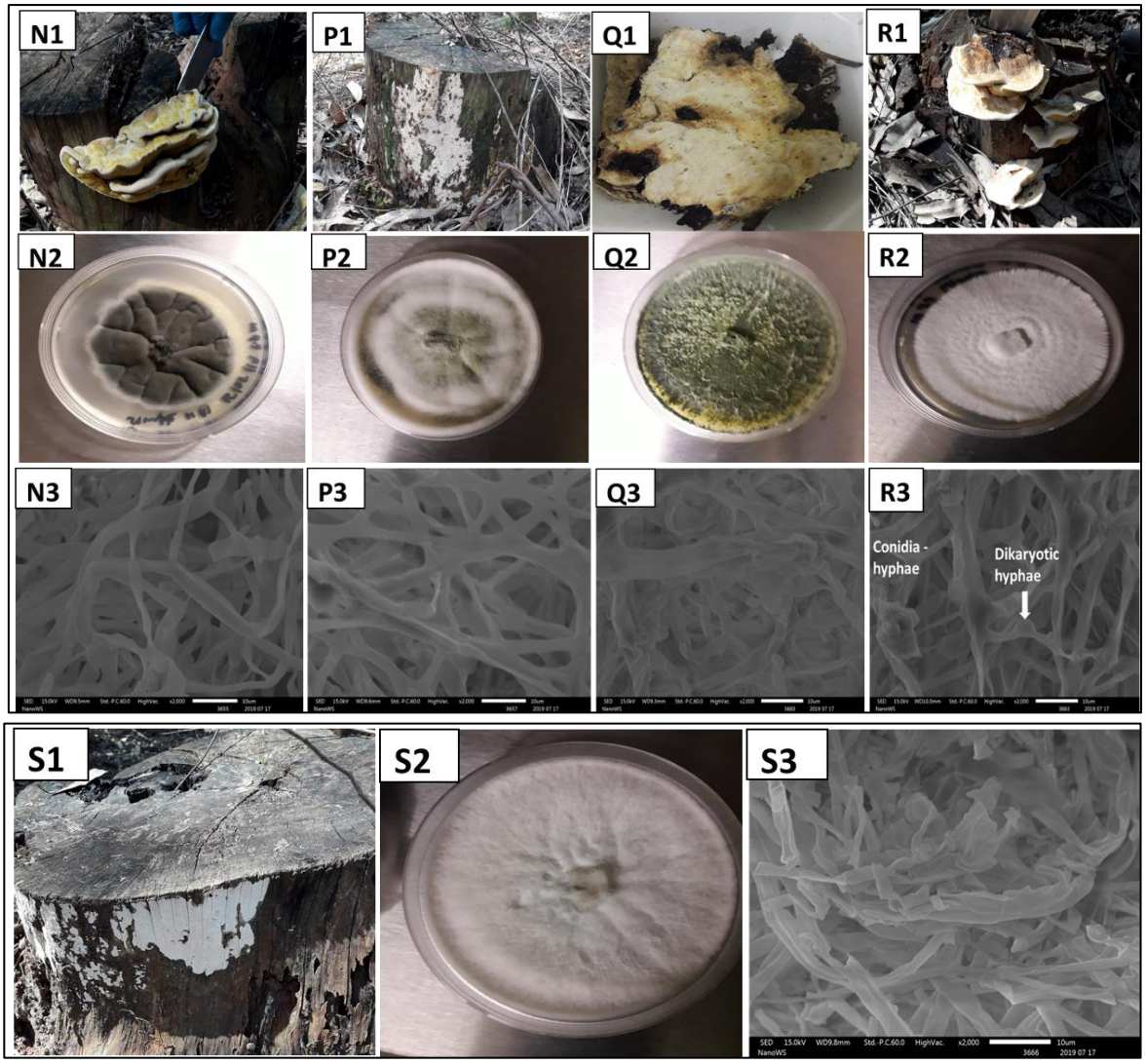


**Figure 5.1**: Showing fruiting bodies (1) and pure cultures (2) of the fungal isolates investigated. SEM images (3) showing typical morphological features of the fungal isolates used in this study at X2000 magnification, only isolates C at X500 magnification.

### 5.2.1.2 Matrix assisted laser desorption ionisation-Time of Flight (MALDI-TOF) biotyping

Of the 18 fungal isolates collected, only three (A, L and I) were successfully identified with MALDI-TOF Biotyper. The previously identified strain *Issatchenkia orientalis* ATCC 6258 was also run as positive control for identification. The strain

*Issatchenkia orientalis* ATCC 6258 was obtained from the Nanotechnology and Water Sustainability (NanoWS) laboratory at the University of South Africa. The mass spectrum generated by MALDI-TOF Biotyper of the identified species is shown in **Figure 5.2**. The strain ATCC 6258 was identified as *Issatchenkia orientalis* with a high confident score level of 2.09 showing high intensity at a mass to charge ratio of between 6000-6500 m/z. Of the three isolates identified by MALDI-TOF Biotyper, only isolate L showed a high confident score level (2.09) and was identified as *Trichoderma longibrachiatum* DD. Generally, a score level of ≥2.0 indicates high confident identification level of the species and a score level between 1.7 and 1.999 can be used for genus-level identification, whereas a score level of <1.7 is taken as not reliable results (Riat *et al*., 2015). The other two isolates (A and I) had low confident score levels of 1.79 and 1.83, respectively. Isolate A was identified as *Trichoderma longibrachiatum* and isolate I as *Aspergillus flavus* CCI. High intensities for the isolates A, L and I were obtained at a mass to charge ratio of between 6100-7100, 6000-6700 and 4000-4500 m/z, respectively. The high intensities are an indication that the high amounts of ions of the species are present in the sample and an increase in mass to charge ratio indicates large amounts of ions of the identified species in the sample (Cassagne *et al*., 2016).

Collectively, these results show that using MALDI-TOF Biotyper automation control and the Bruker Biotyper 3.1 software and library (version 3.1.66, encompassing 4613 entries; Bruker Daltonics, Billerica, MA, USA) did not successfully identify most of the fungal isolates. Consist with this observation, several reports reveal poor identification of species as a result of the paucity of representative spectra in the database (De Carolis *et al*., 2014; De Respinis *et al*., 2014). Therefore, expanding the database with additional extended MS library, especially MALDI-TOF MS spectra from more reference strains has been suggested (De Carolis *et al*., 2014; Rizzato *et al*., 2015).

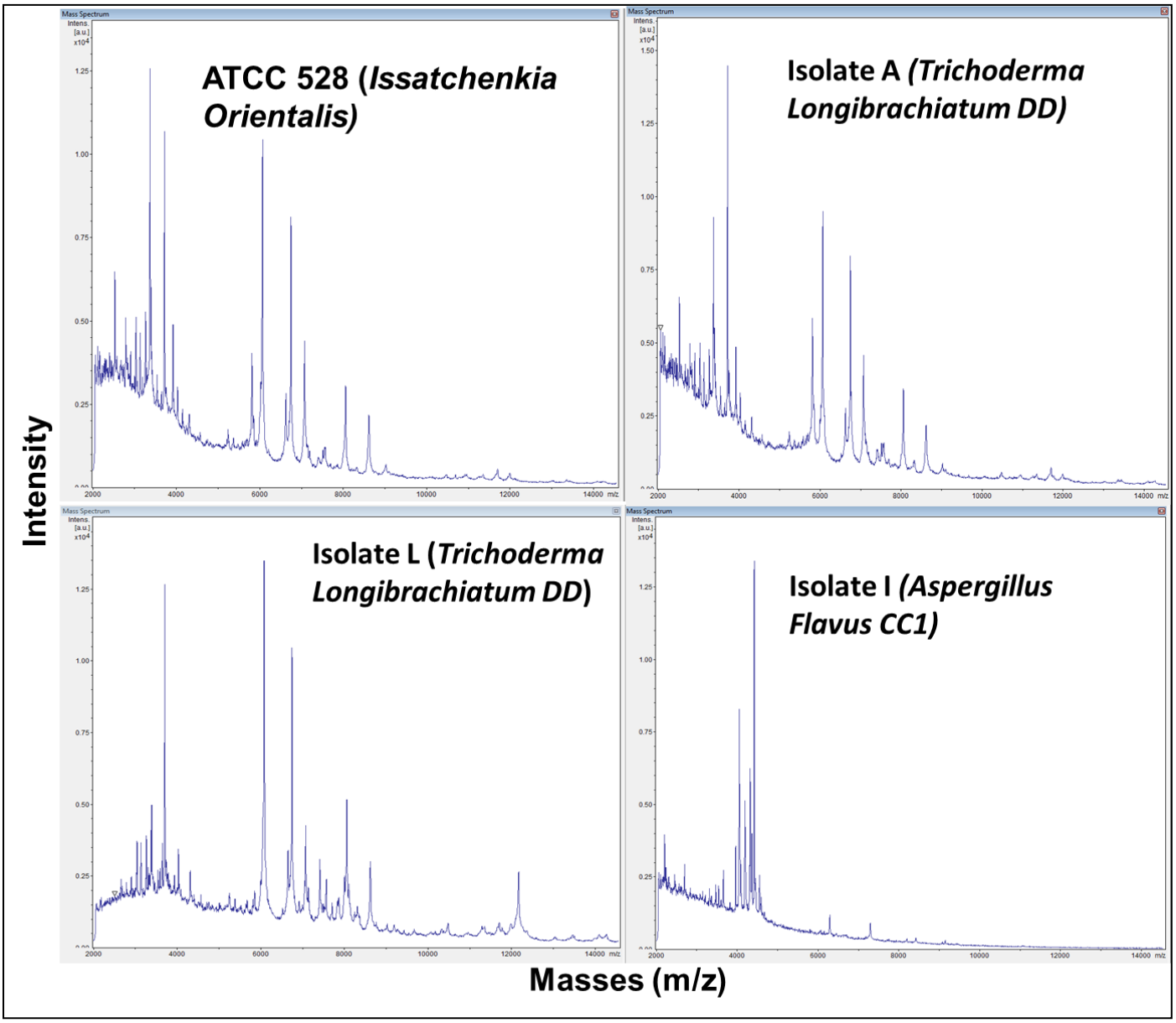


**Figure 5.2**: Mass spectrum of the identified isolates (A, L and I) and reference (strain ATCC 6258) produced by MALDI-TOF Bruker Biotyper.

### 5.2.1.3 Molecular characterization

Due to inability to successfully identify fungal isolates using MALDI-TOF biotyping, molecular identification-based polymerase chain reaction (PCR) amplification and sequencing of internal transcribed sequence (ITS) gene was performed. The PCR product of the ITS region (ITS1 –ITS4) were within the expected size of ~750bp (base pair) **(Figure 5.3),** which is within the range of filamentous fungi region. The ITS PCR product indicate that there was no contamination since the controls (C1

and C2) did not show any presence of deoxyribonucleic acid (DNA). Lane M1 and M2 represent the 100 bp molecular size ladder used, whereas lanes A-M and N-N1 were the ITS PCR for the 18 fungal isolates under study.

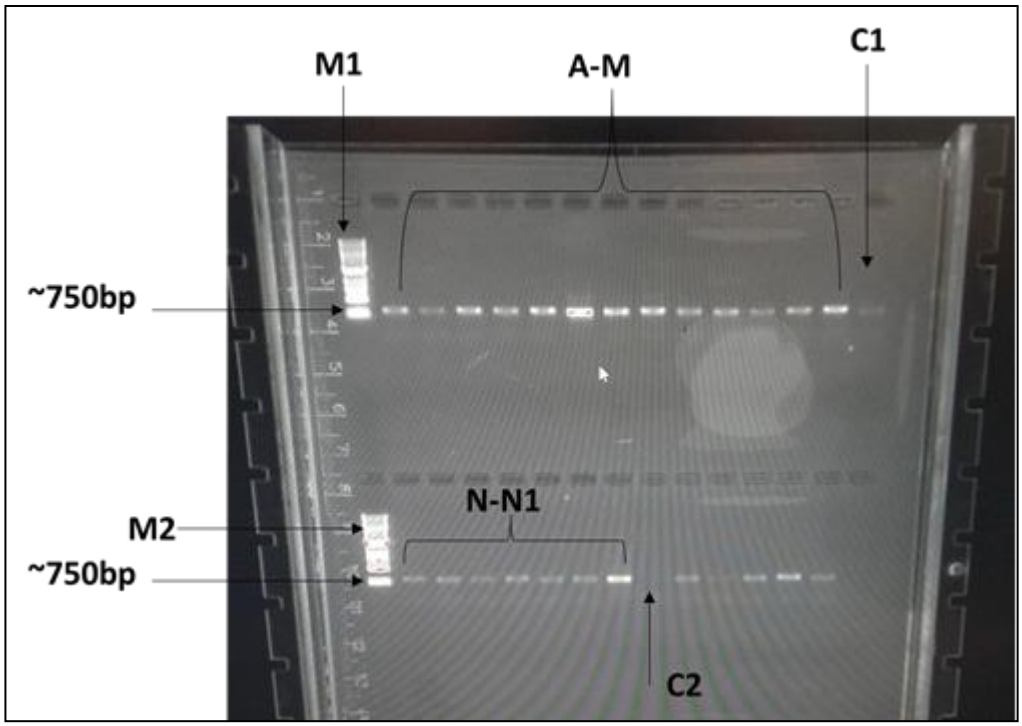


**Figure 5. 3**: Showing a gel electrophoresis image of the PCR product of the fungal isolates in this study.

Basic local alignment search tool (BLAST) search of the resultant 17 ITS sequences on GenBank confirmed that the isolates belonged to phylum *Ascomycota* (13 isolates), *Basidiomycota* (3 isolates) and *Zygomycota* (1 isolate). The descriptions, accession number, E value and percentage identity of the identified species are presented in **Table 5.2**. Isolate H could not give enough data to be successfully processed for sequencing and was thus omitted from **Table 5.1**. The species were chosen based on the highest percentage identity and the lowest E value. From the results obtained, the percentage identity ranged between 97.5 -100 % and most of the E values were 0.0 **(Table 5.1)**. Consistent with results obtained from MALDI-TOF Biotyper **(Figure 5.2)**, analysis of isolates A, I and L concur with results of the molecular identification, which identified isolates A, I and L as *Trichoderma*

*longibrachiatum*, *Aspergillus flavus* and *Trichoderma koningiopsis* isolate upmd, respectively. Although, isolate I was identified as *Trichoderma longibrachiatum* using the MALDI-TOF Biotyper, it still belongs to the same division as *Trichoderma koningiopsis*.

**Table 5.1**: Descriptions of the species identified from ITS gene sequencing analysis

| Isolate | Closest relative | Taxonomic classification | E. value | Identity (%) | Accession No. |
|---|---|---|---|---|---|
| A, E, Q | *Trichoderma longibrachiatum* GS45 | Ascomycota; | 0.0 | 100.00 | MN511324.1 |
| C, K | *Trichoderma ghanense* isolate CTCCSJ-W-SD22035 | Sordariomycetes; Hypocreales; | 0.0 | 99.82 | MF383137.1 |
| F | *Trichoderma erinaceum* isolate SWFU000006 | Hypocreaceae | 0.0 | 99.45 | MK 862245.1 |
| L | *Trichoderma koniniopsis* isolate upmd | | 0.0 | 100.00 | MK 027312.1 |
| P | *Trichoderma deliquescens* isolate CTCCSJ-F-KZ23239 | | 0.0 | 100.00 | MF 408466.1 |
| S | *Trichoderma ovalisporum* strain LHL1-1 | | 0.0 | 100.00 | MN 509070.1 |
| G | *Aspergillus fumigatus* isolate IF1SW-F4 | Ascomycota; | 0.0 | 99.81 | KX 675260.1 |
| I | *Aspergillus flavus* strain ND34 | Eurotiomycetes; Eurotiales; Trichocomaceae | 0.0 | 100.00 | MG 659628.1 |
| M | *Verrucaria polysticta* isolate MM10 | Ascomycota; Eurotiomycetes; Verrucariales; Verrucariaceae | 3e-10 | 100.00 | MK 773877.1 |

**Table 5.1 (continued)**

| Isolate | Closest relative | Taxonomic classification | E. value | Identity (%) | Accession No. |
|---|---|---|---|---|---|
| N | *Setosphaeria rostrate* strain UAS 467D | Ascomycota; Dithideomycetes; Pleosporales; Pleosporaceae | 0.0 | 100.00 | MH 201156.1 |
| D | *Perenniporia* sp. UOCKAUNP MK65 | Basidiomycota; | 0.0 | 100.00 | KR907878.1 |
| R | *Polyporaceae* sp.6 GMB-2014 | Agaricomycetes; Polysporales; Polyporaceae | 0.0 | 97.54 | KP013025.1 |
| B | *Schizophyllum* sp.KN4 | Basidiomycota; Agaricomycetes; Agaricales; Schizophyllaceae | 0.0 | 99.82 | KU253771.1 |
| J | *Umbelopsis isabelline* strain B-3A | Zygomycota; Umbelopsidomycetes; Mucorales; Umbelopsidaceae | 0.0 | 99.64 | MK 358980.1 |

Evolutionary interrelations amongst the identified fungal isolates was carried out by conducting a phylogenic analysis using the maximum likelihood method and Kimura 2-parameter model described by Kimura, (1980). The evolutionary analysis was conducted in MEGA X (Kumar et al., 2018). **Figure 5.4** indicate an ancestral relationship between the fungal isolates. Partial deletion option was selected to eliminate <5 % alignment gaps and missing data. The phylogenic tree shows evolutional relationship amongst the species, which mostly identified as evolved from the *Trichoderma* group of fungi.

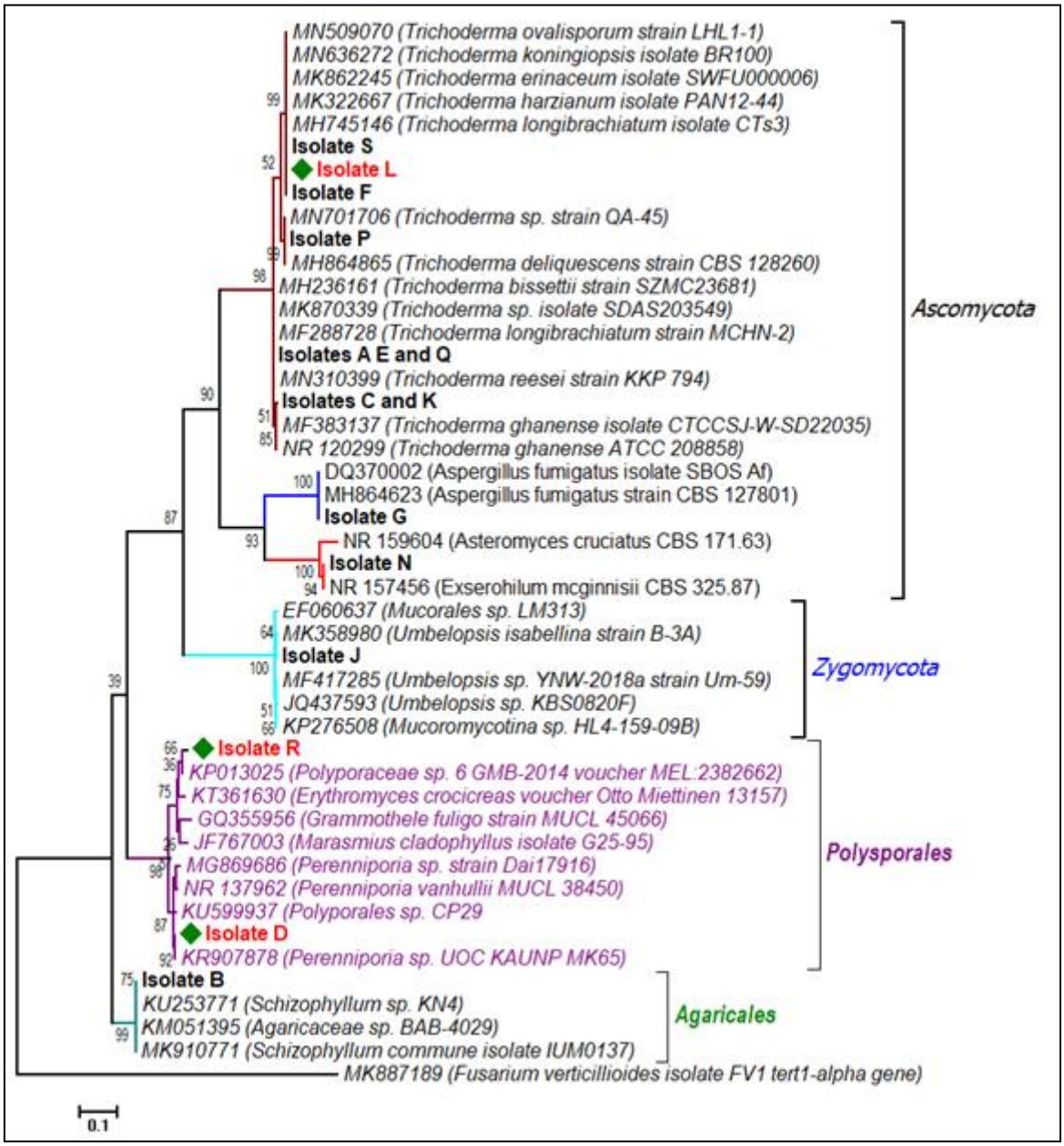


**Figure 5.4**: A phylogenetic tree indicating an ancestral relationship between the identified isolates (500 rounds of bootstrap resampling).

## 5.3 Screening of fungal isolates

### 5.3.1 Primary screening of fungal isolates

All the fungal isolates were screened for their capability to produce laccase using guaiacol plate screening method on Sabouraud dextrose agar (SDA) media as discussed in **Section 3.2.2.3**. The isolates were further screened for their ability to utilise humic acid (HA) as their sole carbon source on solid media as previously discussed in (see **Section 3.2.4.1**). The screening results are shown in **(Figure 5.5 and Table 5.2)**. Among the 18 fungal isolates screened, only three (D, L and R) showed promising results for enzyme production on 0.1 % guaiacol as evidenced by the reddish-brown colour at the top and bottom view of the agar plate **(Figure 5.5)**. The reddish-brown zone at the bottom and edges of the mycelium growth is due to the oxidation of guaiacol by the fungal enzymes (Alfarra *et al*., 2013; Ghebreslasie *et al*., 2016). The three isolates showed a colour change within 10 min of inoculating with mycelium disks on agar plates. Guaiacol can be a unique laccase substrate in the absence of hydrogen peroxide ($H_2O_2$), thereby confirming that the enzyme is a true laccase. However, peroxidases are also able to oxidize guaiacol in presence of hydrogen peroxide as an electron donor (Doerge *et al*., 1997). Generally, laccases catalyse the oxidation of guaiacol to phenoxy radicals, which subsequently undergo oxidative polymerization to form tetraguaiacol producing reddish-brown zone around laccases positive colonies on agar plates (D'Souza *et al*., 1999). Therefore, guaiacol can be used as a marker for extracellular oxidative enzymes, and the immediate colour change may be an indication of high enzyme activity, either laccases and/or peroxidases produced by the fungi (More *et al*., 2011). Similar to this study, Metuku *et al*. (2011) screened white rot fungi (WRF) based on the polymerization of guaiacol in wood powder agar plates caused by extracellular phenoloxidases and or peroxidases excreted by the fungi. Savitha *et al*. (2011) also screened laccase producing WRF on potato dextrose agar (PDA) media containing tannic acid and observed for development of brown coloured precipitate on the plates and observed reddish hallow zone in guaiacol containing plates.

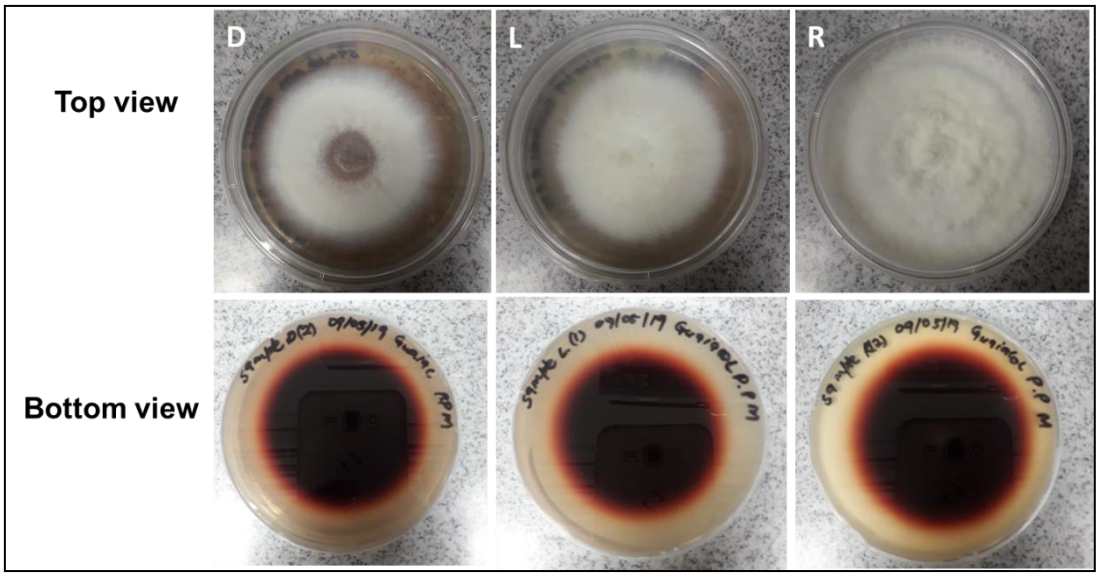


**Figure 5.5**: Lignolytic enzyme activity of *Perenniporia* sp. isolate D, *Polyporaceae* sp isolate R and *Trichoderma koniniopsis* Isolate L on solid media supplemented with guaiacol as a substrate for enzyme laccase detection.

The eighteen (18) isolates were also sub-cultured individually on selective agar plates to screen for their ability to utilise HA as the sole carbon source. **Table A2** shows the actual growth of the mycelium (radius in mm) on HA solid media. As indicated in **Table 5.2**, the mycelium growth for all isolates were observed visually following 4, 7, 10 and 15 days of incubation. The mycelium growth, in terms of colony radius in mm, was used to monitor the fungal isolate's ability to utilise HA as carbon source for growth. As shown in **Table 5.2**, most of the fungal isolates exhibited partial growth on the agar plates containing HA as sole carbon source. However, the mycelium growth for the three isolates D, L, and R was comparatively intense (>30mm) than other isolates, illustrating their ability to efficiently utilise HA as a carbon source. According to Zahmatkesh *et al*. (2016), decolourization of HA in solid media is an indication of degradation of the HA. However, decolourization does not necessarily confirm complete degradation of HA. In this work, no bleaching of the HA was observed, possibly due to the presence of low concentrations of HA in the solid media. The same trend in the growth behaviour of the three isolates (D, L and R) on HA selected media was observed in **Figure 5.6**. With these results, it could

be an indication that the isolates may be producing a similar cocktail of lignolytic enzymes for the diminution of HA for their growth.

**Table 5.2**: Screening of fungal isolates for lignolytic enzymes and growth on humic acid as a carbon source.

| Isolate | Colour change in 0.1% Guaiacol[a] | Growth on humic acid[b] |
|---|---|---|
| A | - | ++ |
| B | - | + |
| C | - | + |
| **D** | **+++** | **+++** |
| E | - | ++ |
| F | - | ++ |
| G | - | ++ |
| H | - | ++ |
| I | - | ++ |
| J | - | + |
| K | - | ++ |
| **L** | **+++** | **+++** |
| M | - | + |
| N | - | + |
| O | - | - |
| P | - | + |
| Q | - | + |
| **R** | **+++** | **+++** |
| S | - | + |

[a] Change in the media colour from colourless to reddish brown: - no change, + slight change, +++ intense colour change.

[b] Colony radius: - no growth, + slight growth (<10mm), ++ good growth (<30mm) and +++ Intense growth (>30mm).

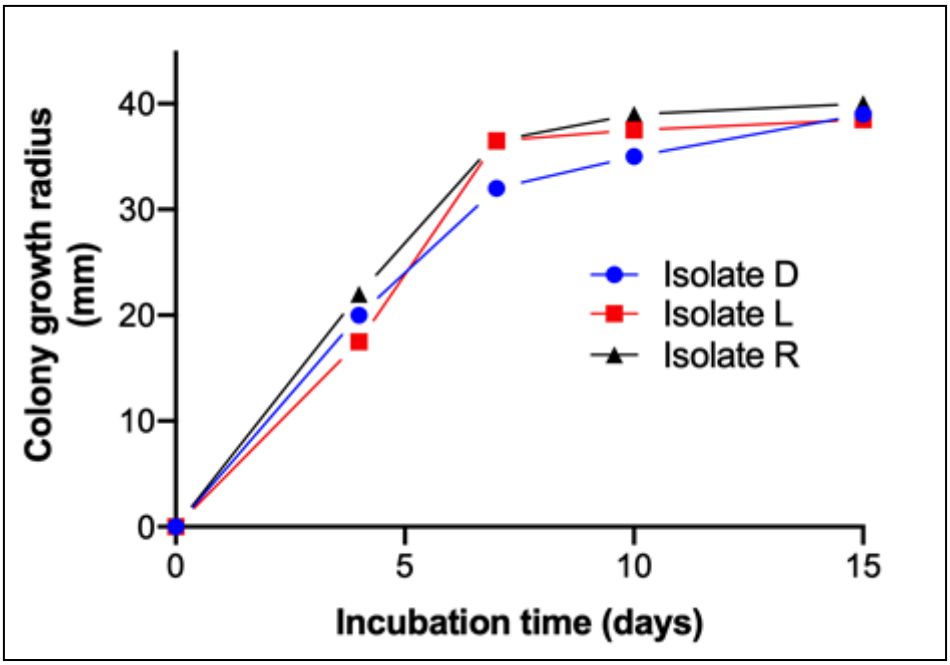


**Figure 5.6**: Growth curve of *Perenniporia* sp. isolate D, *Polyporaceae* sp. isolate R and *Trichoderma koniniopsis* Isolate L on solid media having HA as the sole carbon source.

Members of *Deutromycetes*, *Ascomycetes* and a wide range of *Basidiomycetes* are known fungal producers of laccases, which are exceptionally abundant in many lignin degrading WRF (Bourbonnais *et al*., 1995; Leontievsky *et al*., 1997; Thurston, 1994). Consistent with these reports, the isolates exhibiting guaiacol oxidative capacity were identified as two *Basidiomycetous* fungi (*Perenniporia* sp. (isolate D) and *Polyporaceae* sp (isolate R) and an *Ascomycete Trichoderma koniniopsis* (Isolate L) based on ITS gene sequencing **(Table 5.1)**. There are reports in literature that fungi, especially *saprotrophic* fungi, are able to breakdown the most recalcitrant humic substance structures via the processes of oxidation, aromatic cleavage, and demethylation and utilise the intermediates as carbon sources for growth (Klein *et al*., 2014; Grinhut *et al*., 2007). These compounds are not taken up by the microbial cell but are degraded initially by non-specific extracellular oxidizing enzymes such as manganese peroxidases (MnPs), lignin peroxidases (LiPs) and laccases (Grinhut *et al*., 2007). Therefore, the observed intense growth on HA by the fungal isolates D, L and R could be due to their ability to produce these extracellular lignolytic enzymes for efficient utilisation of HA as carbon source.

### 5.3.2 Humic acid degradation in liquid media

According to Zahmatkesh *et al*. (2016), decolourization of high-molecular-mass HAs in solid media can be used as an indicator for their degradation/conversion into low-molecular-mass fluvic acid (FA) and carbon dioxide. There are several reports for number of white rot fungi (WRF) under cometabolic conditions (i.e., in the presence of an assimilable carbon source such as glucose) to decolourize HAs. For example, WRF such as *Trametes versicolor*, *Phanerochaete Chrysosporium, Bjerkandera adusta and Collybia dryophila* were found to degrade HA from soil, peat and brown coal (Hurst *et al*., 1963; Ralph & Catheside, 1994; Willman & Fakousa, 1997; Steffen *et al*., 2002). However, in this work there was no bleaching of HA observed, possibly due to low concentration of HA used in the solid media. Therefore, *Perenniporia* sp. isolate D, *Polyporaceae* sp isolate R and *Trichoderma koniniopsis* Isolate L were further screened for their ability to decolourize HA in liquid media using HA as the sole source of carbon for the fungal growth as discussed in **Section 3.2.4.2**.

**Figure 5.7** shows decolourization of HA following fungal treatment. The side and top view images of the samples were taken after they were filtered through a 0.45 µm Whatman filter. High decolourization was observed in cultures inoculated with isolates D and R and the reddish-brown colour of the control changed to a less intense reddish-brown colour **(Figure 5.7)**. This colour change is an indication of HA removal by the fungal isolates either through degradation or absorption by the fungal mycelia (Badis *et al*., 2009). The decolourization results concur with the percentage removal of HA in **Figure 5.8**.

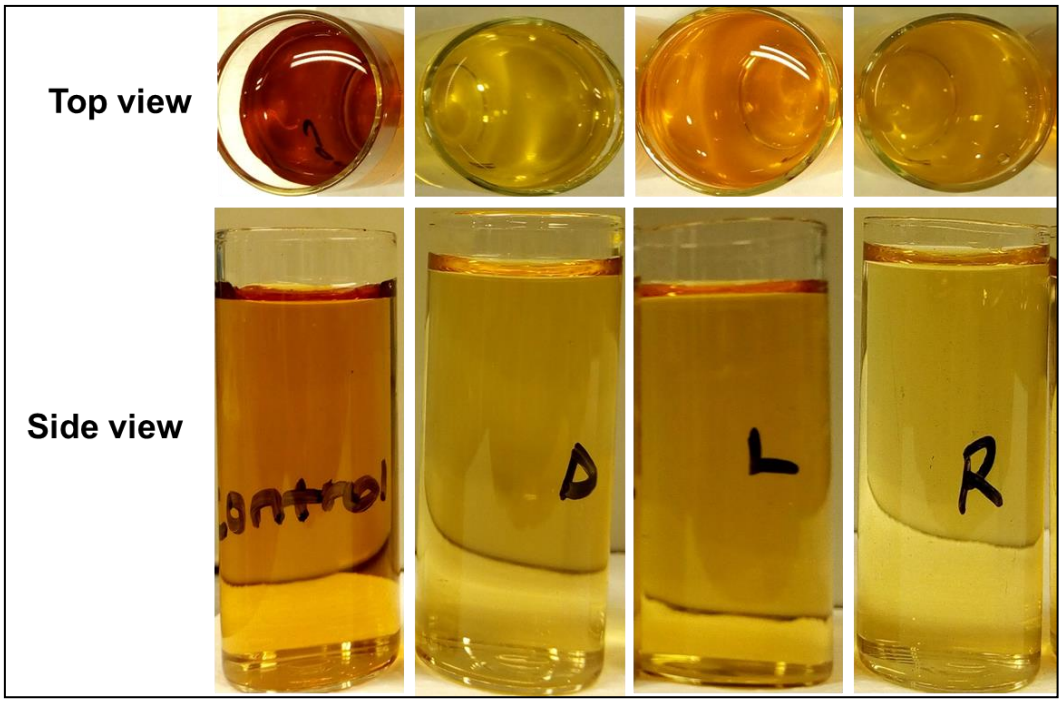


**Figure 5.7**: Comparison of HA decolourization in liquid media by *Perenniporia* sp. isolate D, *Polyporaceae* sp isolate R and *Trichoderma koniniopsis* Isolate L, and the negative control.

### 5.3.3 Humic acid removal capacity

Ultraviolet and visible (UV-Vis) spectrometry and dissolved organic carbon (DOC) are some of the characterization methods that can be used for studying the change in molecular structure and quantity of natural organic matter in water (Cheng *et al*., 2019; Matilainen *et al*., 2011). Humic acid degradation based on $UV_{254}$ and DOC analysis was carried out by fungal treatment of *Perenniporia* sp. isolate D, *Polyporaceae* sp. isolate R and *Trichoderma koniniopsis* Isolate L according to a procedure outlined in **Section 3.4.7**. As shown in **Figure 5.8**, the highest degradation percentage of HA (27.30 % $UV_{254}$; 52.0 % DOC) was achieved using *Polyporaceae* sp. isolate R. On the other hand, the lowest HA degradation percentage (11.65 % $UV_{254}$; 23.05 % DOC) was obtained using *Trichoderma koniniopsis* Isolate L **(Figure 5.8)**. These degradation results suggest strong correlation between $UV_{254}$ and DOC analysis for the removal of HA.

Within the WRF, correlation has been observed between the activities of extracellular peroxidases production and HA degradation, with manganese-dependent peroxidase (MnP) and laccase playing a major role in depolymerizing and mineralizing different HAs in vitro (Zahmatkesh *et al*., 2016). Thus, differences observed in HA degradation between the isolates could be due to differences in their production potential of this enzyme cocktail.

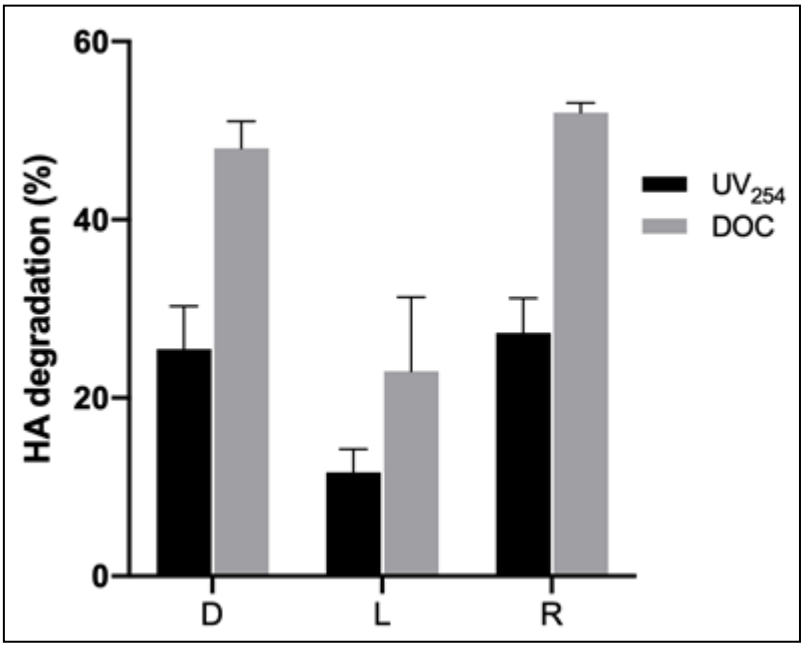


**Figure 5.8**: Percent HA degradation by three selected fungal isolates based on UV absorption spectra ($UV_{254nm}$) and DOC analysis.

### 5.4 Enzyme production during solid-state fermentation (SSF)

When compared with *Trichoderma koniniopsis* Isolate L, far more superior removal rates of HA in liquid media were achieved with *Perenniporia* sp. isolate D, and *Polyporaceae* sp. isolate R. As outlined in **Section 3.2.5.1**, further investigations were therefore conducted on the ability of the two isolates to produce lignin degrading enzymes in an SSF process. Enzyme activity was determined spectrophotometrically after 7, 10, 15 and 21 days of incubation to determine whether there was any increase or decrease in the production of enzymes (**Table**

**A3-A5**). The enzyme activity results indicated high peroxidases production for both isolates as compared to laccase (see **Figure 5.9 (a)-(b)**). On the 10$^{th}$ and 15$^{th}$ days of incubation, the activity of MnP decreased from 1.523 ± 0.0011 U/mL to 0.690 ± 0.000185 U/mL for *Perenniporia* sp. isolate D (**Figure 5.9 (a)**) and from 3.941 ± 0.000389 U/mL to 1.416 ± 0.000113 U/mL for *Polyporaceae* sp. isolate R (**Figure 5.9 (b)**). The decreased activity could be a result of an interplay in the depletion of carbon source to support the growth of the fungal isolates. Whereas the highest concentration of lignin peroxidase (LiP) was produced by *Polyporaceae* sp. isolate R (3.738 ± 0.00018 U/mL) on day 15, the highest activity levels of LiP (1.397 ± 0.00047 U/mL) were obtained only in day 10 for *Perenniporia* sp. isolate D. Interestingly, *Perenniporia* sp. isolate D produced high levels of laccase on day 10 (0.467 ± 0.00016 U/mL), which subsequently decreased to 0.178 ± 0.000312 U/mL at day 21 (**Figure 5.9 (a)**). Following an almost similar trend, *Polyporaceae* sp. isolate R was found to produce high laccase activity on day 7, which subsequently decreased from 0.316 ± 0.00017 to 0.068 ± 0.00018 U/mL at day 21 (**Figure 5.9 (b)**). The results obtained by Ergun & Urek (2017) were different from those generated in this research study; laccase production was found to be the highest compared to the peroxidases produced by *Pleurotus ostreatus* in SSF using potato peel waste (Ergun & Urek, 2017). In another study by Damia´n-Robles *et al*. (2017), white rot fungi species *Irpex lacteus* and *Phlebiopsis* were found to produce lower levels of laccase when basal media was used for the growth of the fungi. The results of this and the above cited studies suggest that the production of lignolytic enzymes is dependent on the type of species and the fungal growth conditions (e.g. type of carbon source) used.

Since high enzyme activity was obtained during 10 days of incubation, SSF experiment was carried out once more over a 10-day period and the enzymes were extracted for purification. While the activity of *Perenniporia* sp. isolate D enzyme was found to be 0.311, 0.746 and 0.329 U/mL for laccase, MnP and LiP, respectively, and the respective activities of 0.263, 1.367 and 0.184 U/mL for laccase, MnP and LiP, were recorded for isolate R identified as *Polyporaceae* sp. The enzymes were partially purified according to an ammonium sulfate purification method outlined in **Section 3.2.5.4**. **Figure 5.19(c)** shows enzyme activity after

purification process. MnP activity was found to be the highest for both isolates (**Table A6**). Activity levels of 0.869 U/mL and 0.724 U/mL were recorded for *Perenniporia* sp. Isolate D and *Polyporaceae* sp. isolate R. While lowest levels of LiP activities were produced with both *Perenniporia* sp. Isolate D and *Polyporaceae* sp. isolate R, respective laccase activity levels of 0.152 and 0.298 U/mL were on the other hand recorded. In some instances, enzyme precipitation using ammonium sulfate increases or decreases enzyme activity depending on the type of method used (Othman *et al*., 2014). In the current work, enzyme activity following purification was slightly increased from 0.746 to 0.869 U/mL (MnP) for *Perenniporia* sp. isolate D, and from 0.263 to 0.297 U/mL (laccase) and from 0.184 to 0.298 U/mL (LiP) for *Polyporaceae* sp. isolate R (see **Figure 5.9(c)**).

Although not efficient, the SSF and partial purification resulted in enzyme extract that could be utilised for the downstream enzyme immobilisation for HA removal as discussed in **Chapter 6**.

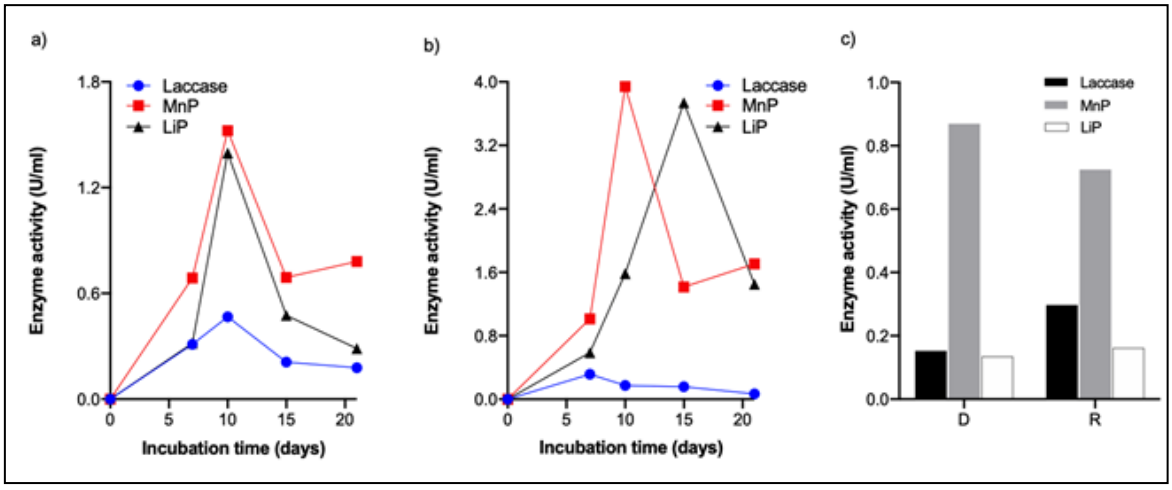


**Figure 5.9**: Change in lignolytic enzyme production during solid state fermentation by *Perenniporia* sp. isolate D (a) and *Polyporaceae* sp isolate R (b), and the final enzyme activities of partially purified extracts (c).

## 5.5 Conclusion

In the study, a combination of culture-dependent (fruiting bodies morphology, colony characteristic and SEM) and molecular (based on MALDI-TOF biotyping and ITS gene sequencing) methods were used for identification of 18 fungal isolates collected from *Eucalyptus* trees forest in eSwatini. The 18 fungal isolates were identified as belonging to phylum *Ascomycota* (14 isolates), *Basidiomycota* (3 isolates) and *Mucoromycotina/Zygomycota* (1 isolate). Based on guaiacol plate assay, two *Basidiomycetous* fungi *Perenniporia* sp. isolate D and *Polyporaceae* sp. isolate R and an *Ascomycete Trichoderma koniniopsis* Isolate L qualitatively exhibited ability to produce lignin degrading enzyme laccase. The three isolates also exhibited ability to use HA as a sole carbon source on solid media and HA and its decolourization (bleaching) in vitro. Reduction in dissolved organic carbon and $UV_{254}$ analysis results indicated subtle differences in HA degradation in liquid media. Comparatively, the results also indicated that white rot fungi (WRF) *Perenniporia* sp. isolate D and *Polyporaceae* sp. isolate R were two-fold efficient in degrading HA than the *Ascomycetous Trichoderma koniniopsis* Isolate L. The study also showed the capacity of the two WRF *Perenniporia* sp. isolate D and *Polyporaceae* sp. isolate R to produce lignolytic enzymes MnP, laccase and LiP, under solid-state fermentation system, which optimal production observed between 10-15 days. However, further studies are required to optimise conditions for maximal enzymes production. Moreover, enzyme purification, and biochemical characterization to understand the novel features that can be of importance regarding application in HA degradation also need to be investigated.

## 5.6 References

Alfarra, H.Y., Hasali, N.H.M. and Omar, M.N., 2013. A lignolytic fungi with laccase activity isolated from Malaysian local environment for phytochemical transformation purposes. *International Research Journal of Biological Sciences*, *2*(2), pp.51-54.

Badis, A., Ferradji, F.Z., Boucherit, A., Fodil, D. and Boutoumi, H., 2009. Characterization and biodegradation of soil humic acids and preliminary identification of decolorizing actinomycetes at Mitidja plain soils (Algeria). *African Journal of Microbiology Research*, *3*(13), pp.997-1007.

Bourbonnais, R., Paice, M.G., Reid, I.D., Lanthier, P. and Yaguchi, M., 1995. Lignin oxidation by laccase isozymes from Trametes versicolor and role of the mediator 2, 2'-azinobis (3-ethylbenzthiazoline-6-sulfonate) in kraft lignin depolymerization. *Applied Environmental and. Microbiology.*, *61*(5), pp.1876-1880.

Carolis, E.D., Hensgens, L.A., Vella, A., Posteraro, B., Sanguinetti, M., Senesi, S. and Tavanti, A., 2014. Identification and typing of the Candida parapsilosis complex: MALDI-TOF MS vs. AFLP. *Sabouraudia*, *52*(2), pp.123-130.

Cassagne, C., Normand, A.C., L'Ollivier, C., Ranque, S. and Piarroux, R., 2016. Performance of MALDI-TOF MS platforms for fungal identification. *Mycoses*, *59*(11), pp.678-690.

Cheng, G., Niu, Z., Zhang, C., Zhang, X. and Li, X., 2019. Extraction of Humic Acid from Lignite by KOH-Hydrothermal Method. *Applied Sciences*, *9*(7), pp.1356.

D'souza, T.M., Merritt, C.S. and Reddy, C.A., 1999. Lignin-modifying enzymes of the white rot basidiomycete Ganoderma lucidum. *Applied Environmental and Microbiology.*, *65*(12), pp.5307-5313.

Damián-Robles, R.M., Castro-Montoya, A.J., Saucedo-Luna, J., Vázquez-Garciduenas, M.S., Arredondo-Santoyo, M. and Vázquez-Marrufo, G., 2017. Characterization of ligninolytic enzyme production in white-rot wild fungal strains suitable for kraft pulp bleaching. *3 Biotech*, *7*(5), p.319.

De Respinis, S., Monnin, V., Girard, V., Welker, M., Arsac, M., Cellière, B., Durand, G., Bosshard, P.P., Farina, C., Passera, M. and Van Belkum, A., 2014. Matrix-assisted laser desorption ionization–time of flight (MALDI-TOF) mass spectrometry using the Vitek MS system for rapid and accurate identification of dermatophytes on solid cultures. *Journal of Clinical Microbiology*, *52*(12), pp.4286-4292.

Doerge, D.R., Divi, R.L. and Churchwell, M.I., 1997. Identification of the coloured guaiacol oxidation product produced by peroxidases. *Analytical Biochemistry*, *250*(1), pp.10-17.

Ergun, S.O. and Urek, R.O., 2017. Production of ligninolytic enzymes by solid state fermentation using Pleurotus ostreatus. *Annals of Agrarian Science*, *15*(2), pp.273-277.

Ghebreslasie, Z., Premjet, D. and Permjet, S., 2016. Screening of fungi producing ligninolytic enzymes. *Asia-Pacific Journal of Science and Technology*, *21*(2), pp.200-209.

Grinhut, T., Hadar, Y. and Chen, Y., 2007. Degradation and transformation of humic substances by saprotrophic fungi: processes and mechanisms. *Fungal Biology Reviews*, *21*(4), pp.179-189.

Haarhoff, J., Mamba, B., Krause, R.W.M., Van Staden, S., Nkambule, T., Dlamini, S. and Lobanga, K.P., 2013. Natural organic matter in drinking water sources: Its characterisation and treatability. *Water Research Commission* Report No. 1883/1/12.

Hopkins, A.J., 2007. *The taxonomy and ecology of wood decay fungi in Eucalyptus obliqua trees and logs in the wet sclerophyll forests of southern Tasmania* (Doctoral dissertation, University of Tasmania).

Hurst, H.M., Burges, A. and Latter, P., 1962. Some aspects of the biochemistry of humic acid decomposition by fungi. *Phytochemistry*, *1*(4), pp.227-231.

Kimura, M., 1980. A simple method for estimating evolutionary rates of base substitutions through comparative studies of nucleotide sequences. *Journal of Molecular Evolution*, *16*(2), pp.111-120.

Klein, O.I., Isakova, E.P., Deryabina, Y.I., Kulikova, N.A., Badun, G.A., Chernysheva, M.G., Stepanova, E.V. and Koroleva, O.V., 2014. Humic substances enhance growth and respiration in the basidiomycetes Trametes maxima under carbon limited conditions. *Journal of Chemical Ecology*, *40*(6), pp.643-652.

Kumar, S., Stecher, G., Li, M., Knyaz, C. and Tamura, K., 2018. MEGA X: molecular evolutionary genetics analysis across computing platforms. *Molecular Biology and Evolution*, *35*(6), pp.1547-1549.

Leontievsky, A.A., Vares, T., Lankinen, P., Shergill, J.K., Pozdnyakova, N.N., Myasoedova, N.M., Kalkkinen, N., Golovleva, L.A., Cammack, R., Thurston, C.F. and Hatakka, A., 1997. Blue and yellow laccases of ligninolytic fungi. *FEMS Microbiology Letters*, *156*(1), pp.9-14.

Matilainen, A., Gjessing, E.T., Lahtinen, T., Hed, L., Bhatnagar, A. and Sillanpää, M., 2011. An overview of the methods used in the characterisation of natural organic matter (NOM) in relation to drinking water treatment. *Chemosphere*, *83*(11), pp.1431-1442.

Metuku, R.P., Burra, S., Nidadavolu, S.V., Bindu, S.H., Pabba, S. and Singaracharya, M., 2011. Selection of highest lignolytic white rot fungus and its molecular identification. *Journal of Cell and Tissue Research*, *11*(1), pp.2557.

More, S.S., PS, R. and Malini, S., 2011. Isolation, purification, and characterization of fungal laccase from Pleurotus sp. *Enzyme Research*, *2011*, p.248737.

Nkambule, T.I., Krause, R.W.M., Haarhoff, J., & Mamba, B.B.,2012. Natural organic matter ( NOM ) in South African waters : NOM characterisation using combined assessment techniques. *Water SA Vol*. 38(5), pp.697–706.

Othman, A.M., Elshafei, A.M., Hassan, M.M., Haroun, B.M., Elsayed, M.A. and Farrag, A.A., 2014. Purification, biochemical characterization and applications of Pleurotus ostreatus ARC280 laccase. *British Microbiology Research Journal*, *4*(12), pp.1418-1439.

Ralph, J.P. and Catcheside, D.E.A., 1994. Decolourisation and depolymerisation of solubilised low-rank coal by the white-rot basidiomycete Phanerochaete chrysosporium. *Applied Microbiology and Biotechnology*, *42*(4), pp.536-542.

Riat, A., Hinrikson, H., Barras, V., Fernandez, J. and Schrenzel, J., 2015. Confident identification of filamentous fungi by matrix-assisted laser desorption/ionization time-of-flight mass spectrometry without subculture-based sample preparation. *International Journal of Infectious Diseases*, *35*, pp.43-45.

Rizzato, C., Lombardi, L., Zoppo, M., Lupetti, A. and Tavanti, A., 2015. Pushing the Limits of MALDI-TOF mass spectrometry: beyond fungal species identification. *Journal of Fungi*, *1*(3), pp.367-383.

Savitha, S.D., Gururaj, B.T., Nityanand, C., Anup, A.C., Gouri, D. and Azhar, M.B., 2011. Isolation of laccase producing fungi and partial characterization of laccase Research Article. *Biotechnology. Bioinformatics Bioengineering*, *1*(4), pp.543-549.

Steffen, K.T., Hatakka, A. and Hofrichter, M., 2002. Degradation of humic acids by the litter-decomposing basidiomycete Collybia dryophila. *Applied Environmental and Microbiology.*, *68*(7), pp.3442-3448.

Thurston, C.F., 1994. The structure and function of fungal laccases. *Microbiology*, *140*(1), pp.19-26.

Willmann, G. and Fakoussa, R., 1997. Extracellular oxidative enzymes of coal-attacking fungi. *Fuel Processing Technology*, *52*(1-3), pp.27-41.

Zahmatkesh, M., Spanjers, H., Toran, M.J., Blánquez, P. and Van Lier, J.B., 2016. Bioremoval of humic acid from water by white rot fungi: exploring the removal mechanisms. *AMB Express*, *6*(1), p.118.

# CHAPTER 6

# ENZYME-MODIFIED POLY ETHERSULFONE (PES) MEMBRANE FOR THE REMOVAL AND DEGRADATION OF HUMIC ACID

---

## 6.1 Introduction

In **Chapter 4**, the methods in preparing a poly ethersulfone (PES) membrane that possesses high permeate flux by varying the composition of the dope solution and parameters that influence the phase inversion process was introduced. On the other hand, **Chapter 5** introduced methods for isolation and identification of white rot fungi (WRF) isolates using three identification methods. In addition, **Chapter 5** also introduced the method for the production and extraction of lignin-degrading enzymes. In this chapter, the modification of PES membranes through immobilisation of enzyme laccase on the membranes surface for simultaneous degradation and removal of humic acid as a model compound for NOM is presented.

## 6.2 Experimental methods

### 6.2.1 Modification experiments

Previously prepared flat sheets of PES membranes were cut into small fragments and placed in 500 mL beakers (M.5 clear membrane as a blank, M.5a membrane with substrate only, M.5b membrane with the enzymes only, and M.5c membrane with enzyme and substrate). The beakers contained 40 mL of 0.1 M sodium acetate buffer (pH 5.0), 50 mL of 28.8 mM 4-hydroxybenzoic acid and 10 mL of crude enzyme laccase with 0.297 U/mL for isolate R and 0.152 U/mL for isolate D. The contents of the beakers were incubated for 24 h at 30 °C under stirring conditions (120 rpm). After the incubation and prior to use, the membranes were kept in desiccators containing silica gel. The change in the colour of the membranes was

visually observed after 24 h of incubation. Further colour changes were observed after rinsing the membranes with ultra-pure water and after undertaking rejection studies.

### 6.2.2 Membrane characterization

Characterization of the membranes in terms of surface morphology using scanning electron microscopy and wettability measurements using drop shape analyzer were carried out. The respective methods are outlined in **Sections 3.4.4** and **3.4.2**, respectively.

### 6.2.5 Membrane filtration tests

Humic acid (HA) rejection was carried out by passing through the membranes using a dead-end cell system ~30 mg/L of HA solution as feed stream. For every h, the permeate was monitored for every 15 and 30 min. The effective area of the membranes was 0.00113 $m^2$. The permeate flux was calculated using (**Equation 2**) as described in **Section 3.41**. Membrane water permeability was calculated as follows using (**Equation 5**).

$$\boldsymbol{A = \frac{V}{Am\Delta tP}} \qquad \textbf{(5)}$$

where: A is the membranes permeability (L/h.$m^2$.bar), V is the permeate volume (L), $A_m$ is the membrane area ($m^2$), $\Delta t$ is the filtration time (h) and P is the pressure applied (bar).

The permeate analysis was carried out using ultraviolet visible (UV-vis) spectrometry, with particular attention given to 254 nm as an absorbing wavelength for HA (Nkambule et al., 2012) and dissolved organic carbon (DOC) (see **Section 3.4.8**). UV-Vis analysis was conducted for all the permeate samples and DOC analysis were conducted after a 30 min filtration of the permeate samples. The

removal percentage for HA was calculated according to **Equation 3** outlined in **Section 3.4.1**.

## 6.4 Results and discussion

### 6.4.1 Colour observation

A visual change in colour of the modified membranes was considered as confirmation for successful grafting of the enzymes and the substrate onto the membrane surface. As expected, no colour change was observed for the blank membrane **(**see **Figure 6.1)**. A colour change was observed for membranes incubated with enzymes and substrate. The change in colour was particularly intense for M.5c when compared with M.5b, especially with enzymes extracted from isolate D (see **Figure 6.1 (a)**). The change in colour for M.5b was ascribed to the adsorption of enzymes onto the membrane surface. The intense colour change in M.5c is indicative of an enzymatic free radical reaction taking place between the substrate and the sulfonate groups of the membranes (Nady *et al*., 2012). The membranes were kept for 24 h in a desiccator prior to use and no colour change was observed after storage.

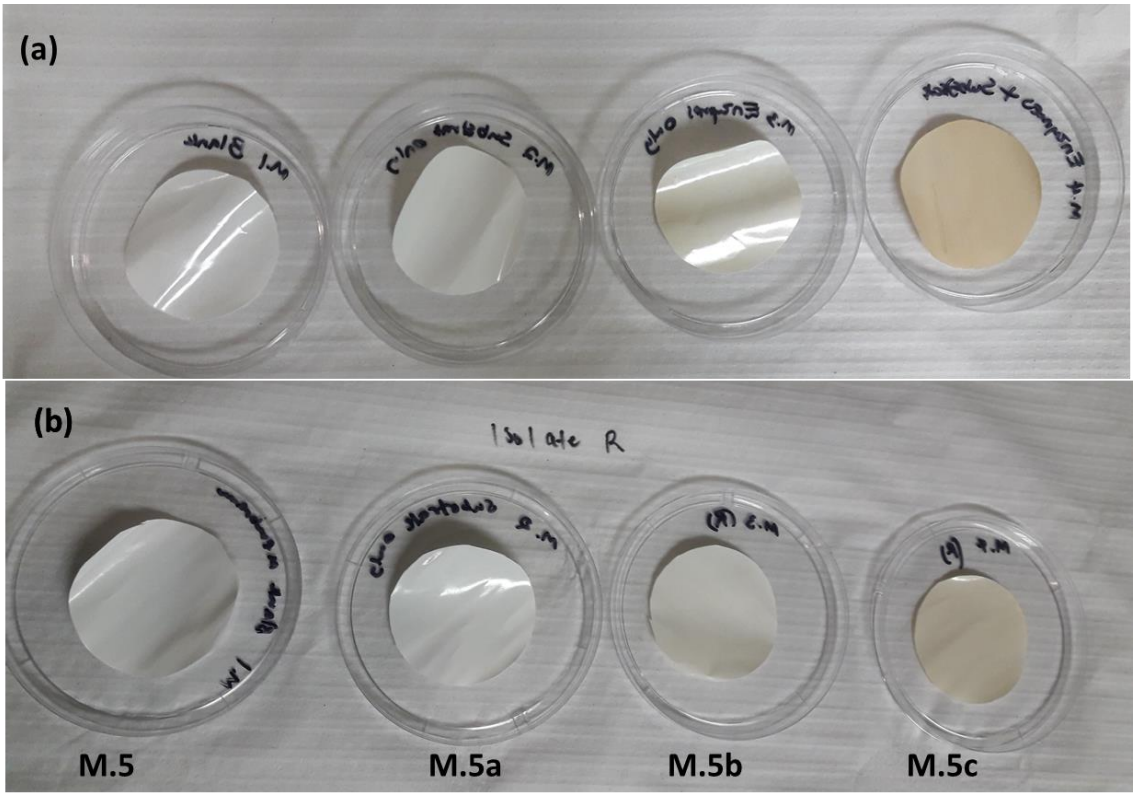


**Figure 6.1**: Images of unmodified and modified membranes using enzymes produced by isolate D (a) and isolate R (b).

### 6.4.2 Surface morphological examination

A morphological analysis of the membranes was carried out to confirm the enzyme immobilisation on the surface of the membranes. The appearance of large rough spherically shaped enzymes on enzyme modified membranes is evident in **Figure 6.2c, d, g and h**. As expected, a clear surface was observed on the blank membrane M.5 **(Figure 6.2(a))**. Membranes incubated with enzymes from isolate D (M.5b and M.5c) were found to possess well distributed enzymes on the membrane surface (see **Figure 6.2 (c) and (d)**) when compared with membranes modified with enzymes from isolate R (see **Figure 6.2 (g) and (h)**). The good distribution of the enzymes could be attributed to complete physical adhesion of isolate D enzymes on the membranes surface since all the membranes were subjected to the same incubation conditions. The structural changes observed on the enzyme modified membranes were similar to that obtained by Nady et al. (2016). To verify if enzyme leakage occurred during filtration, the morphology of the enzyme modified

membranes were examined after filtration. As depicted in **Figure 6.2 (e, f, i and j)**, no major changes in the morphology of enzyme modified membranes were observed since small spherically shaped enzymes were still present on the surface of the membranes. It is possible no leaching ever took place and the enzymes were therefore linked to the substrate that is covalently bonded to the membrane. Based on stable membrane permeabilities observed 60 min following filtration of enzyme modified membranes, possibilities exist of the enzymes becoming saturated **(Figure 6.4)**. However, this does not mean the enzymes were washed off after filtration; this was confirmed by SEM results (see on **Figure 6.2 e, f, i and j**).

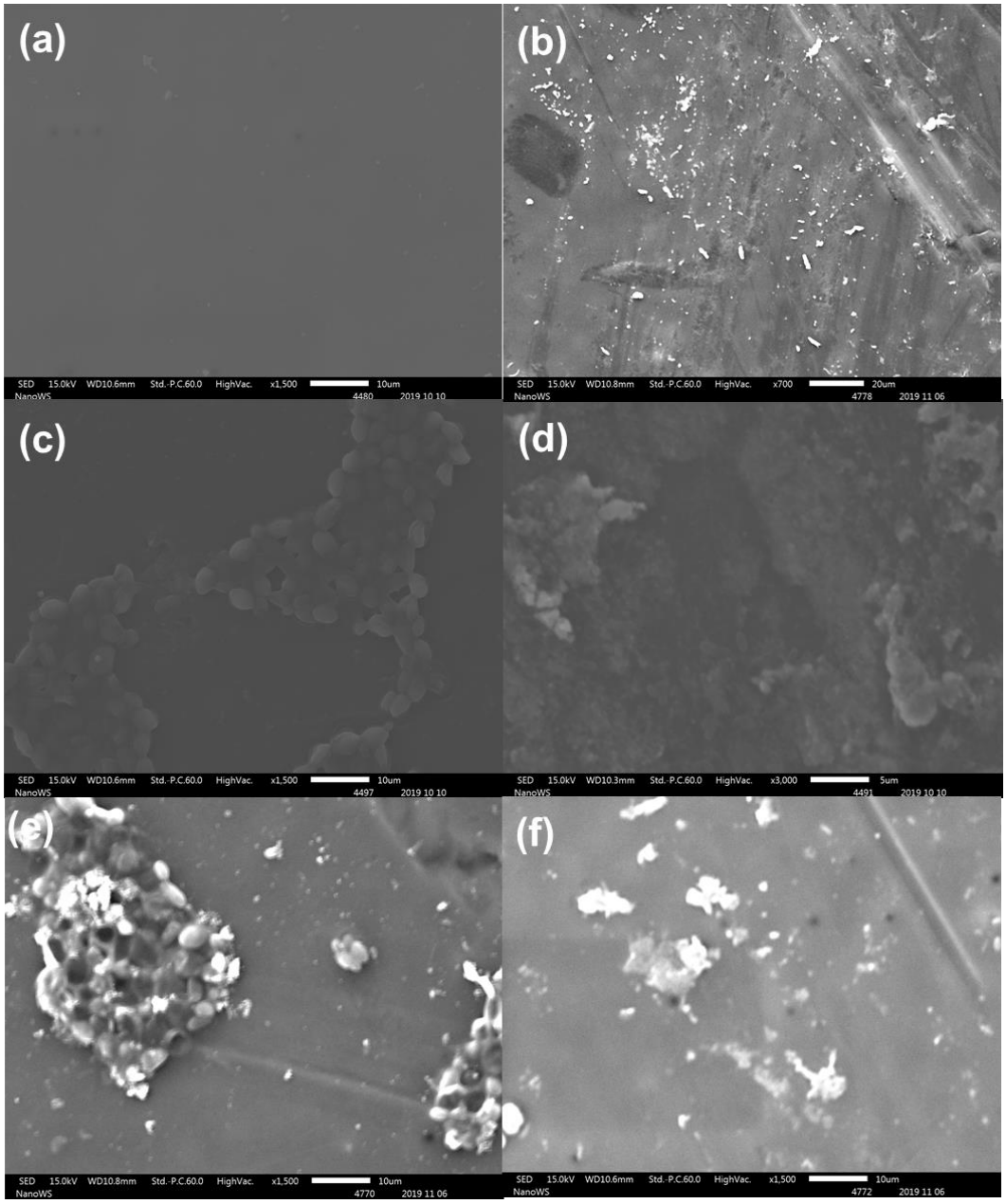


**Figure 6.2**: SEM images of all membranes investigated (a) M.5 blank membrane, (b) M.5a membrane with substrate only, (c) M.5b(D) membrane with enzyme only, (d) M.5c(D) membrane with enzyme and substrate, (e) M.5b(D) used membrane, (f) M.5c(D) used membrane, (g) M.5b(R) membrane with enzyme only, (h) M.5c(R) membrane with enzyme and substrate, (i) M.5b(R) used membrane and (j) M.5c(R) used membrane. The membranes were taken at x1500 magnification except for M.5a and M.5c(R) which were taken at x700.

### 6.4.3 Wettability

The measured contact angles for all membranes investigated are presented in **Figure 6.3**. All the measured contact angles were found to be greater than 60°, indicating that the membranes are slightly hydrophobic. According to Malczewska & Zak (2019), a hydrophobic membrane is characterised by a contact angle of >60°. The grafting of the enzymes on the membranes surface increased the contact angles from 68.1°± 5.8 (M.5) to 71.94°± 2.41 (M.5b) and 72.84°± 4.72 (M.5b) for the isolate D and R enzymes, respectively. The increased contact angles suggest successful immobilisation of the enzymes on the membranes. However, upon addition of the substrate, the contact angles decreased slightly to 59.3°± 4.2, 63.83°± 2.07 and 61.25°± 5.11 for the M.5a, M.5c isolate D enzyme and M.5c isolate R enzyme, respectively. In addition, the slight decrease in the contact angle was accompanied by an enhancement in the hydrophilicity of the membranes. The reported contact angle measurements herein are in agreement with the contact angle measurements obtained by Nady *et al*. (2011). The increase in hydrophilicity is attributed to the polar carbonyl groups present in the 4-hydroxybenzoic acid substrate, which are covalently bonded to the sulfonate groups of poly ethersulfone membranes (Nady *et al*., 2012).

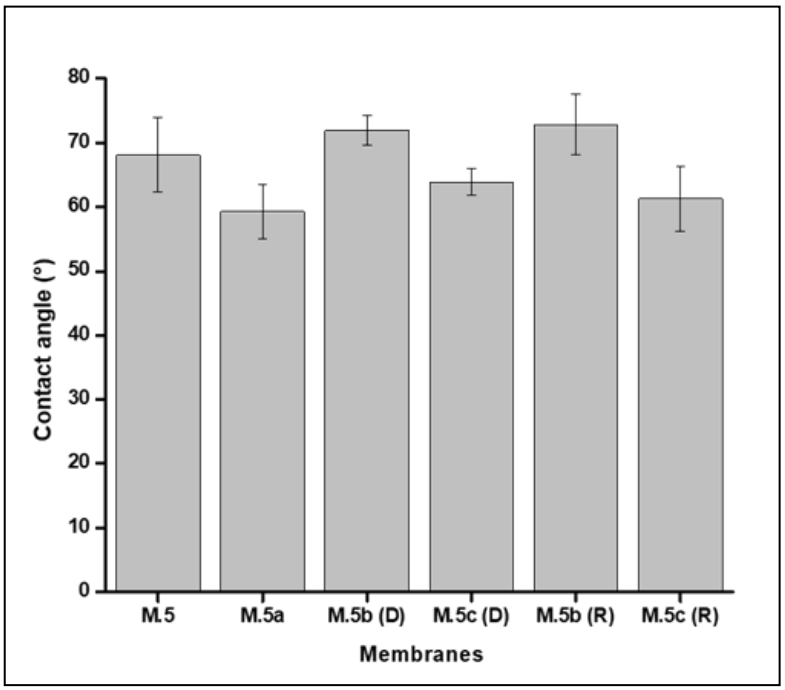


**Figure 6. 3**: Contact angle for all the membranes studied.

### 6.4.4 Permeability and Rejection experiments

The membranes performance in terms of permeability and filtration period is illustrated in **Figure 6.4**. **Table A7-A12** shows raw data of the permeabilities of unmodified and modified membranes. As expected, the results obtained indicate a high permeability of 30.09 L/h.m$^2$.bar (M.5) and 21.24 L/h.m$^2$.bar (M.5a) during the first 15 min of filtration for the unmodified membranes compared with enzyme modified membranes (**Figure 6.4**). However, the respective permeabilities of the same membranes decreased to 3.98 L/h.m$^2$.bar (M.5) and 2.65 L/h.m$^2$.bar (M.5a) after 180 min of filtration. The decrease in permeability could results from the deposition of humic acid (HA) on the surface of the membrane resulting from the increased concentration of HA in the feed stream brought about by the membrane rejection of HA. The initial 15 min permeabilities of 6.73 L/h.m$^2$.bar (M.5b) and 4.96 L/h.m$^2$.bar (M.5c) obtained for the membranes modified with isolate D enzymes were found to decrease over time. The decrease in permeabilities is attributed to the reduction of membrane pores, caused by the grafting of the enzymes on the membranes surface as well as the formation of an extra permeate flow resistant layer (Luo *et al*., 2014; Koloti *et al*., 2018). A reduction in permeate flux, which is related to permeability, was also reported by Nady (2016) when laccase modified PES membranes were used for the rejection of bovine serum albumin. The permeability results obtained for M.5c from isolate D contradict with contact angle results obtained in **Figure 6.3**. As upon incorporating the substrate in the incubation solution, the hydrophilicity of the membranes slightly increased which was expected to increase the permeability. A decrease in the permeability of the M.5c (D) membrane from 6.726 to 4.956 L/h.m$^2$.bar was not expected.

A similar trend was observed for the isolate R enzyme modified membranes. However, contact angle results obtained for M.5b (R) and M.5c (R) are in alignment with the corresponding increase in permeability from 4.956 to 6.726 L/h.m$^2$.bar that was observed after 15 min of filtration. The increase in permeability could be due to the incorporation of the substrate 4-hydroxybenzoic acid onto the membrane M.5c (R) which led to an increase in the hydrophilicity of the membrane. Similar results were reported by Koloti *et al*. (2017). No significant difference in the permeabilities

of membranes modified with D and R enzymes was noted. This implies that the extent of enzyme grafting does not affect the permeability of membranes.

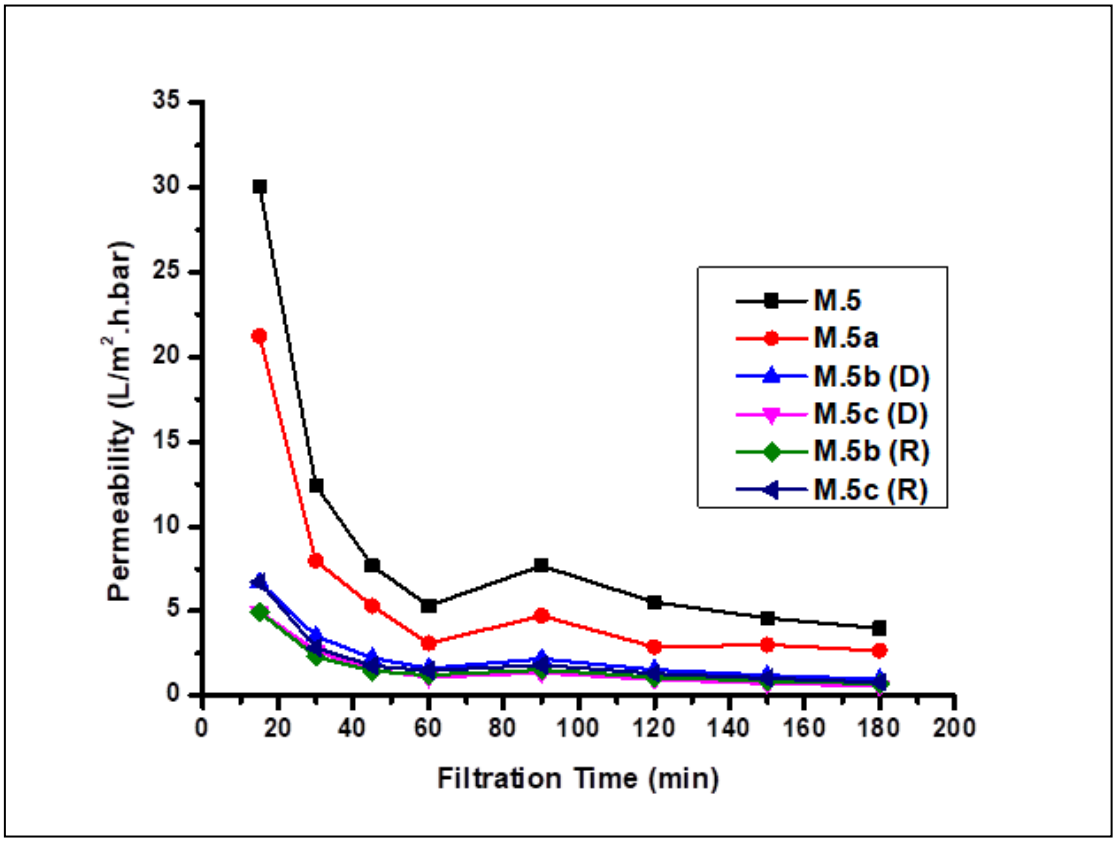


**Figure 6. 4**: Permeabilities of unmodified membranes (M.5 and M.5a) at 1 bar and enzyme modified membranes at 5 bars.

For all the membranes investigated in this research study (**Figure 6.5**), the $UV_{254}$ removal percentage of HA was found to be high during the first filtration period (i.e. 15 min); thereafter, it decreased with time. A high HA removal rates for M.5b (D) (84.8%) and M.5b (R) (81.1%) membranes were observed during first 15 min filtration period. However, after 180 min of filtration, the HA removal rate decreased to 57.18% and 60.13% for the respective M.5b (D) and M.5b (R) membranes. The decreased HA removal rate is attributable to saturation of the active sites of the enzymes. After 90 min of filtration, a constant HA removal rate was observed for M.5, M.5a, M.5c (D) and M.5c (R) membranes **(Figure 6.5)**. This implies that these membranes are stable between the filtration periods of 30 and 120 min. Low removal percentage rates were obtained for M.5c D (41.9%) and M.5 (42.0%) membranes. It is evident from the results obtained that the HA removal rates for the

modified membranes with enzymes are higher than those of the other membranes investigated. This suggests that enzymes are much more effective in the removal of HA when used without the substrate on membranes as a support material for immobilisation.

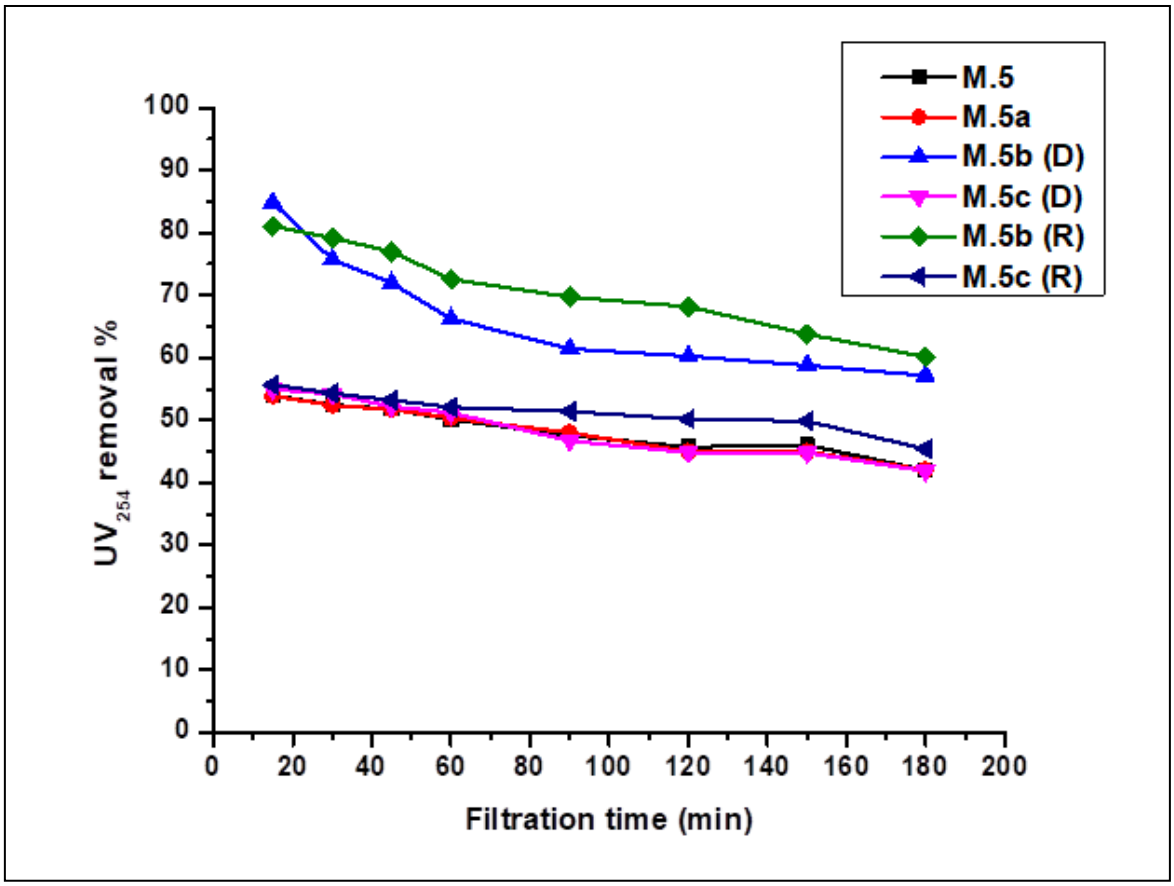


**Figure 6.5**: UV-Vis spectrum for all membranes studied; M.5 blank membrane, M.5a membrane with substrate only, M.5b (D) membrane with enzyme only, M.5c (D) membrane with enzyme and substrate, M.5b (R) membrane with enzyme only and M.5c (R)membrane with enzyme and substrate.

The removal of HA as measured by dissolved organic carbon (DOC) is shown in **Figure 6.6**. The DOC concentration was initially high and thereafter decreased as the filtration progressed over time. A similar trend in terms of total organic carbon degradation by laccase was reported by Mahvi *et al*. (2009). In this work, degradation rate within the first 90 min was initially high for the modified and it then declined with time. At 120 min interval, membranes modified with enzymes extracted from isolate D displayed a DOC concentration reduction of 6.06 to 3.43

mg/L and 7.99 to 6.01 mg/L for M.5b (D) and M.5c (D) membranes, respectively. After 180 min, the DOC concentration increased slightly from 3.43 to 3.77 mg/L and 6.01 to 6.55 mg/L for M.5b (D) and M.5c (D) membranes, respectively (see **Figure 6.6 (a)**). This sudden increase in the DOC concentration could be due to over deposition of HA on the surface of the membrane resulting from the continuous filtration through the membranes. Alternatively, the sudden increase in the DOC concentration might be due to over saturation of the reactive sites of the enzymes. For membranes modified with enzymes extracted from isolate R, the DOC concentration decreased from 2.33 to 0.15 mg/L at 120 min and 1.99 to 0.30 mg/L at 90 min for M.5b (R) and M.5c (R) membranes, respectively. Later, the DOC concentration increased from 0.15 to 1.47 mg/L and 0.30 to 1.98 mg/L for M.5b and M.5c membranes, respectively, after 180 min filtration (see **Figure 6.6 (a)**).

As shown in **Figure 6.6**, the DOC results correspond to UV results in **Figure 6.5**. The highest HA removal rate was achieved (99.5%) within 120 min of filtration using the M.5b (R) membrane modified with enzymes extracted from isolate R. On the other hand, the lowest removal percentage was achieved (51.8 %) within filtration 30 min using the unmodified M.5a membrane (see **Figure 6.6 (b)**). These removal percentage figures are similar to those obtained by Barrios-Estrada *et al*. (2018) and Bilal *et al*. (2019), which involved the degradation of Bisphenol A (BPA) using laccase produced from white rot fungi species.

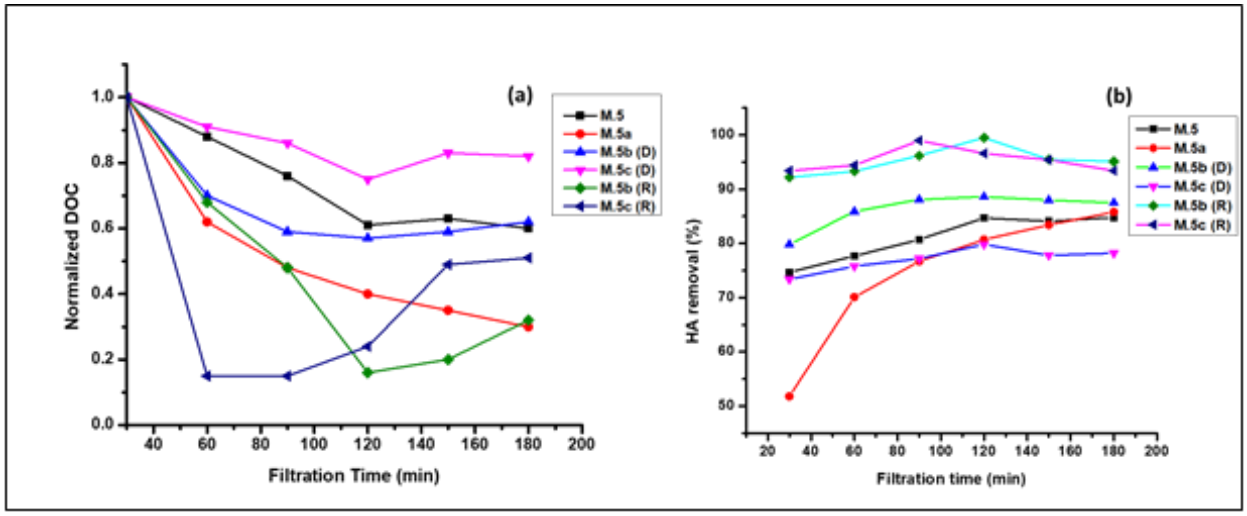


**Figure 6.6**: Normalized DOC (a) and HA removal % (b) over 180 min filtration time for all the membranes studied.

## 6.5 Conclusion

Laccase substrate, 4-hydroxybenzoic acid was used to maintain the stability of enzyme laccase on the membrane surface through formation of C-O covalent bond between the enzyme and the sulfonate groups of the membranes. It was observed that the substrate led to an improvement of the hydrophilicity of PES membranes modified with enzymes extracted from *Polyporaceae* sp. isolate R. The intense colour of the enzyme modified membranes confirmed the interaction between the enzyme, substrate and membranes. The appearance of the spherically shaped structures on the SEM images of M.5b and M5.c enzyme modified membranes was used as confirmation for the successful immobilisation of the enzyme. Moreover, a reduction in the permeability of the modified membranes served as confirmation for the enzyme immobilisation, which could have resulted from the reduced porosity (clogged pores) of the membranes. Rejection results suggest that the enzyme modified membranes can be used for the removal of HA and other similar compounds from water since 95 % HA removal rate was achieved when the M.5c (*Polyporaceae* sp. Isolate R) membrane modified was used.

## 6.6 References

Barrios-Estrada, C., de Jesús Rostro-Alanis, M., Parra, A.L., Belleville, M.P., Sanchez-Marcano, J., Iqbal, H.M. and Parra-Saldívar, R., 2018. Potentialities of active membranes with immobilized laccase for Bisphenol A degradation. *International Journal of Biological Macromolecules*, *108*, pp.837-844.

Bilal, M., Iqbal, H.M. and Barceló, D., 2019. Mitigation of bisphenol A using an array of laccase-based robust bio-catalytic cues–a review. *Science of The Total Environment*, *689*, pp.160-177.

Koloti, L.E., 2017. *Biodegradation of bisphenol a on an enzyme modified nanofibrous membrane for water treatment* (Doctoral dissertation, University of Johannesburg).

Koloti, L.E., Gule, N.P., Arotiba, O.A. and Malinga, S.P., 2018. Laccase-immobilized dendritic nanofibrous membranes as a novel approach towards the removal of bisphenol A. *Environmental Technology*, *39*(3), pp.392-404.

Luo, J., Meyer, A.S., Mateiu, R.V., Kalyani, D. and Pinelo, M., 2014. Functionalization of a membrane sublayer using reverse filtration of enzymes and dopamine coating. *ACS Applied Materials & Interfaces*, *6*(24), pp.22894-22904.

Mahvi, A., Maleki, A., Rezaee, R. and Safari, M., 2009. Reduction of humic substances in water by application of ultrasound waves and ultraviolet irradiation. *Journal of Environmental Health Science & Engineering*, *6*(4), pp.233-240.

Malczewska, B. and Żak, A., 2019. Structural Changes and Operational Deterioration of the Uf Polyethersulfone (Pes) Membrane Due to Chemical Cleaning. *Scientific Reports*, *9*(1), p.422.

Nady, N., 2016. PES surface modification using green chemistry: New generation of antifouling membranes. *Membranes*, *6*(2), p.23.

Nady, N., El-Shazly, A., Soliman, H. and Kandil, S., 2016. Protein-Repellence PES Membranes Using Bio-grafting of Ortho-aminophenol. *Polymers*, *8*(8), p.306.

Nady, N., Franssen, M., Zuilhof, H., Boom, R. and Schroën, K., 2012. Enzymatic modification of polyethersulfone membranes. *Water*, *4*(4), pp.932-943.

Nady, N., Schroën, K., Franssen, M.C., Lagen, B.V., Murali, S., Boom, R.M., Mohyeldin, M.S. and Zuilhof, H., 2011. Mild and highly flexible enzyme-catalyzed modification of poly (ethersulfone) membranes. *ACS Applied Materials & Interfaces*, *3*(3), pp.801-810.

Nkambule, T.I., Krause, R.W.M., Haarhoff, J. and Mamba, B.B., 2012. Natural organic matter (NOM) in South African waters: NOM characterisation using combined assessment techniques. *Water SA*, *38*(5), pp.697-706.

# CHAPTER 7

# CONCLUSIONS AND RECOMMENDATIONS

## 7.1 Conclusion

The aim of this work was to evaluate the performance of an enzyme enabled poly ethersulfone (PES) membranes in the degradation and removal of natural organic matter from water. In accomplishing the aim of this work, the following objectives were successfully achieved; preparation of high performing PES membrane in terms of permeate flux by altering the composition of the dope solution and parameters that influences the phase inversion process; isolation and identification of eighteen (18) fungal isolates using three (3) well-defined methods; screening of the isolates for the production of lignolytic enzymes using guaiacol as a substrate, and for removal of humic acid (HA) from liquid media; production of lignolytic enzymes using solid-state fermentation method, purification of the enzymes using ammonium sulfate and extraction of the crude lignolytic enzymes; modification of the high performing membrane by immobilising the extracted crude enzyme laccase on the membrane surface; and application and evaluation of the enzyme-modified membranes in the biodegradation and removal of HA as a model compound for NOM.

The following conclusions were drawn from this study:

I. In membrane preparation, the addition of water of up to 5 wt.% did not have any effect on the structure of the membranes. However, for the PES membrane M.6, an increase in the content of the poreformer polyethylene glycol (PEG) from 20 wt.% to 36 wt.% and water content of 5.5 wt.% changed the finger-like structure of the membrane to spongy-like. Extensive surface characterization of PES membrane M.5 (with 36 wt.% PEG and 0 wt.% water) revealed that the membrane was hydrophilic (with a contact angle of < 45°) with the highest water flux of 276.72 $L.m^{-2}.h^{-1}$. Further enhancement of the permeability of the membrane M.5 through the addition of the solvent

(15 wt.%) into the coagulation bath improved the permeate flux to 568.66 L. $m^{-2}.h^{-1}$. Rejection results showed that the order of rejection was as follows: BSA>HA>acid blue dye, which indicates that the removal was mostly governed by the size exclusion mechanism.

II. Only three (D, L and R) of the 18 isolates screened exhibited the production of enzyme laccase when guaiacol was used as a substrate. The three isolates (D,L and R) were further screened for their ability to remove HA from liquid media. About 48, 23 and 52 % removal were achieved from isolates D, L and R, respectively. This indicates that fungal enzymes from WRF have the potential to degrade organic compounds in aqueous media and can be therefore used to degrade NOM in surface water.

III. Characterization of the isolates using molecular methods has revealed that the isolates belong to the family of *Perenniporia* sp. (D), *Trichoderma koniniopsis* (L) and *Polyporaceae* sp. (R). This corroborates the difference in the degradation of HA, which was ascribed to the variation in species. Thus, it can be concluded that the organic compound degradation is species dependent.

IV. The solid-state fermentation method was used to enhance enzyme production by the two isolates (D and R). Results demonstrated a decrease in enzyme activity after 10 days of incubation, suggesting that the optimal duration for enzyme extraction was less than 10 days. A slight increase in enzyme activity was observed after purification, with isolate R exhibiting high laccase activity when compared with isolate *Perenniporia* sp. (Isolate D). This serves as further confirmation that enzyme production differs from species to species. The purified crude enzyme laccase from *Perenniporia* sp. (isolates D) and *Polyporaceae* sp. (isolate R) were immobilised onto the surface of the PES membrane for the degradation and removal of humic acid.

V. The high flux membrane M.5 was used as a support material (film) to maintain the stability of the enzyme laccase on the membrane. The substrate

4-hydroxybenzoic acid increased the membrane hydrophilicity owing to its polar carbonyl groups. An intense colour change was observed that is indicative of an interaction amongst the enzyme, the substrate and the sulfonate functional groups of the membrane. Morphological examination with scanning electron microscope and reduced permeability confirmed the successful enzyme immobilisation on the surface of the membranes.

VI. The highest $UV_{254}$ degradation efficiency of 85 % was obtained with membranes immobilised with *Perenniporia* sp. (isolate D) enzymes during the first 15 min of filtration. The highest dissolved organic carbon (DOC) removal efficiency of 99.5 % was achieved with membranes immobilised with *Polyporaceae* sp. (isolate R) enzymes. This implies that the enzymes are much more active on their own than with the substrate. However, a decrease in DOC removal was observed after 90 min of filtration. This could be due to saturation of the enzyme active sites or deposition of HA on the membrane surface. It can be concluded that the best retention time for HA removal from water is between 15 to 90 min of filtration.

## 7.2 Recommendations

The study could be extended to cover the following:

- **High flux membrane preparation**
  Results emanating from this work showed that it is possible to fabricate a polymeric membrane with high performance and high mechanical strength without adding nanomaterials. However, detailed knowledge on the fundamentals of membrane fouling are needed to fully understand performance and determine the lifespan of the membranes.

- **Screening of fungal isolates for enzymes production and humic acid degradation**

This study was focused on the production of enzymes from three isolates (D, L and R) on solid media using guaiacol as a substrate. The use of other substrates for enzyme detection is recommended. Although the investigated isolates (D, L and R) showed an ability to remove humic acid from liquid media, the screening of other fractions of natural organic matter (NOM) such as protein-like, and polysaccharides-like compounds as well as other NOM model compounds is also recommended.

- **Enzyme-modified PES membrane characterization**

  The removal of HA as a model NOM constituent by enzyme-modified membranes was achieved. Future work on the removal of other NOM fractions in real water samples is recommended. Future work involving the application of the enzyme-modified membranes on membrane bioreactors using hydraulic retention times of between 15 and 90 min of filtration with the view to enhance membrane performance and process application is recommended.

## APPENDIX

**Table A1**: Flux measurements and permeabilities of the prepared membranes at 3 bars.

| Area | 0.00335 $m^2$ | **Prepared membranes** | | | | | | | | |
|---|---|---|---|---|---|---|---|---|---|---|
| Time | 0.5 H | 20 PES/20 PEG | | | | 20 PES/36 PEG | | | 22 PES/36 PEG | |
| | | **M.1** | **M.2** | **M.3** | **M.4** | **M.5** | **M.6** | **M.7** | **M.8** | **M.9** |
| | | **0 wt.% H20** | **2.5 wt. % H20** | **3.5 wt.% H20** | **5 wt.% H20** | **0 wt.% H20** | **5.5 wt.% H20** | **6.5 wt.% H20** | **0 wt.% H20** | **2.5 wt.% H20** |
| | **3 bars** | 65 | 38 | 37 | 94 | 478 | 81 | 250 | 116 | 430 |
| | | 29 | 29 | 50 | 101 | 449 | 72 | 330 | 101 | 455 |
| | | 45 | 30 | 46 | 100 | 322 | 56 | 200 | 102 | 555 |
| | **Average (mL)** | 37 | 29.5 | 48 | 100.5 | 463.5 | 76.5 | 225 | 101.5 | 442.5 |
| | **Average (L)** | 0.037 | 0.0295 | 0.048 | 0.1005 | 0.4635 | 0.0765 | 0.225 | 0.1015 | 0.4425 |
| | **Flux (LMH)** | 22.08955224 | 17.6119403 | 28.65671642 | 179.6407186 | 276.716418 | 45.67164 | 134.3283582 | 60.59701493 | 264.1791045 |
| | **Permeability** | 7.36318408 | 5.870646766 | 9.552238806 | 59.88023952 | 92.238806 | 15.22388 | 44.7761194 | 20.19900498 | 88.05970149 |
| | **STD** | 11.3137085 | 0.707106781 | 2.828427125 | 0.707106781 | 20.5060967 | 6.363961 | 56.56854249 | 0.707106781 | 17.67766953 |

**Table A2**: Mycelium growth (radius in mm) of all the fungal isolates on HA solid media.

| Isolates | Day 4 | Day 7 | Day 10 | Day 15 |
|---|---|---|---|---|
| **A** | 29.5 | 37.5 | 38.5 | 40 |
| **B** | 9.5 | 14 | 15 | 15.5 |
| **C** | 31.5 | 37 | 37 | 38 |
| **D** | 20 | 32 | 35 | 39 |
| **E** | 15.5 | 32 | 33 | 34.5 |
| **F** | 29.5 | 40 | 40 | 40 |
| **G** | 10 | 36 | 36.5 | 37 |
| **H** | 32.5 | 36 | 36.5 | 37 |
| **I** | 25 | 36 | 36.5 | 37 |
| **J** | 10 | 25 | 27 | 27.5 |
| **K** | 12.5 | 36.5 | 36.5 | 36.5 |
| **L** | 17.5 | 36.5 | 37.5 | 38.5 |
| **M** | 18 | 35 | 35.5 | 36 |
| **N** | 19 | 34.5 | 36.5 | 37.5 |
| **O** | - | - | - | - |
| **P** | 30 | 36 | 3.65 | 37 |
| **Q** | 29.5 | 35 | 35.5 | 35.5 |
| **R** | 22 | 36.5 | 39 | 40 |
| **S** | 20 | 35.5 | 37.5 | 38.5 |

**Table A3**: Enzyme laccase activity for isolate D and R over 21 incubation period on SSF.

| Laccase activity | | | | | |
|---|---|---|---|---|---|
| **Isolate** | **Abs before incubation** | **Abs after incubation** | **Difference** | **Enzyme Activity (U/mL)** | **E.A * 1000 (U/mL)** |
| R(a) 7 d | 2.424 | 3.31 | 0.886 | 0.000328635 | 0.328635015 |
| R(b) 7 d | 2.076 | 2.894 | 0.818 | 0.000303412 | 0.303412463 |
| | | | | | |
| R(a) 10 d | 1.449 | 2.307 | 0.858 | 0.000318249 | 0.318249258 |
| R(b) 10 d | 0.35 | 0.432 | 0.082 | 3.04154E-05 | 0.03041543 |
| | | | | | |
| D(a) 7 d | 2.208 | 3.078 | 0.87 | 0.0003227 | 0.322700297 |
| D(b) 7 d | 2.286 | 3.095 | 0.809 | 0.000300074 | 0.300074184 |
| | | | | | |
| R(a) 15 d | 1.428 | 2.243 | 0.815 | 0.0003023 | 0.302299703 |
| R(b) 15 d | 0.284 | 0.325 | 0.041 | 1.52077E-05 | 0.015207715 |
| | | | | | |
| D(a) 10 d | 1.501 | 2.748 | 1.247 | 0.000462537 | 0.462537092 |
| D(b) 10 d | 0.982 | 2.255 | 1.273 | 0.000472181 | 0.472181009 |
| | | | | | |
| R(a) 21 d | 1.551 | 1.85 | 0.299 | 0.000110905 | 0.110905045 |
| R(b) 21 d | 0.439 | 0.509 | 0.07 | 2.59644E-05 | 0.025964392 |
| | | | | | |
| D(a) 15 d | 1.935 | 2.592 | 0.657 | 0.000243694 | 0.243694362 |
| D(b) 15 d | 1.563 | 2.043 | 0.48 | 0.000178042 | 0.178041543 |
| | | | | | |
| D(a) 21 d | 1.745 | 2.287 | 0.542 | 0.000201039 | 0.201038576 |
| D(b) 21 d | 1.376 | 1.796 | 0.42 | 0.000155786 | 0.15578635 |

**Table A4**: Manganese-dependent peroxidase activity for isolate D and R over 21 incubation period on SSF.

| Manganese peroxidase | | | | | |
|---|---|---|---|---|---|
| **Isolate** | **Abs before peroxide addition** | **Abs after peroxidase addition** | **Difference** | **Enzyme Activity** | **E.A * 1000** |
| R(a) 7 d | 2.129 | 1.7135 | 0.4155 | 0.001203999 | 1.203998841 |
| R(b) 7 d | 1.431 | 1.147 | 0.284 | 0.00082295 | 0.82294987 |
| | | | | | |
| R(a) 10 d | 1.981 | 0.716 | 1.265 | 0.003665604 | 3.665604173 |
| R(b) 10 d | 2.191 | 0.736 | 1.455 | 0.004216169 | 4.216169226 |
| | | | | | |
| D(a) 7 d | 1.286 | 1.0145 | 0.2715 | 0.000786728 | 0.786728484 |
| D(b) 7 d | 1.007 | 0.804 | 0.203 | 0.000588235 | 0.588235294 |
| | | | | | |
| R(a) 15 d | 2.28 | 1.819 | 0.461 | 0.001335845 | 1.335844683 |
| R(b) 15 d | 2.32 | 1.804 | 0.516 | 0.001495219 | 1.495218777 |
| | | | | | |
| D(a) 10 d | 1.222 | 0.971 | 0.251 | 0.000727325 | 0.727325413 |
| D(b) 10 d | 0.973 | 0.173 | 0.8 | 0.002318169 | 2.318168647 |
| | | | | | |
| R(a) 21 d | 2.63 | 2.0775 | 0.5525 | 0.001600985 | 1.600985222 |
| R(b) 21 d | 2.683 | 2.057 | 0.626 | 0.001813967 | 1.813966966 |
| | | | | | |
| D(a) 15 d | 0.962 | 0.769 | 0.193 | 0.000559258 | 0.559258186 |
| D(b) 15 d | 1.357 | 1.0735 | 0.2835 | 0.000821501 | 0.821501014 |
| | | | | | |
| D(a) 21 d | 0.776 | 0.657 | 0.119 | 0.000344828 | 0.344827586 |
| D(b) 21 d | 1.468 | 1.048 | 0.42 | 0.001217039 | 1.21703854 |

**Table A5**: Lignin peroxidase activity for isolate D and R over 21 incubation period on SSF.

| Lignin peroxidase | | | | | |
|---|---|---|---|---|---|
| **Isolate** | **Abs before peroxide addition** | **Abs after peroxidase addition** | **Difference** | **Enzyme Activity** | **E.A * 1000** |
| R(a) 7 d | 2.736 | 2.5935 | 0.1425 | 0.000766129 | 0.766129032 |
| R(b) 7 d | 1.822 | 1.7455 | 0.0765 | 0.00041129 | 0.411290323 |
| | | | | | |
| R(a) 10 d | 2.366 | 2.0905 | 0.2755 | 0.001481183 | 1.481182796 |
| R(b) 10 d | 2.629 | 2.315 | 0.314 | 0.001688172 | 1.688172043 |
| | | | | | |
| D(a) 7 d | 1.52 | 1.4545 | 0.0655 | 0.000352151 | 0.352150538 |
| D(b) 7 d | 1.206 | 1.1535 | 0.0525 | 0.000282258 | 0.282258065 |
| | | | | | |
| R(a) 15 d | 0.194 | 0.8655 | 0.6715 | 0.003610215 | 3.610215054 |
| R(b) 15 d | 0.177 | 0.896 | 0.719 | 0.003865591 | 3.865591398 |
| | | | | | |
| D(a) 10 d | 0.183 | 0.5045 | 0.3215 | 0.001728495 | 1.728494624 |
| D(b) 10 d | 0.189 | 0.387 | 0.198 | 0.001064516 | 1.064516129 |
| | | | | | |
| R(a) 21 d | 0.828 | 0.946 | 0.118 | 0.000634409 | 0.634408602 |
| R(b) 21 d | 0.492 | 0.9135 | 0.4215 | 0.002266129 | 2.266129032 |
| | | | | | |
| D(a) 15 d | 0.329 | 0.404 | 0.075 | 0.000403226 | 0.403225806 |
| D(b) 15 d | 0.487 | 0.589 | 0.102 | 0.000548387 | 0.548387097 |
| | | | | | |
| D(a) 21 d | 0.338 | 0.403 | 0.065 | 0.000349462 | 0.349462366 |
| D(b) 21 d | 0.534 | 0.576 | 0.042 | 0.000225806 | 0.225806452 |

**Table A6**: Enzyme activity for isolate D and R after purification.

| Laccase | | | | | |
|---|---|---|---|---|---|
| Isolate | Absorbance before incubation | Absorbance after incubation | Difference | Enzyme activity | E.A *1000 (U/mL) |
| R | 0.57 | 1.37 | 0.8 | 0.000296736 | 0.296735905 |
| D | 2.735 | 3.145 | 0.41 | 0.000152077 | 0.152077151 |

| Manganese-peroxidase | | | | | |
|---|---|---|---|---|---|
| Isolate | Absorbance before $H_2O_2$ addition | Absorbance after $H_2O_2$ addition | Difference | Enzyme activity | E.A *1000 (U/mL) |
| R | 1.81 | 1.56 | 0.25 | 0.000724428 | 0.724427702 |
| D | 2.37 | 2.07 | 0.3 | 0.000869313 | 0.869313243 |

| Lignin-peroxide | | | | | |
|---|---|---|---|---|---|
| Isolate | Absorbance before $H_2O_2$ addition | Absorbance after $H_2O_2$ addition | Difference | Enzyme activity | E.A *1000 (U/mL) |
| R | 0.92 | 0.89 | 0.03 | 0.00016129 | 0.161290323 |
| D | 0.945 | 0.97 | 0.025 | 0.000134409 | 0.134408602 |

**Table A7**: Permeabilities of unmodified membrane

Area 0.00113 $m^2$

| M.5 | | | | | |
|---|---|---|---|---|---|
| **Filt Time(min)** | **hours** | **Volume (mL)** | **L** | **Flux** | **permeability** |
| 15 | 0.25 | 8.5 | 0.0085 | 30.08849558 | 30.08849558 |
| 30 | 0.5 | 7 | 0.007 | 12.38938053 | 12.38938053 |
| 45 | 0.75 | 6.5 | 0.0065 | 7.669616519 | 7.669616519 |
| 60 | 1 | 6 | 0.006 | 5.309734513 | 5.309734513 |
| 90 | 1.5 | 13 | 0.013 | 7.669616519 | 7.669616519 |
| 120 | 2 | 12.5 | 0.0125 | 5.530973451 | 5.530973451 |
| 150 | 2.5 | 13 | 0.013 | 4.601769912 | 4.601769912 |
| 180 | 3 | 13.5 | 0.0135 | 3.982300885 | 3.982300885 |

**Table A8**: Permeabilities of unmodified membrane with substrate only

Area 0.00113 $m^2$

| M.5a | | | | | |
|---|---|---|---|---|---|
| **Filt Time(min)** | **hours** | **Volume (mL)** | **L** | **Flux** | **permeability** |
| 15 | 0.25 | 6 | 0.006 | 21.23893805 | 21.23893805 |
| 30 | 0.5 | 4.5 | 0.0045 | 7.96460177 | 7.96460177 |
| 45 | 0.75 | 4.5 | 0.0045 | 5.309734513 | 5.309734513 |
| 60 | 1 | 3.5 | 0.0035 | 3.097345133 | 3.097345133 |
| 90 | 1.5 | 8 | 0.008 | 4.719764012 | 4.719764012 |
| 120 | 2 | 6.5 | 0.0065 | 2.876106195 | 2.876106195 |
| 150 | 2.5 | 8.5 | 0.0085 | 3.008849558 | 3.008849558 |
| 180 | 3 | 9 | 0.009 | 2.654867257 | 2.654867257 |

**Table A9**: Permeabilities of membranes modified with enzymes only

Area 0.00113 $m^2$

| M.5b isolate D | | | | | |
|---|---|---|---|---|---|
| **Filt Time(min)** | **hours** | **Volume (ml)** | **L** | **Flux** | **permeability** |
| 15 | 0.25 | 9.5 | 0.0095 | 33.62831858 | 6.725663717 |
| 30 | 0.5 | 10 | 0.01 | 17.69911504 | 3.539823009 |
| 45 | 0.75 | 9.5 | 0.0095 | 11.20943953 | 2.241887906 |
| 60 | 1 | 9.2 | 0.0092 | 8.14159292 | 1.628318584 |
| 90 | 1.5 | 18.5 | 0.0185 | 10.91445428 | 2.182890855 |
| 120 | 2 | 17.5 | 0.0175 | 7.743362832 | 1.548672566 |
| 150 | 2.5 | 17 | 0.017 | 6.017699115 | 1.203539823 |
| 180 | 3 | 16.5 | 0.0165 | 4.867256637 | 0.973451327 |

**Table A10**: Permeabilities of membranes modified with enzymes and substrate

Area 0.00113 $m^2$

| M.5c isolate D | | | | | |
|---|---|---|---|---|---|
| **Filt Time(min)** | **hours** | **Volume (ml)** | **L** | **Flux** | **permeability** |
| 15 | 0.25 | 7 | 0.007 | 24.77876106 | 4.955752212 |
| 30 | 0.5 | 7.5 | 0.0075 | 13.27433628 | 2.654867257 |
| 45 | 0.75 | 6.5 | 0.0065 | 7.669616519 | 1.533923304 |
| 60 | 1 | 6.3 | 0.0063 | 5.575221239 | 1.115044248 |
| 90 | 1.5 | 11.5 | 0.0115 | 6.784660767 | 1.356932153 |
| 120 | 2 | 11 | 0.011 | 4.867256637 | 0.973451327 |
| 150 | 2.5 | 10.5 | 0.0105 | 3.716814159 | 0.743362832 |
| 180 | 3 | 10 | 0.01 | 2.949852507 | 0.589970501 |

**Table A11**: Permeabilities of membranes modified with enzymes only

Area 0.00113 $m^2$

| M.5b isolate R | | | | | |
|---|---|---|---|---|---|
| **Filt Time(min)** | **hours** | **Volume (ml)** | **L** | **Flux** | **permeability** |
| 15 | 0.25 | 7 | 0.007 | 24.77876106 | 4.955752212 |
| 30 | 0.5 | 6.5 | 0.0065 | 11.50442478 | 2.300884956 |
| 45 | 0.75 | 6.2 | 0.0062 | 7.315634218 | 1.463126844 |
| 60 | 1 | 7 | 0.007 | 6.194690265 | 1.238938053 |
| 90 | 1.5 | 13 | 0.013 | 7.669616519 | 1.533923304 |
| 120 | 2 | 12.5 | 0.0125 | 5.530973451 | 1.10619469 |
| 150 | 2.5 | 12.5 | 0.0125 | 4.424778761 | 0.884955752 |
| 180 | 3 | 12.2 | 0.0122 | 3.598820059 | 0.719764012 |

**Table A12**: Permeabilities of membranes modified with enzymes and substrate

Area 0.00113 $m^2$

| M.5c isolate R | | | | | |
|---|---|---|---|---|---|
| **Filt Time(min)** | **hours** | **Volume (ml)** | **L** | **Flux** | **permeability** |
| 15 | 0.25 | 9.5 | 0.0095 | 33.62831858 | 6.725663717 |
| 30 | 0.5 | 8 | 0.008 | 14.15929204 | 2.831858407 |
| 45 | 0.75 | 7.5 | 0.0075 | 8.849557522 | 1.769911504 |
| 60 | 1 | 8.5 | 0.0085 | 7.522123894 | 1.504424779 |
| 90 | 1.5 | 15.5 | 0.0155 | 9.144542773 | 1.828908555 |
| 120 | 2 | 15 | 0.015 | 6.637168142 | 1.327433628 |
| 150 | 2.5 | 14.8 | 0.0148 | 5.238938053 | 1.047787611 |
| 180 | 3 | 13.6 | 0.0136 | 4.01179941 | 0.802359882 |